ANALYSIS OF A NUMERICAL AND ADAPTIVE CONTROL SERVOMECHANISM

ANALYSIS OF A NUMERICAL AND ADAPTIVE CONTROL SERVOMECHANISM

by

MOHAMED A.A. ELBESTAWI, B.Sc. (Eng.)

A Thesis

Submitted to the School of Graduate Studies

in Partial Fulfilment of the Requirements

for the Degree

Master of Engineering

McMaster University

April, 1976

TO THE MEMORY OF MY FATHER

MASTER OF ENGINEERING (1976) McMaster University
(Mechanical Engineering) Hamilton, Ontario

TITLE: Analysis of a Numerical and Adaptive Control Servomechanism

AUTHOR: MOHAMED ABDEL AZIZ ELBESTAWI
B.Sc. (Production Eng.)
(Alexandria University, Alexandria, Egypt)

SUPERVISOR: Professor J. Tlusty

NUMBER OF PAGES: xii, 170

ABSTRACT:

The purpose of this project was to analyze the Numerical and Adaptive Control system of a CNC milling machine, in order to improve the time response of the system while maintaining its stability. The available linear control theory as well as the state space method were used to study and simulate the behaviour of the N/C loop. The N/C system was tested to determine the practically optimum values of position and velocity gains. The Adaptive Control system consists of a cutting force transducer, and an Analog to Digital Processor which supply input to an A/C routine resident in the HR-2100A minicomputer. Both classical control theory and the state space technique were also used to investigate the operation of the A/C loop and to predict the response of the actual system.

ACKNOWLEDGEMENTS

It is my pleasure to express my sincere gratitude to Dr. J. Tlusty for his expert guidance, valuable advice and continuous encouragement throughout the duration of the present investigation.

The author also expresses his appreciation to Ms. Theresa MacFarlane for her expert typing of the manuscript.

The financial assistance from McMaster University is gratefully acknowledged.

TABLE OF CONTENTS

LIST OF FIGURES

CHAPTER 1

INTRODUCTION

The use of a digital computer to automatically control and program machine tools shows promise of leading to a new era in manufacturing techniques. The largest single benefit of a digital computer is its ability to do simultaneously a number of unrelated tasks.

Beyond N/C, there are two areas of possible improvement in machining. The first involves decreasing the non-machining time by improving loading, unloading, scheduling and shop routing. The second involves decreasing the actual machining time. It is in this second area that Adaptive control (AC) lies.

Adaptive control is a logical extension from N/C in the further automation of metalworking machinery. Under adaptive control, the cutting process is continuously monitored by observing certain important process variables. The A/C controller, using these process variables as input alters selected control variables to improve the cutting process. In metal cutting the term "improvement of the cutting process" means either increasing the metal removal rate (MRR), or decreasing the unit cost. This leads to two conflicting requirements. On the one hand the MRR is

linearly dependent on the product of the feed and cutting speed. But on the other hand increasing feed and speed causes a faster tool failure. Tool failure requires stopping of the machine for tool change which in turn decreases the MRR (when the unit cost is the criterion, an additional factor - the cost of the tool - must be taken into account as well).

Although the field of adaptive control has witnessed many very complex and cumbersome systems, there remains a need for simple yet efficient A/C systems.

In the present work an attempt to analyze the entire CNC-A/C system is performed. The N/C loop was first analyzed using the available linear control theory. The response of the loop to different inputs was simulated using the state space method. The actual N/C loop was tested and the results were compared with those obtained from using the simulation technique. The purpose is to explore ways of obtaining a faster response of the N/C loop while still maintaining its stability.

The A/C system was next analyzed by using first the classical linear control theory assuming linearization of the loop. The state space method was used to simulate the operation of the entire CNC-A/C system including all its non-linearties. The effect of the time lag between the cutting force and the table velocity, the force sampling interval and the current limitation constraint on the

behaviour of the system was investigated using mainly the simulation technique. A linear A/C algorithm is suggested and the A/C strategy has been altered sufficiently to produce stable control as well as improving the response time of the system.

The work discussed in this thesis follows that of reference 7 where in an adaptive control system controlling the feed rate of a CNC milling machine based on a non-linear algorithm was simulated and developed, and the design of a force transducer was discussed.

CHAPTER 2

Literature Survey

A numerical control system[1,2] regulates the action of one or more machines by the automatic interpretation of instructions expressed as numerals. A typical numerically controlled machine tool receives information in digital form. Coded numbers indicating dimensions of the parts to be produced are punched in cards or in paper tape, or electronically recorded on magnetic tape. A conventional NC Contouring Controller is generally organized as shown in figure 1[21]. The data tape and manual input are read into the core unit, which provides buffer storage, decoding and sequencing logic, decimal-to-binary conversion, and other related functions. Virtually all conventional NC Contouring Control systems utilize pulse-oriented digital circuitry. Both position command and position measurement are digital pulses, each pulse associated with an increment of axis displacement. The path generation or interpolation logic converts the tape position coordinates and velocity commands into a command-pulse series of correct frequency.

The main advantages of NC over conventional machining[1,2] are the capability of accurate machining of complex shapes, decreased set-up times and more management

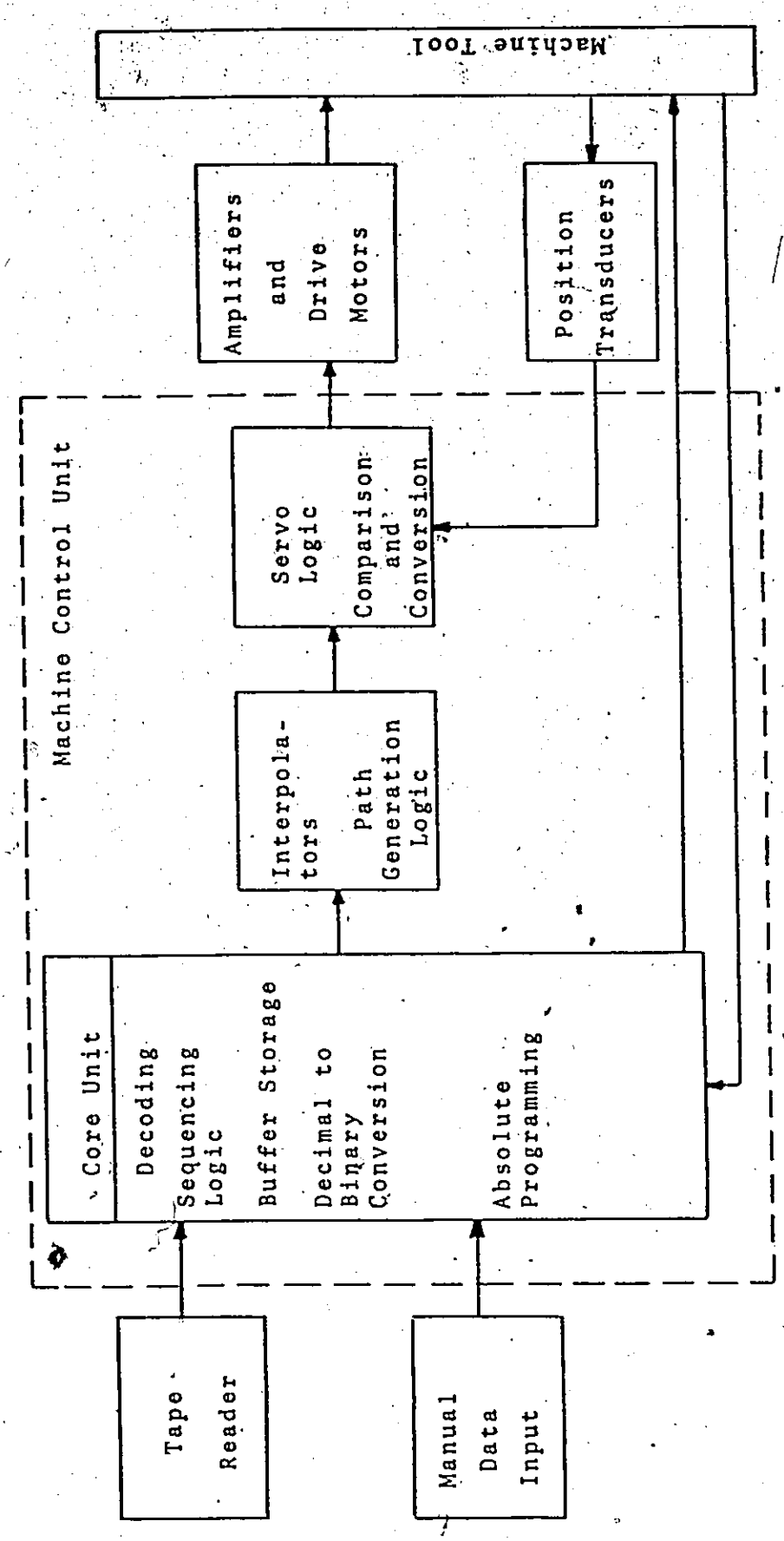

Block Diagram of a Conventional Hardwired NC Control System

FIGURE 1

control of shop operations, as well as a general increase in productivity over manual methods.

The CNC concept[9,20,21,22] means to have a mini-computer for on-line control of a machine tool. Two basic approaches have been used for CNC alternatives to conventional control:

1. A hybrid combination consisting of a computer and hard-wired logic, where a general-purpose mini-computer replaces the functions of the conventional core unit and conventional hardwired circuits are retained for the interpolation and position loop logic. This system is shown in figure 2A.
2. A complete minicomputer system where all control functions, including interpolation and position-loop closure, are performed in the computer software as shown in figure 2B.

The basic difference between a conventional N/C and a CNC system is the change in the level of flexibility[9]. The conventional N/C is a purely hardware system. To alter or modify a hardware system means rewiring, while a modification in a CNC system means reprogramming. Another advantage of a CNC system is the elimination of on-line reading of the data-tape, thus avoiding the errors which occur during the tape reading. Moreover - if an addition of adaptive control (AC) is desired, the system requires a computer for calculating the "optimal" conditions of the process according to a given policy. In such a CNC/AC system the computer is used

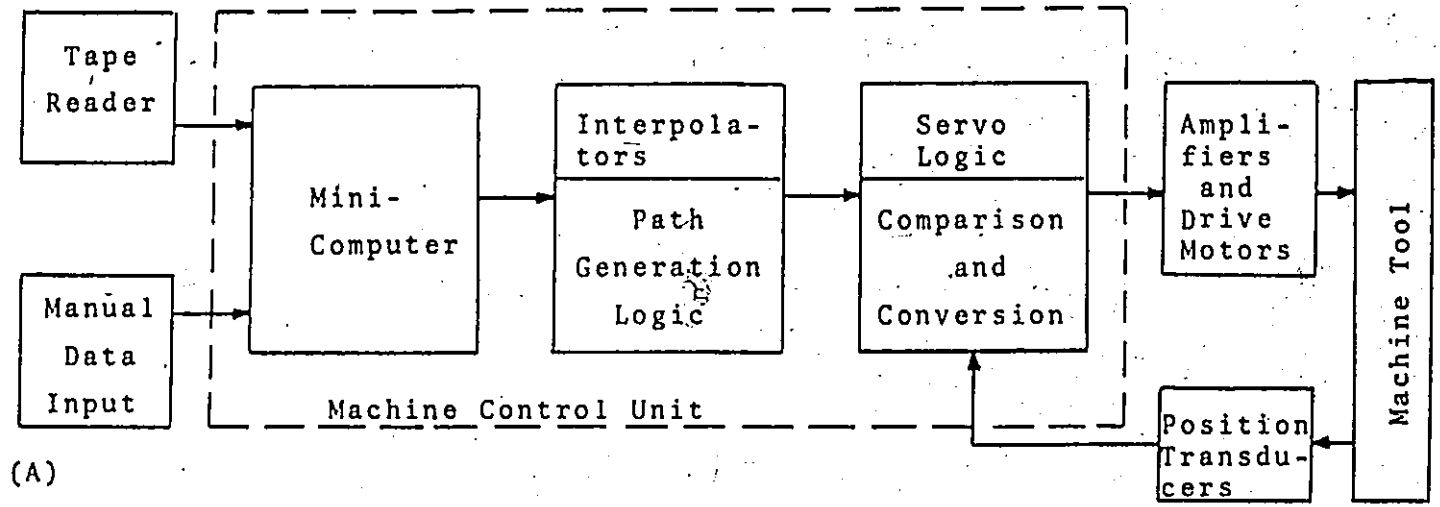

(A)

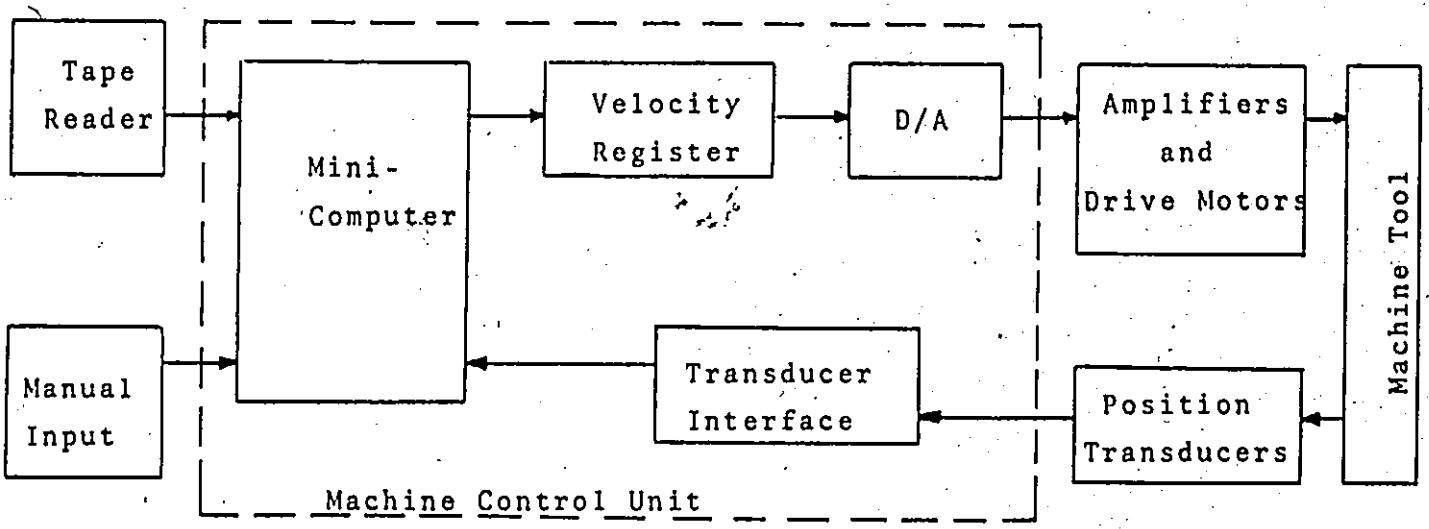

(B)

FIGURE 2

Approaches Commonly Used in CNC Systems

A - Hybrid Configuration

B - Software CNC Configuration

for both purposes and the computation process is switched from the AC program to the N/C program and back.

For complex metal cutting processes, adaptive control can be an effective means of reducing cost, decreasing scrap rate, and increasing productivity. The implementation of Adaptive control technique requires the use of sensors for on-line measurement of process variables. The sensor outputs are generally applied to an adaptive controller which calculates the process performance and then adjusts the input variables to improve performance. The degree to which "optimum" performance can be maintained with adaptive control is dependent largely upon the availability of accurate sensing equipment[19]. Process variables investigated by many researchers included cutting forces, spindle torque, spindle deflection, temperature at the tool-workpiece interface, table vibrations, spindle vibrations and motor current[11,13, 14,15,16,17,18,19]. The controlled variables are generally feed rate and/or spindle speed. The role of using the adaptive control technique is generally more significant in the numerical control field[15], where their use could lighten the programmer's load and increase productivity. The interconnection of an adaptive control system with a numerically controlled milling machine, used as illustrative example, is shown in figure 3[19]. Two feedback loops are closed around the machining process: the primary feedback from the machine tool to the numerical control system; the secondary or

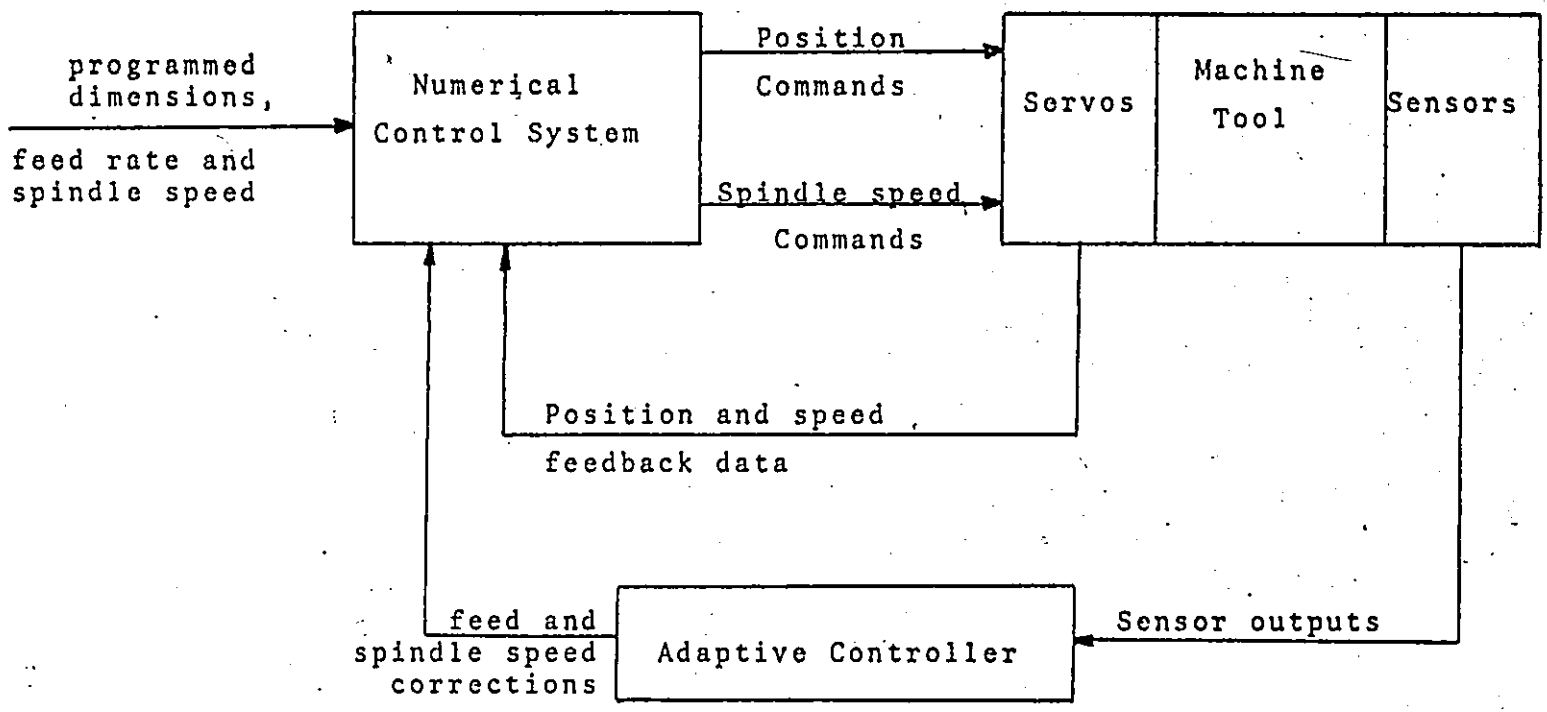

FIGURE 3

Interconnection of an Adaptive Control with a Numerically Controlled Milling Maching

[Ref. 19]

adaptive loop is closed around the entire process.

Adaptive control systems are generally divided according to objective, structure and method into Adaptive Control Constraint (ACC) and Adaptive Control Optimization (ACO) (figure 4)[16]. A further subdivision exists into technological and geometrical AC. An AC optimizing system seeks the best combination of machining rates, at every instant of time, in order to satisfy some predetermined optimum value for metal removal rate and cost[7]. Such an optimizing system would require an on-line tool wear sensor to obtain the economic tool life. Although many researchers have attempted on-line tool wear determination[14,15], by using cutting forces, cutting sound, light reflection and pneumatic methods. a reliable on-line sensor has yet to be developed[7.14]. Therefore, the alternative to full optimization is then an A/C constraint system where in machining rates may be changed within predetermined bounds only. The preset constraints could be:

1. Maximum spindle speed
2. Minimum spindle speed
3. Maximum torque
4. Maximum chip load
5. Maximum feed-rate
6. Impact chip load
7. Maximum vibration
8. Maximum force

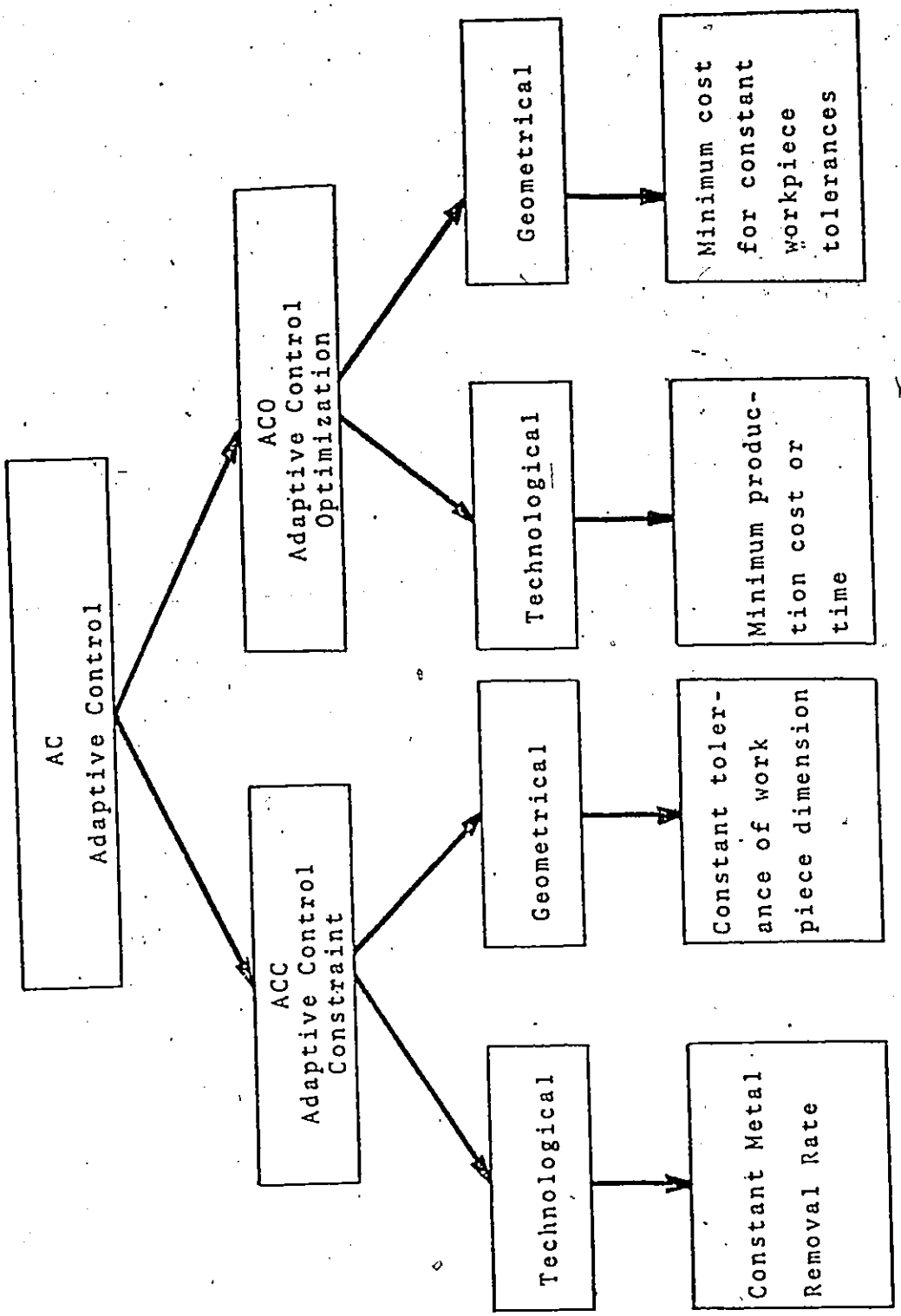

Subdivisions of the Term "Adaptive Control"

FIGURE 4

9. Minimum chip load

Examples of such AC constraint systems could be found in references 7, 11, 13, 14, 16, 17, 18 and 19.. In the practical application of AC constraint system for milling machines, cutting force is often used as the sensed variable while the feed rate is the controlled variable[11,17,18]. Two major problems are often encountered in the application of such a feed rate control.

Stute and Goetz[18] explained that one of the problems encountered in the use of AC constraint systems for milling machines, is the possible large variation of the gain of the controlled process which depends on the machining conditions. For example, according to the variations in width or depth of cut, the ratio of cutting force to feed rate widely changes, and so does the gain of the open loop transfer function of the system. If there is a controlled process in which the gain changes then the behaviour of the control may become worse because the parameters of the controller are constant. If the gain of the controlled process becomes too large, the stability and therefore the safety of machining will be in danger.

A second problem is the time lag of the feed rate response to an actual cutting force variation[7,17], which may cause instability in the AC loop.

With the development of stored programme control systems, the adaptive control function is achieved by

software[7,8,10,11,25], while in the conventional type of adaptive control systems, the adaptive control function was achieved via hardware components.

Bedini and Pinotti[25] used a mini-computer (PDP 11/40 with 16K, 16 bits words of core memory, 900 ns cycle time) operating in real time and connected to the control unit of a milling machine. The computer sets a wide range of spindle speeds and feeds while machining various materials at different depths and widths of cut. The signals received from bending and torque transducers are digitalized for each machining condition and statistically processed. Basically the adaptive controller samples the actual values of bending, torque and power, compares them with those which are assumed to be the optimal ones for the best machine utilization and, taking into account all the technological and mechanical constraints, changes the feed-rate and spindle speed in order to keep the bending, torque and power at the desired values. The use of the digital computer is reported to greatly simplify the testing of the control algorithms which, being software implemented, can be easily modified and improved in their performances simply by changing the programs. Moreover, the computer can be used for collection and processing of the cutting data.

In the system investigated in this thesis the adaptive controller is a software programme which contains the limits of the constraints and the necessary software

to handle the signals from the sensor on the machine and compute the corresponding feed according to a specified strategy. This system is basically designed for the control of die sinking operations [7,8,10,11].

Of all the possible applications of adaptive control in machining the one concerning the die sinking is perhaps the most obvious and straightforward. The reason for this application of adaptive control are, on one side, the practically unpredictable and usually large variation of the load on the cutter, and on the other side, the vulnerability of the usually long end slender end milling cutters used in die work.

CHAPTER 3

ANALYSIS OF THE NC LOOP

3.1 Introduction

The adaptive control (A/C) of metal working processes is a logical extension of numerical control. In the N/C process the cutting speed and feed are prescribed by the part programmer. The determination of these parameters depends on his experience and knowledge about the workpiece and tool materials, coolant conditions, radius of the cutter nose and some other factors.

The main idea in adaptive control is the improvement of the cutting process by automatic on-line determination of the cutting speed and feed. Accordingly, the adaptive control system is basically a feed back system in which the cutting speed and feed automatically adapt themselves to the actual conditions of the process. However, the adaptive controller, often must work in cooperation with other control functions, that is the N/C controller.

The complete NC control function was analysed before the addition of the AC loop. The purpose is to investigate the possible methods that result in a faster response of the NC loop which in turn should be reflected on the response

of the entire system, that is including the AC loop, and in the meanwhile ensure the stability of the system. Both loops were simulated by a digital computer program in order to more easily investigate the effects of changes in either cutting or controlling conditions. This chapter presents a mathematical analysis of the NC loop using different techniques of the classical control theory as well as simulation of the NC loop.

3.2 General Description of the NC Loop

Fig. 5 illustrates the block diagram of any axis of motion of the system. The three axes of motion may be considered as parallel systems, each one complete in itself, with each receiving its input from a Hewlet-Packard 2100A mini computer. A distance command is supplied as an input to the system. Position control in the system is carried out in a closed-loop mode with synchro resolvers as feedback devices. The resolver is connected to the lead screw of the machine. Both the distance command and the actual position of the machine slide as provided by the resolver are subtracted in a phase comparator which produces a control error proportional to the phase difference between command and feed back. The phase-comparator operation is based on the principle of up-down counter, which its outputs are connected to a D/A converter. The output of the latter is smoothed by a low pass-filter and fed as a "velocity

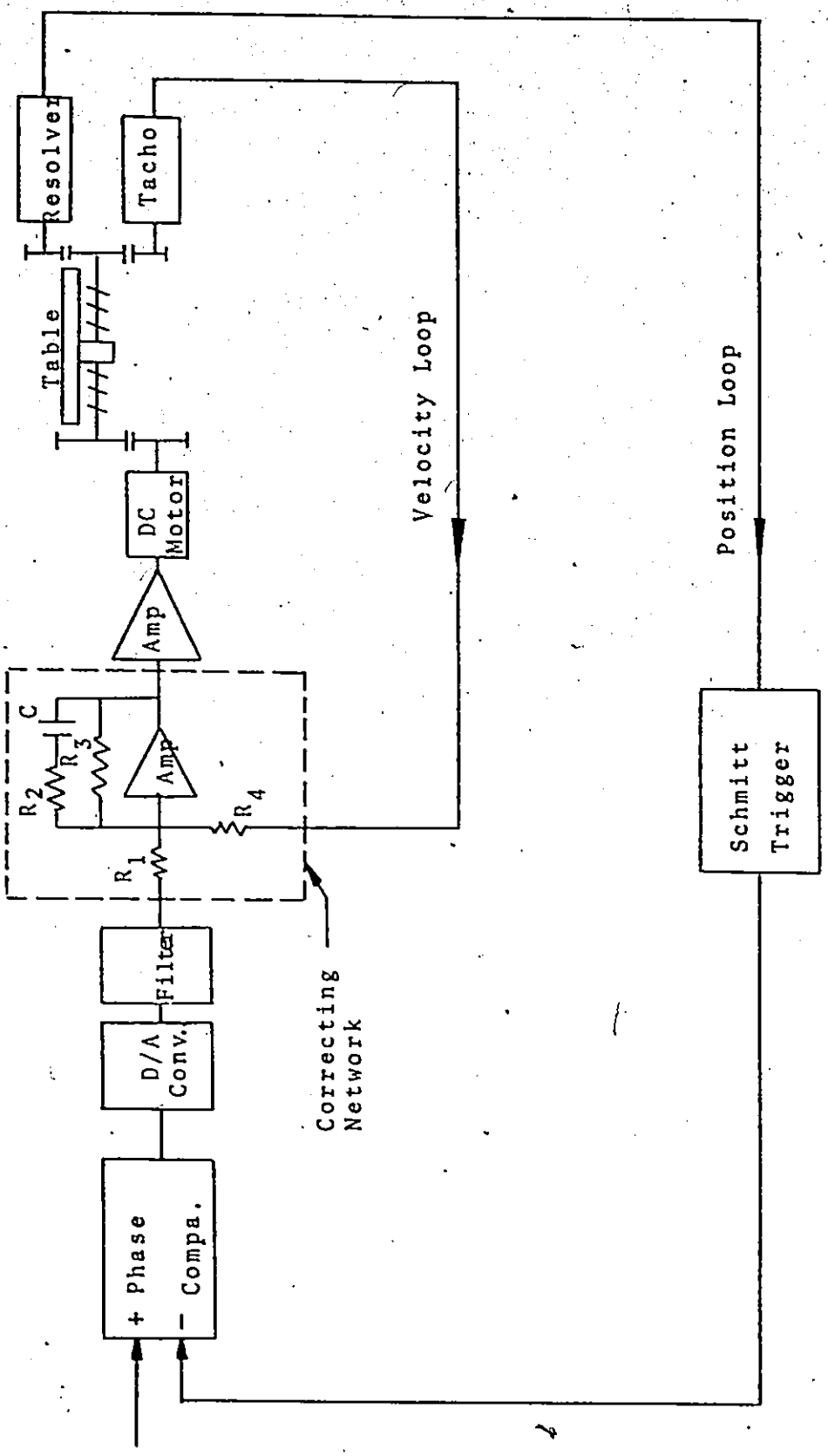

N/C BLOCK DIAGRAM

FIGURE 5

command" to a servo drive unit (SDU). The latter contains a correcting network which acts as a low-pass filter; this provides the velocity loop with a fast initial response without serious overshoot problems. The actual slide velocity indicated by a tacho generator is compared with command at the correcting circuit, thus it acts also as a summing point to the velocity loop. The transfer function of the correcting network is:

$$T(s) = \frac{R_3}{R_1}\left[\frac{1 + ScR_2}{1 + Sc(R_2+R_3}\right]$$

where R_2 = 22 KΩ and R_1 = 10 KΩ

R_3 = 2.2 MΩ and R_4 = 46 KΩ

The output of the correcting network is then amplified and used to control the servomotor. Neglecting the inductance of the armature coil, the general expression for the transfer function of the rotor excited DC motor is:

$$T(s) = \frac{Km}{1 + s\tau m}$$

The value of the motor time constant τ_m was found equal to 32 milliseconds. The motor turns the recirculating ball lead screw through a transmission ratio of 1:2.5. Both the resolver and the tachogenerator then are connected to the lead screw through a 2.5:1 gear ratio, giving both feed back devices the same speed as the servomotor. The resolver, which is considered to be basically an integrator, has a sinusoidal output. This output, is converted by a Schmidt trigger into

a pulse train.

In the analysis that follows, several simplifications were made. In general, the system was considered as a linear control system, where the phase comparator was considered as a simple summing point having no significant frequency characteristics. The time constant of the filter which is equal to 0.4 millisecond was neglected as compared with time constants elsewhere in the system. The gain in the Schmidt trigger was considered equal to unity with no significant delay or frequency characteristics. Finally, backlashe and dead zone in the mechanical part of the system were neglected. Proceeding with the classical control theory approach, each loop within the N/C controller was systematically analysed.

3.3 The Velocity Loop

Fig. 6 illustrates the block diagram of the closed velocity loop. The loop represents a second order system, having a closed loop transfer function:

$$\frac{V_t(s)}{V_c(s)} = 271.25 \left[\frac{s + 45.45}{s^2 + 94.243\ s + 2804.357}\right]$$

The transfer function of the closed velocity loop is derived in Appendix A. The open loop gain is the product of the following gains:

1. The gain of the correcting network $\frac{R_3}{R_1}$

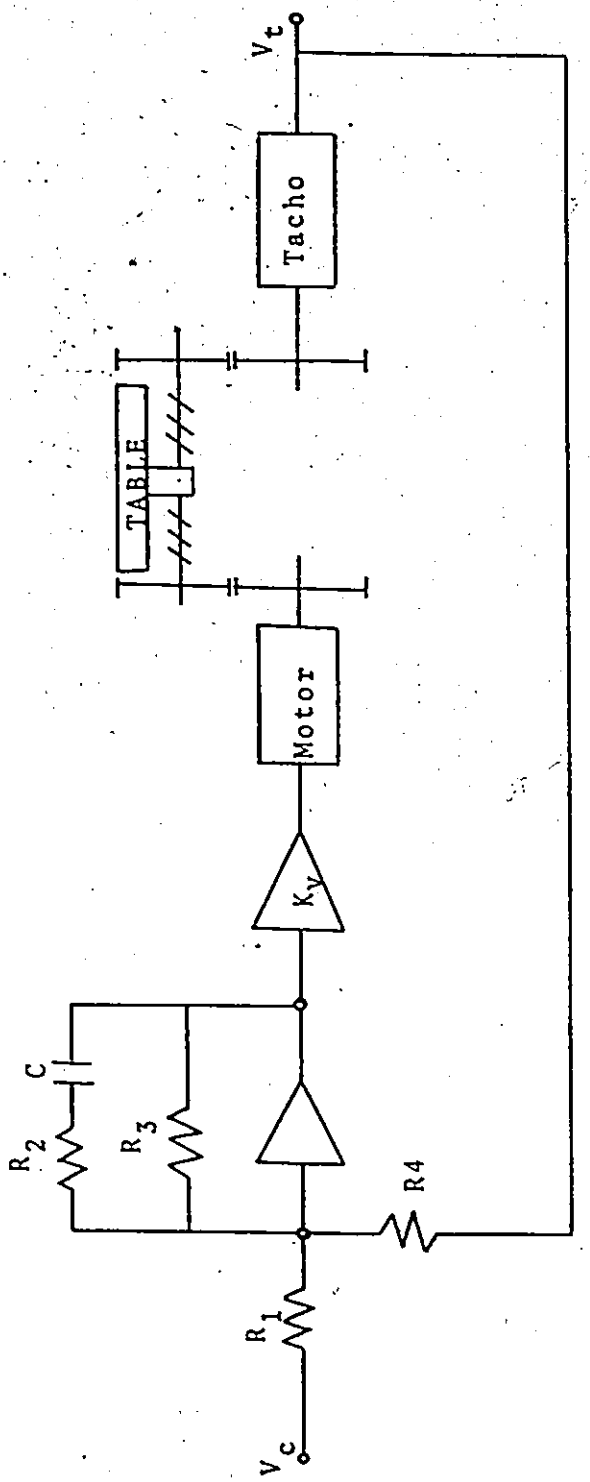

BLOCK DIAGRAM OF THE CLOSED VELOCITY LOOP

FIGURE 6

2. The power amplifier gain $K_v = 10.0$
3. The motor gain $K_m = 0.35$ rev/sec/volt
4. The tacho gain $K_T = 1.24$ volt/rev/sec
5. The velocity feed back $\frac{R_1}{R_4}$

The response of the closed velocity loop to a unit step input of 1.0 volt is:

$$V_t(t) = 4.578\ [1.0 - e^{-t/0.0208} \cos(25.159\ t) + 0.6549\ e^{-t/0.0208} \sin(25.159\ t)]$$

The derivation of the response of the closed velocity loop to a unit step input is also explained in Appendix A. This response is shown in figure 7. The time constant computed was 21 milliseconds. These results were also verified experimentally. The circuit diagram of the correcting network is shown in figure 8. Figure 9 illustrates a schematic representation of the terminal boards located in the servo drive unit which contains essentially the correcting network and amplifier for driving the servo motor. Figure 10 illustrates the arrangement used for the velocity loop measurements.

For open-loop measurement, the feed back in the loop was first disconnected by disconnecting point F of TB-107 (figure 9). A step voltage was applied to TB-107 point H by closing the switch in figure 10. The output of the tacho was recorded on a high speed U-V recorder using the arrangement shown in figure 11. The response of the

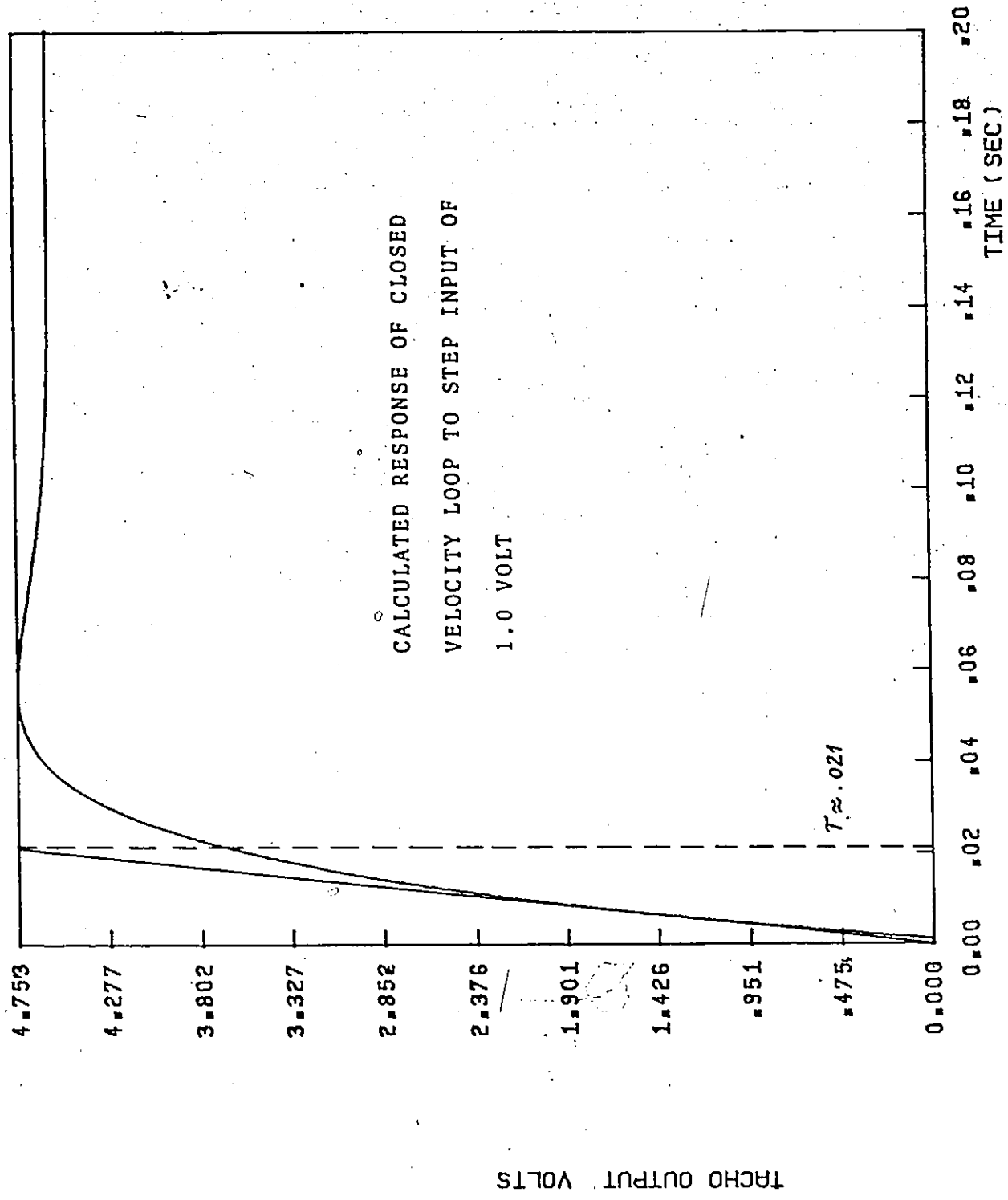
CALCULATED RESPONSE OF CLOSED
VELOCITY LOOP TO STEP INPUT OF
1.0 VOLT
$\tau \approx .021$
TACHO OUTPUT VOLTS
TIME (SEC)
4.753
4.277
3.802
3.327
2.852
2.376
1.901
1.426
.951
.475
0.000
.00
.02
.04
.06
.08
.10
.12
.14
.16
.18
.20

FIGURE 7

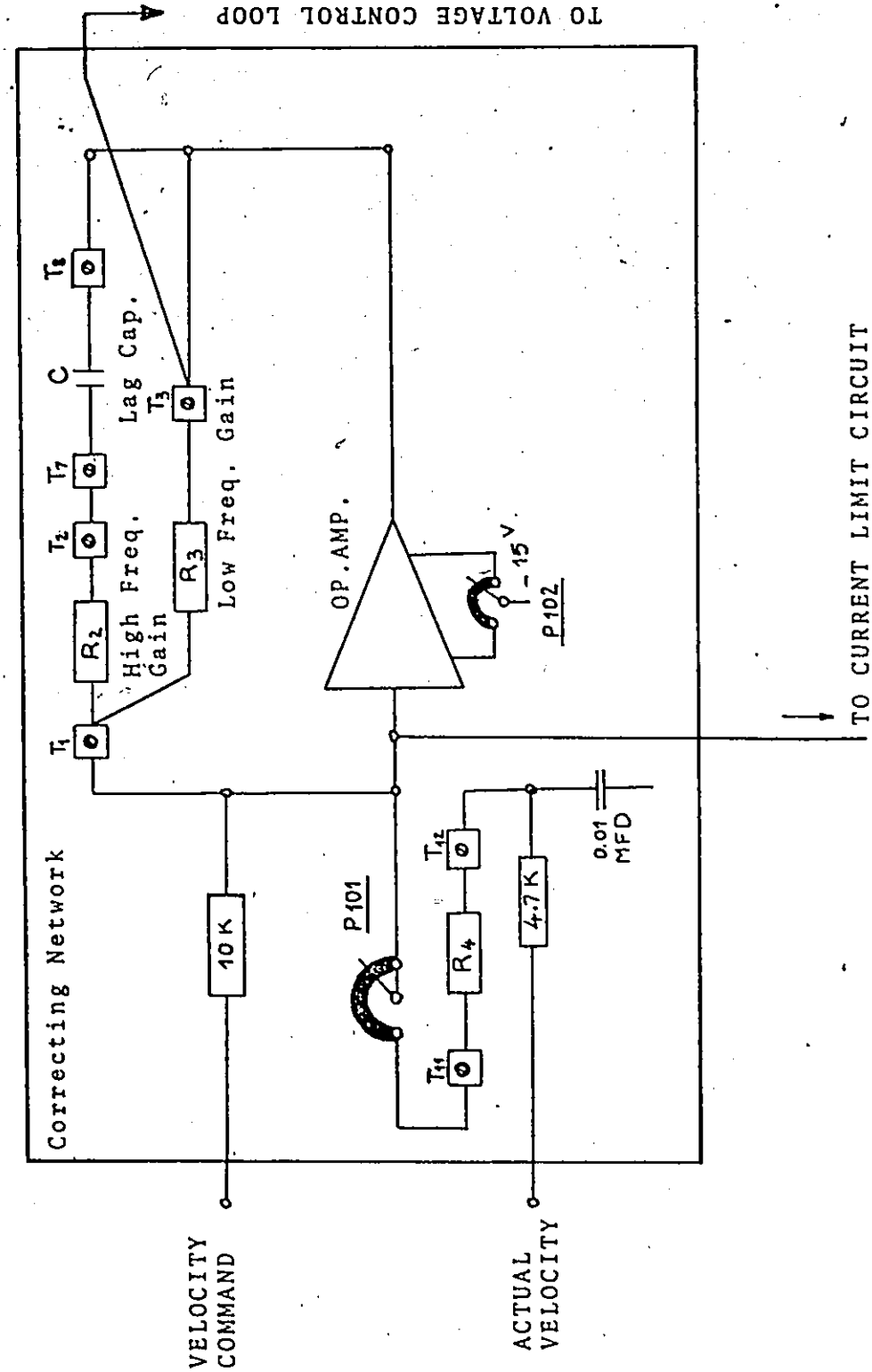

FIGURE 8

CIRCUIT DIAGRAM OF CORRECTING NETWORK

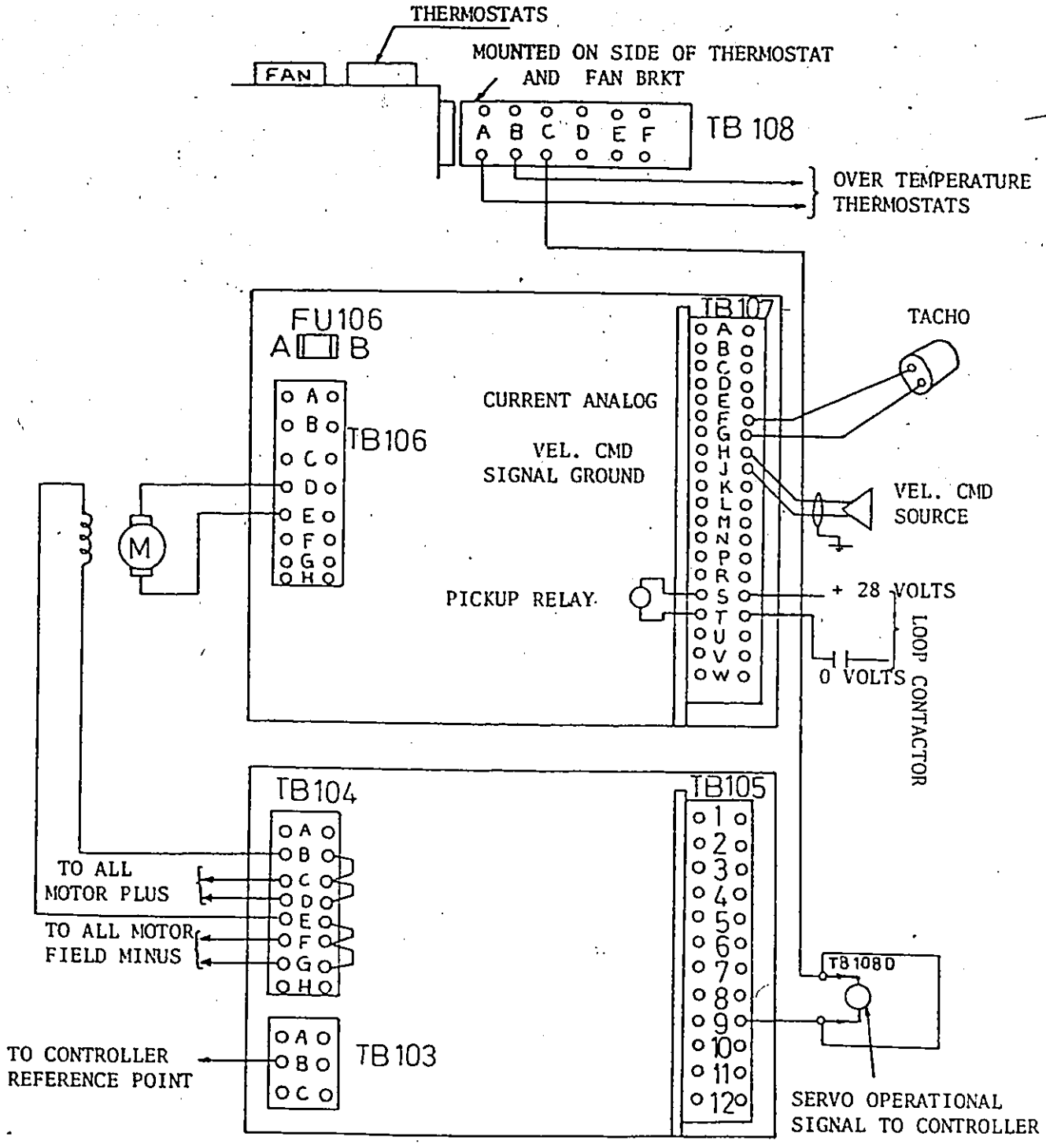

TERMINAL BOARDS SCHEMATIC REPRESENTATION

FIGURE 9

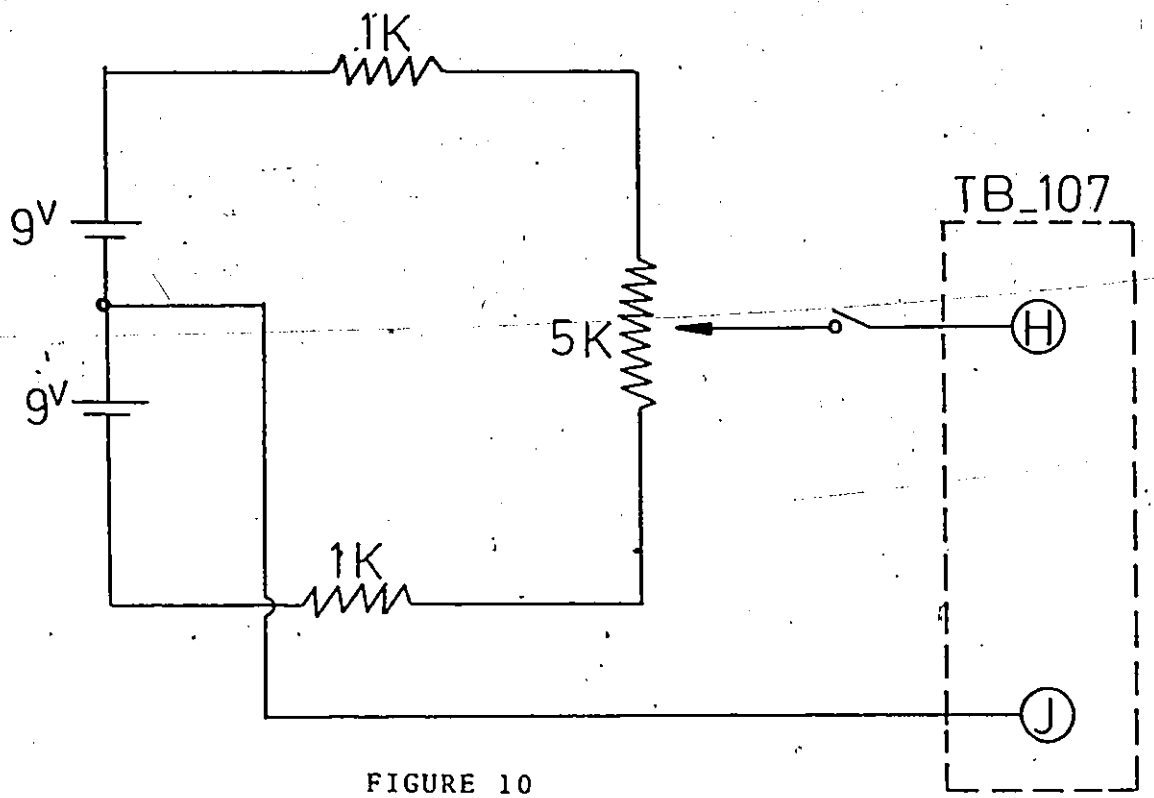

FIGURE 10

ARRANGEMENT USED FOR VELOCITY LOOP MEASUREMENTS

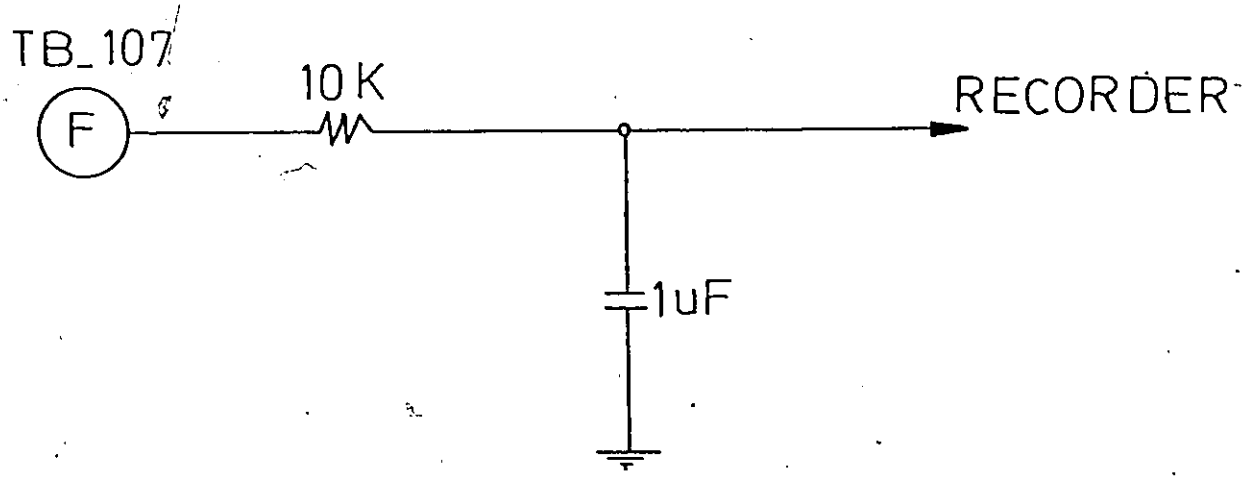

FIGURE 11

ARRANGEMENT USED FOR RECORDING THE TACHO SIGNAL

open velocity loop to a step input is shown in figure 12. The measured gain was found equal to 955.5. For closed loop measurement, point F of TB-107 was reconnected to include the tacho in the loop. A step voltage was again applied to TB-107 point H yielding the response shown in Figure 13. The measured time constant was 25 milliseconds. The results of measuring the open velocity loop gain as well as the loop time constant agreed rather well with those obtained from the computations.

The frequency characteristics of the velocity loop were next investigated both theoretically and experimentally. Experimentally, the frequency characteristics of both loops were investigated using the fourier analyzer. Again referring to figures 8, 9, 10 and 11, the open loop measurement is first considered. An impact piezo-electric transducer was used. Disconnecting point F of TB-107, a hammer was used to supply an input signal approximated as a pulse input to TB-107 point H (the circuit shown in figure 10). Both the tacho output and the input signal were fed to the Fourier Analyzer, which in turn evaluates the Fourier transforms of both signals, and produces their ratio which is the system transfer function. The magnitude of the system transfer function, as well as the phase angle are plotted over a specified range of frequencies. Figure 14 shows both the calculated and experimental frequency response of the open velocity loop. The loop has a corner

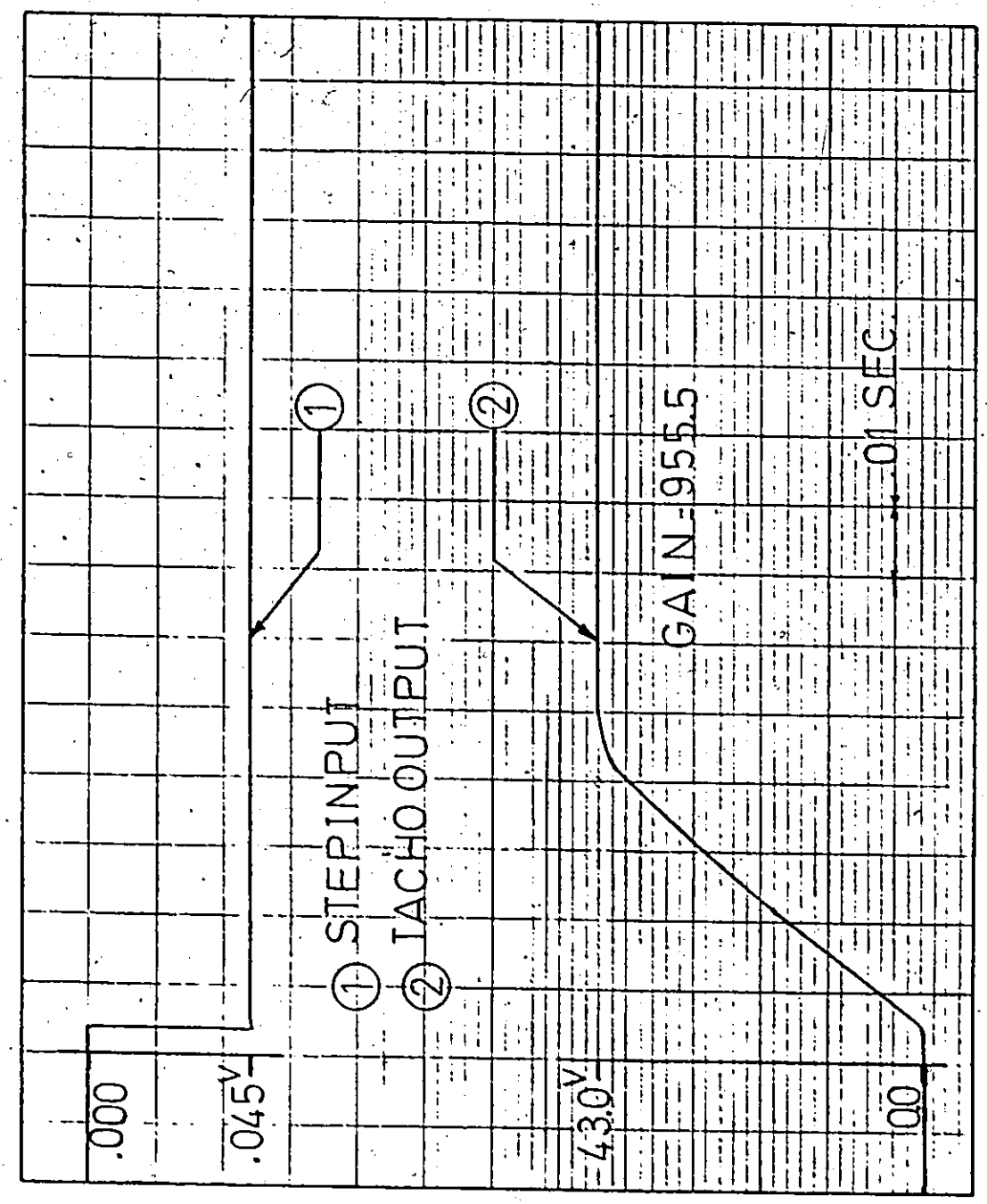

MEASURED RESPONSE OF THE OPEN VELOCITY LOOP TO A STEP INPUT

FIGURE 12

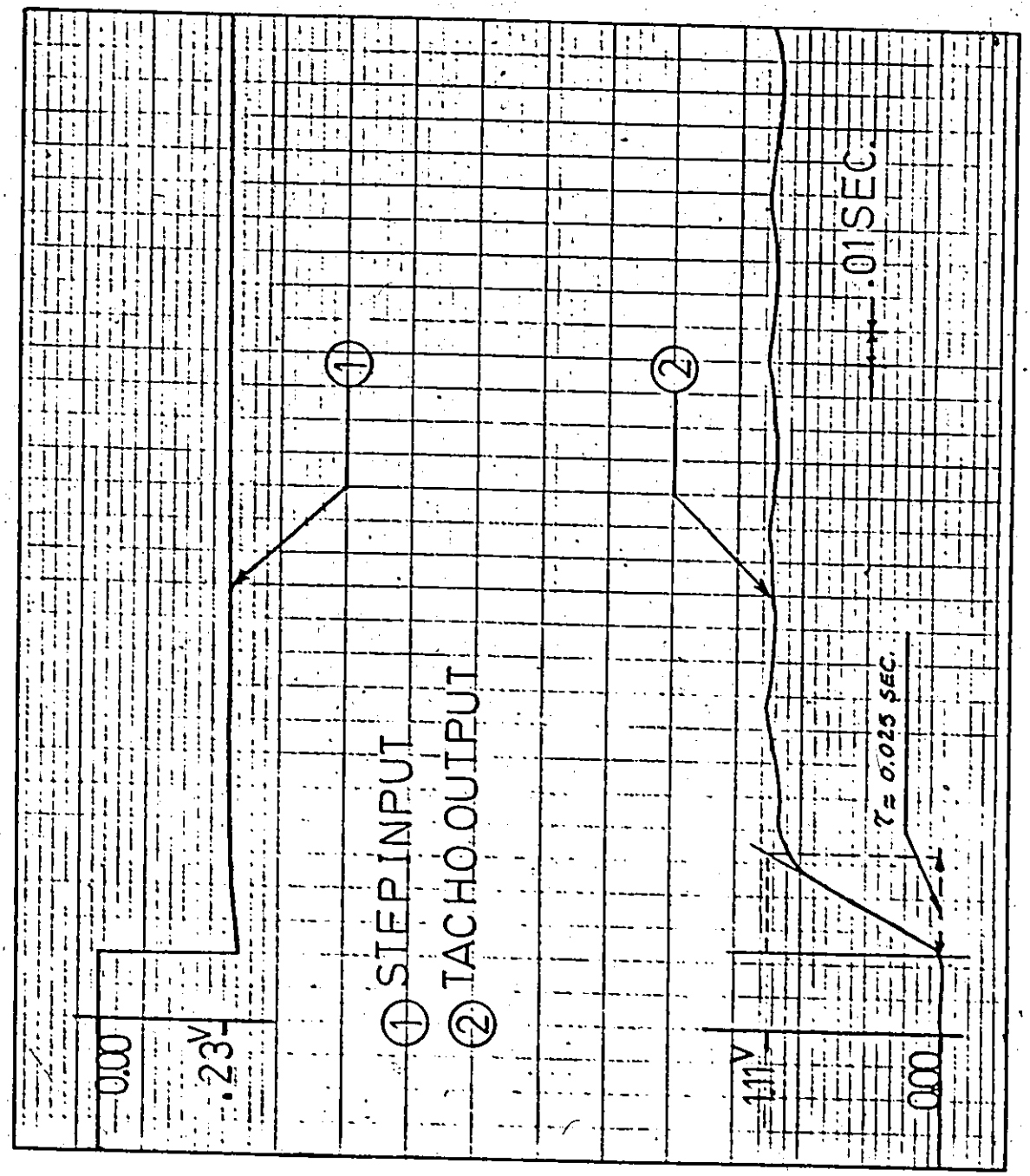

MEASURED RESPONSE OF THE CLOSED VELOCITY LOOP TO A STEP INPUT

FIGURE 13

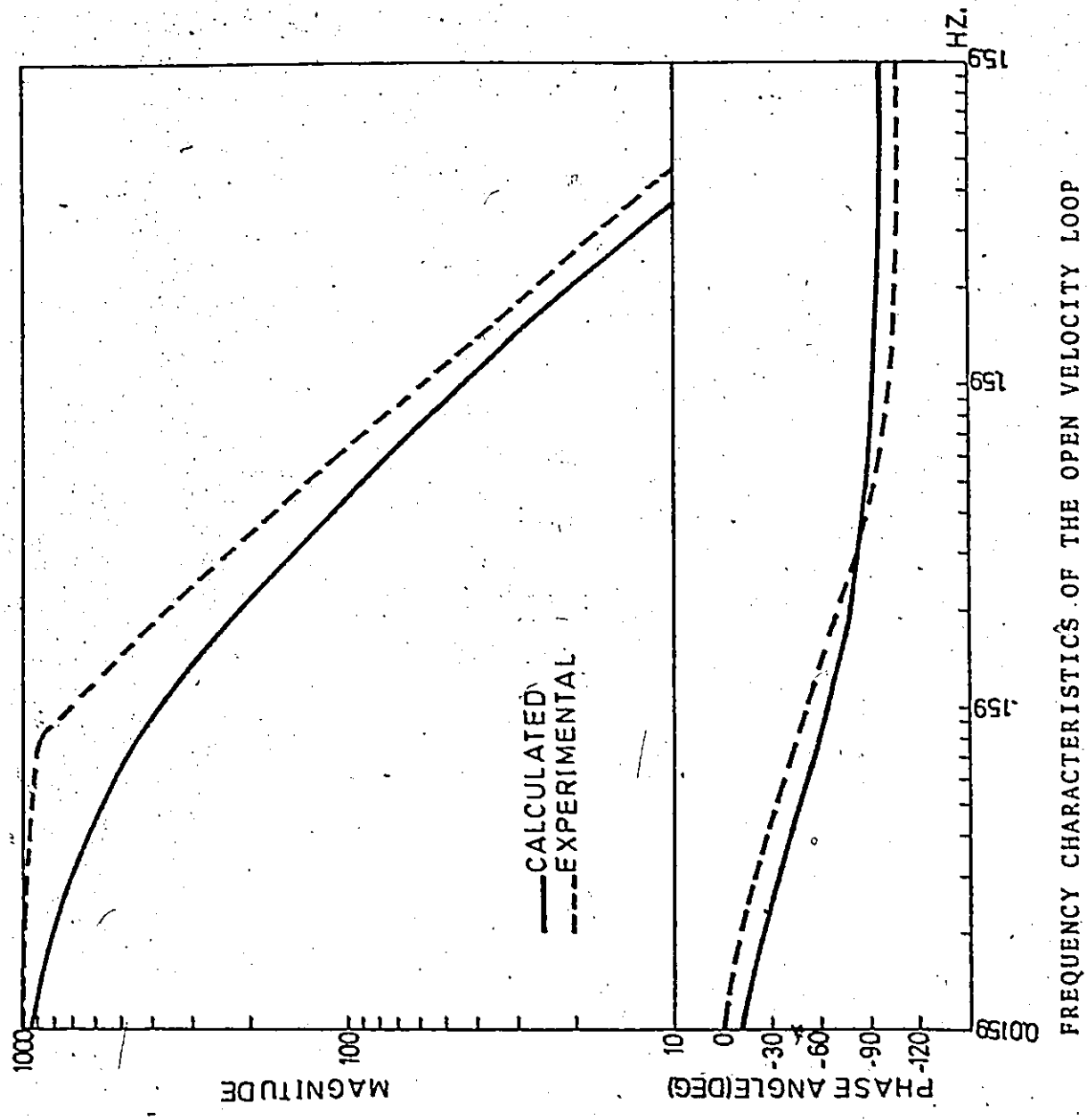

FREQUENCY CHARACTERISTICS OF THE OPEN VELOCITY LOOP

FIGURE 14

frequency at 0.07 H_z, while its calculated natural frequency is equal to 8.610 H_z.

Experimentations with the closed velocity loop are next discussed. Reconnecting point F of TB-107 (i.e. the tacho in the loop), a pulse input is applied to TB-107 point H in the same manner described previously for the open loop measurements. Again both the pulse input and the tacho output were fed to the fourier analyzer to evaluate the system transfer function. Figure 15 shows both the calculated and experimental frequency response of the closed velocity loop. The root locus technique was next used in order to further investigate the transient behaviour of this loop and the effect of changing the gain on its overall performance. Figure 16 shows the root locus plot for the velocity loop. Two roots govern the transient behaviour of this loop, the first starts at - 0.45 where K = 0, the second at - 21.25. At - 20.172 the two roots leave the real axis, follow the circular path shown in the figure, and breaking into the real axis again at - 70.728. Finally one of the roots ends at point - 45.45 where K is infinity, while the other one follows the real axis to infinity. It should be noted that K is the product of both the gain of the feed forward elements in the loop K_1 and K_2 the gain of the feed back element. Obviously, increasing the open loop gain results in a faster response of the loop. However, as seen from the root locus plot, increasing the

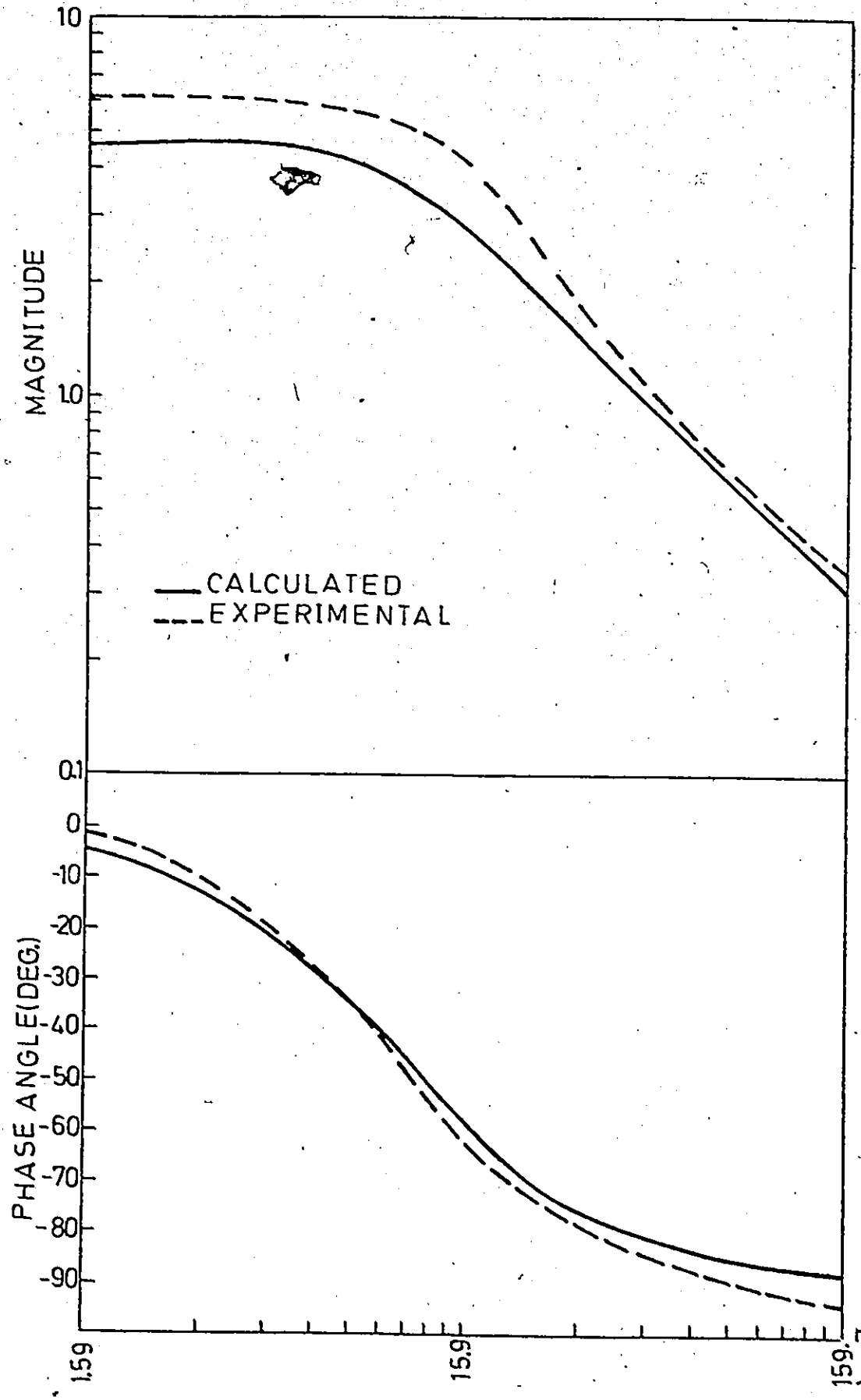

FREQUENCY CHARACTERISTICS OF THE CLOSED VELOCITY LOOP

FIGURE 15

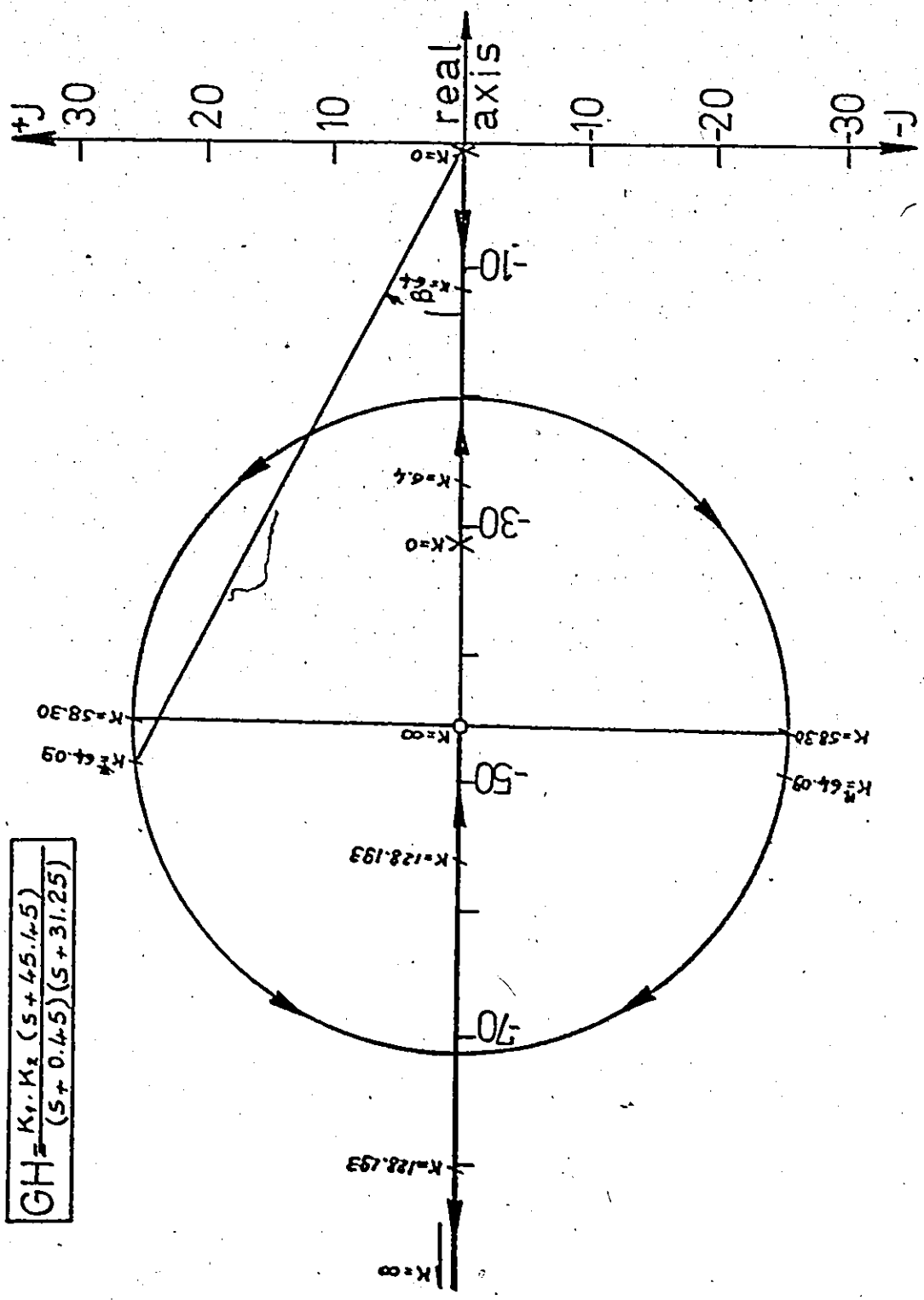

ROOT LOCUS PLOT OF THE VELOCITY LOOP

FIGURE 16

open loop gain tends also to increase the damping factor ξ in the loop. This is due to the fact that increasing K decrease the angle β (figure 16) and accordingly increase ξ. However, the present value of ξ in the loop is 0.885 which is considered quite reasonable for most practical applications. As far as the question of stability is concerned, the loop is seen to be quite stable since the root locus never crosses the imaginary axis of the plot.

3.3.1 Current Limit Circuit

The previous section explains how the velocity loop operational amplifier circuitry referred to as the "correcting network" involves summation of input signal, gain function, and a servo stabilizing network. "Velocity command" and "actual velocity" analog signals are summed to generate an error signal. The error signal is amplified and applied to the D-C motor as the voltage command signal. The third input to the operational amplifier is from the current limit circuitry shown in figure 17 which modifies the velocity command to effect current limit.

The operation of the current limit circuitry is further explained in the following manner. An armature current sensor, which is basically a differential amplifier, senses a differential voltage across a resistor in series with the motor armature. The output known as "current analog" is used to overcome a threshold of a fixed level and injects

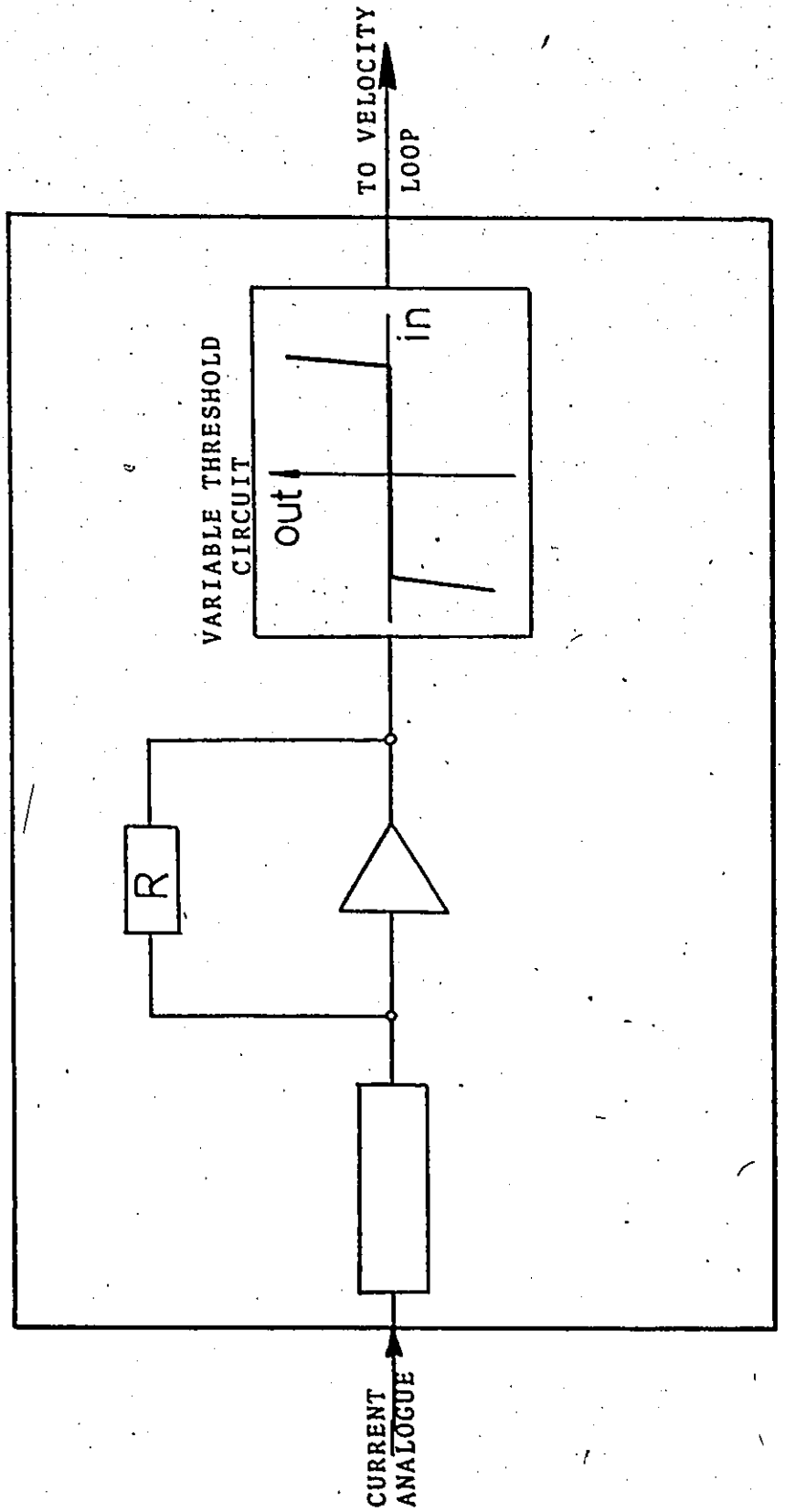
TO VELOCITY LOOP
VARIABLE THRESHOLD CIRCUIT
in
out
R
CURRENT LIMIT CIRCUIT
CURRENT ANALOGUE

FIGURE 17

a signal into a velocity loop input terminal. This injected signal modifies the velocity command in such a way as to effect current limit. To conclude the current limit circuitry does not allow the armature current to exceed a certain limit, and accordingly there exists a maximum armature current value. And as a result, there exists also a limit on the acceleration of the existing feed drives. The influence of the current limit on the overall performance of the system will be investigated later in this chapter.

Experimentations were conducted in order to determine the limit of the current analog. Again referring to figures 4, 5, 6 and 7, a step voltage was applied to TB-107 point H. It should be noted here that these measurements were conducted with the velocity loop closed i.e. the tacho in the loop. Varying the magnitude of the step voltage, the input signal, the tacho output and the current analog signal were recorded for each step.

In order to ensure a step input applied to the motor circuit a jumper was placed across the lag capacitor of the correcting network. Accordingly, the operation of the operational amplifier of the correcting network is now restricted to a simple multiplier having a gain of 2.2.

Figure 18 shows the response of the closed velocity loop to a step input of 200 millivolts. As previously mentioned, the input signal, the tacho output and the

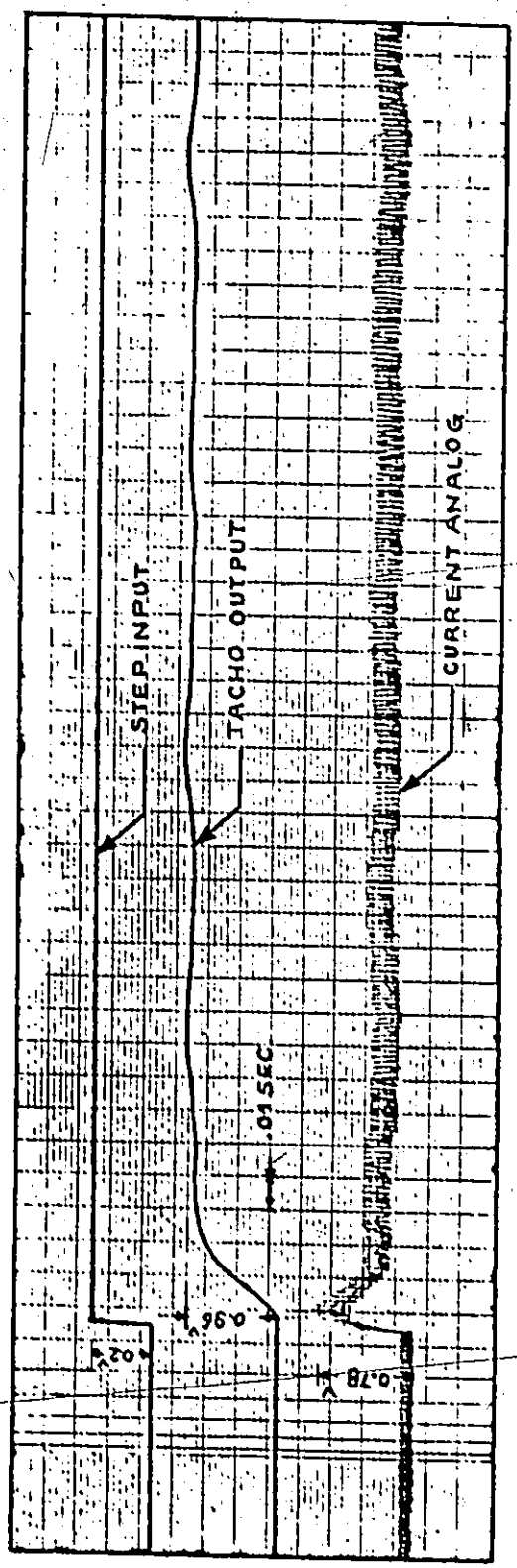

MEASURED RESPONSE OF THE CLOSED VELOCITY LOOP TO A STEP INPUT

FIGURE 18

current analog signal were recorded using a high speed U-V recorder. The current analog signal reaches its peak value almost immediately after applying the step. With no back electro motive force developed yet in the motor circuit, only the time constant of the armature winding is active. However, as seen from the figure, this time constant is negligibly small. The magnitude of the peak value of the current analog signal is in fact an indication of the amount of acceleration of the feed drive. Following this peak, and as a result of the rotation of the motor, a back e.m.f. start developing in the motor circuit. The magnitude of the current analog signal decreases and approaches a constant value, this is when the tacho output reaches its maximum value. Repeating the test with larger step inputs, the peak of the current analog signal increases and accordingly the acceleration of the feed drive. This is clearly shown in figure 19 where a step input of 750 millivolts is applied to the velocity loop. In figures 20, 21 and 22 the results obtained input steps of 1.0, 1.4 and 1.6 volt are shown respectively. It is clearly seen that starting with a step input of 1.0 volt the magnitude of the peak value of the current analog is always constant. This value was measured equal to 3.49 volts and it is then considered as the limit value of the current analog.

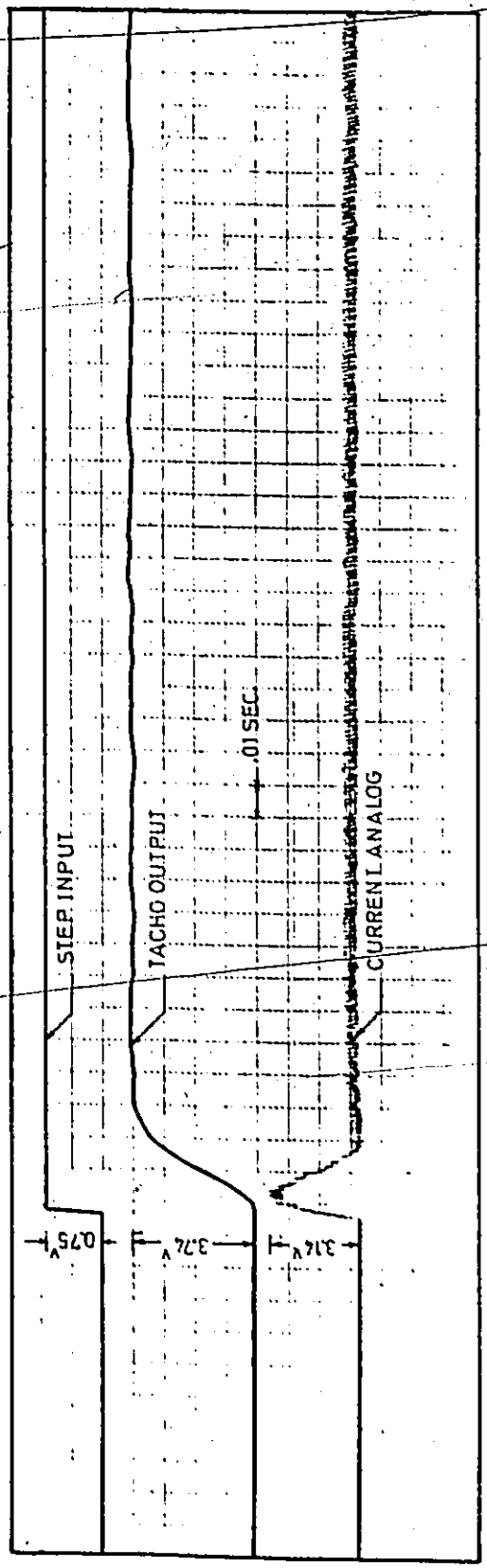

MEASURED RESPONSE OF THE CLOSED VELOCITY LOOP TO A STEP INPUT

FIGURE 19

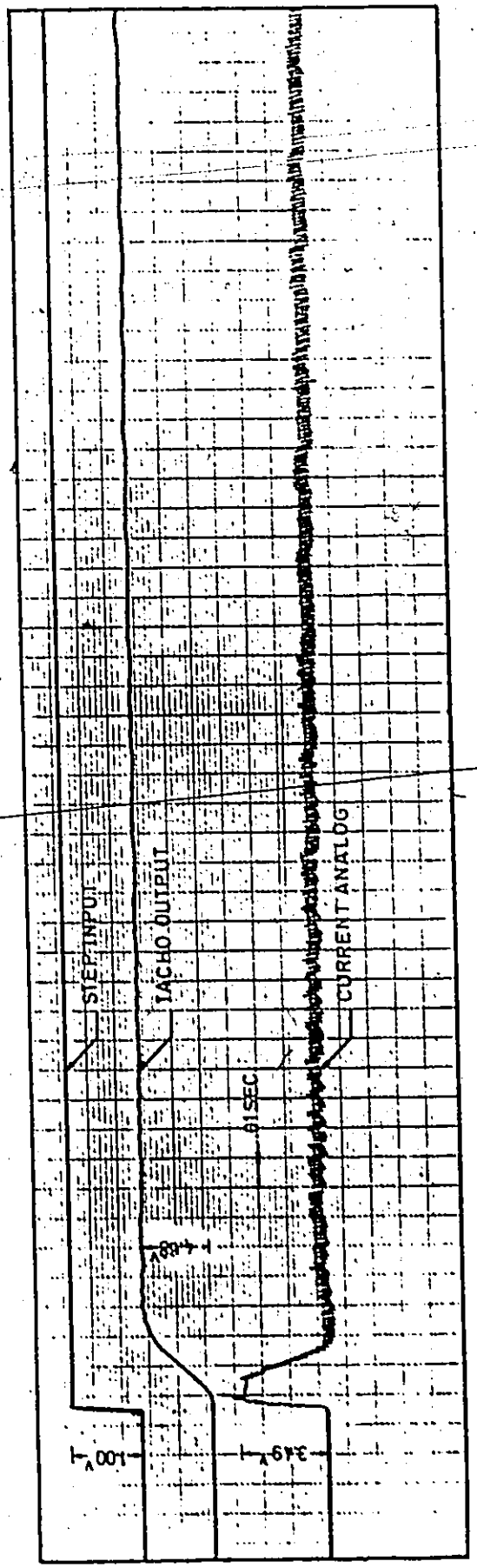

MEASURED RESPONSE OF THE CLOSED VELOCITY LOOP TO A STEP INPUT

FIGURE 20

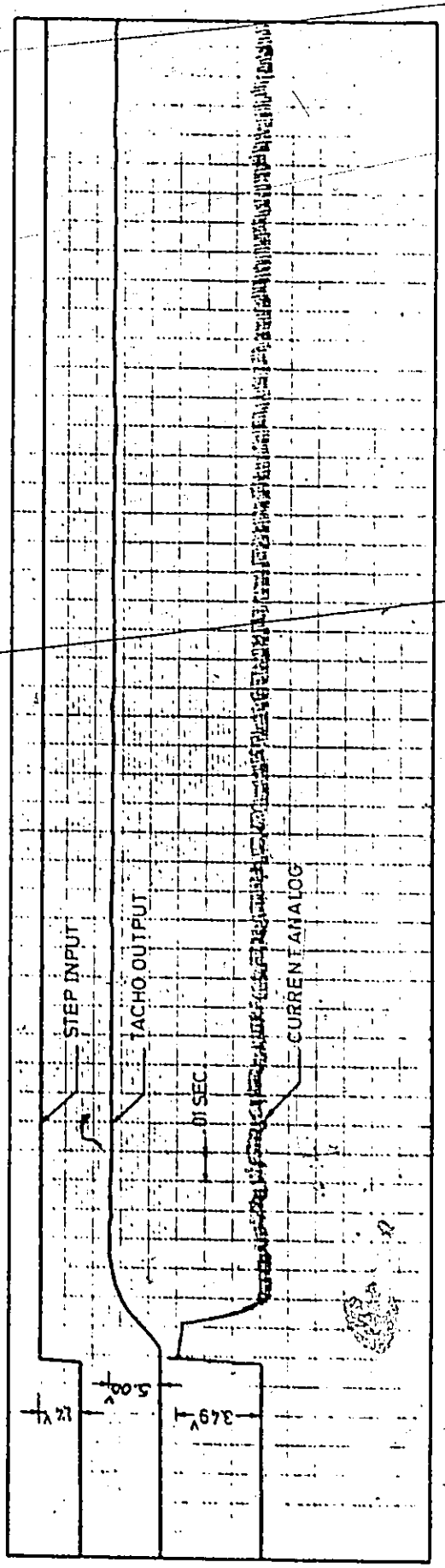

MEASURED RESPONSE OF THE CLOSED VELOCITY LOOP TO A STEP INPUT

FIGURE 21

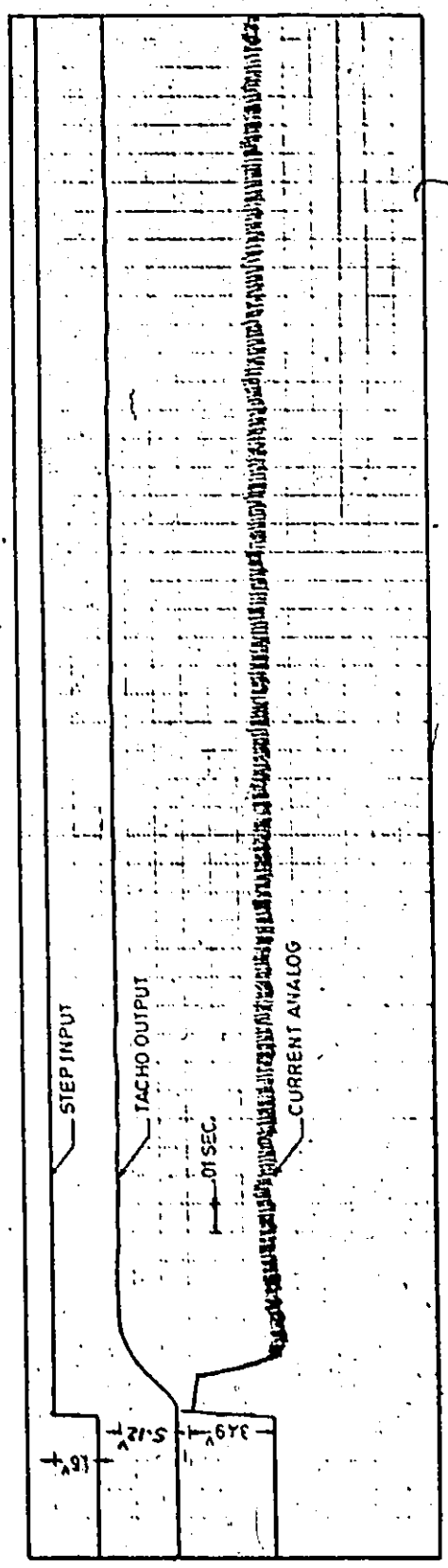

FIGURE 22

MEASURED RESPONSE OF THE CLOSED VELOCITY LOOP TO A STEP INPUT

3.4 The Position Loop

Figure 23 shows a simplified block diagram of the loop. A major problem in the design of control systems is that of providing a system which meets the requirements of both accuracy and stability. Higher accuracies require higher gain factors, but on the other hand, the high gain may cause instability, or at least increase the overshoots. The transfer function of the closed position loop is:

$$\frac{Y(s)}{X(s)} = 1071.932\left[\frac{(s+45.45)}{(s+19.27)(s^2+76.67s+2528.23)}\right]$$

The loop represents a third order system, having a unity feed back. The response of the loop to a step input of 1.0 inch as seen from the resolver output is:

$$Y(t) = 0.999[1.0-1.0246\ e^{-t/0.0518} + 0.02467\ e^{-t/0.026}\cos(32.537\ t) - 0.5764\ e^{-t/0.026}\sin(32.537\ t)] \quad (3.1)$$

and, as seen from the tacho output:

$$V_t(t) = 244.74[e^{-t/0.0518} - e^{-t/0.026}\cos(32.537\ t) + 1.082\ e^{-t/0.026}\sin(32.537\ t)] \quad (3.2)$$

The derivation of these responses is given in detail in appendix B. The resolver and the tacho responses to a unity step input as calculated from equations (3.1) and (3.2) are shown in figures 24 and 25 respectively. The prevalent time constant observed is equal to 96 milliseconds. For experimental investigation it is not possible to apply

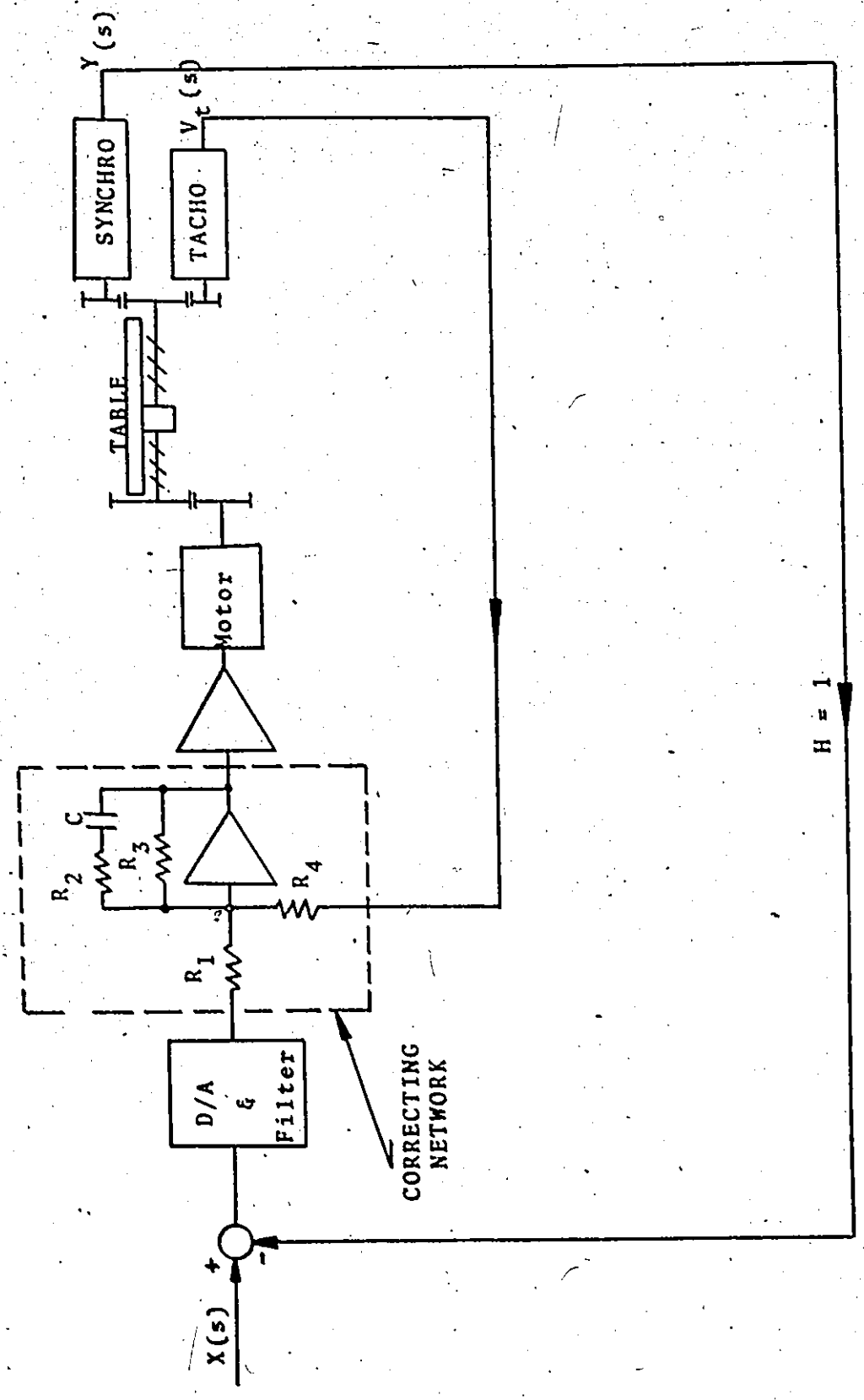

SIMPLIFIED BLOCK DIAGRAM OF THE CLOSED POSITION LOOP

FIGURE 23

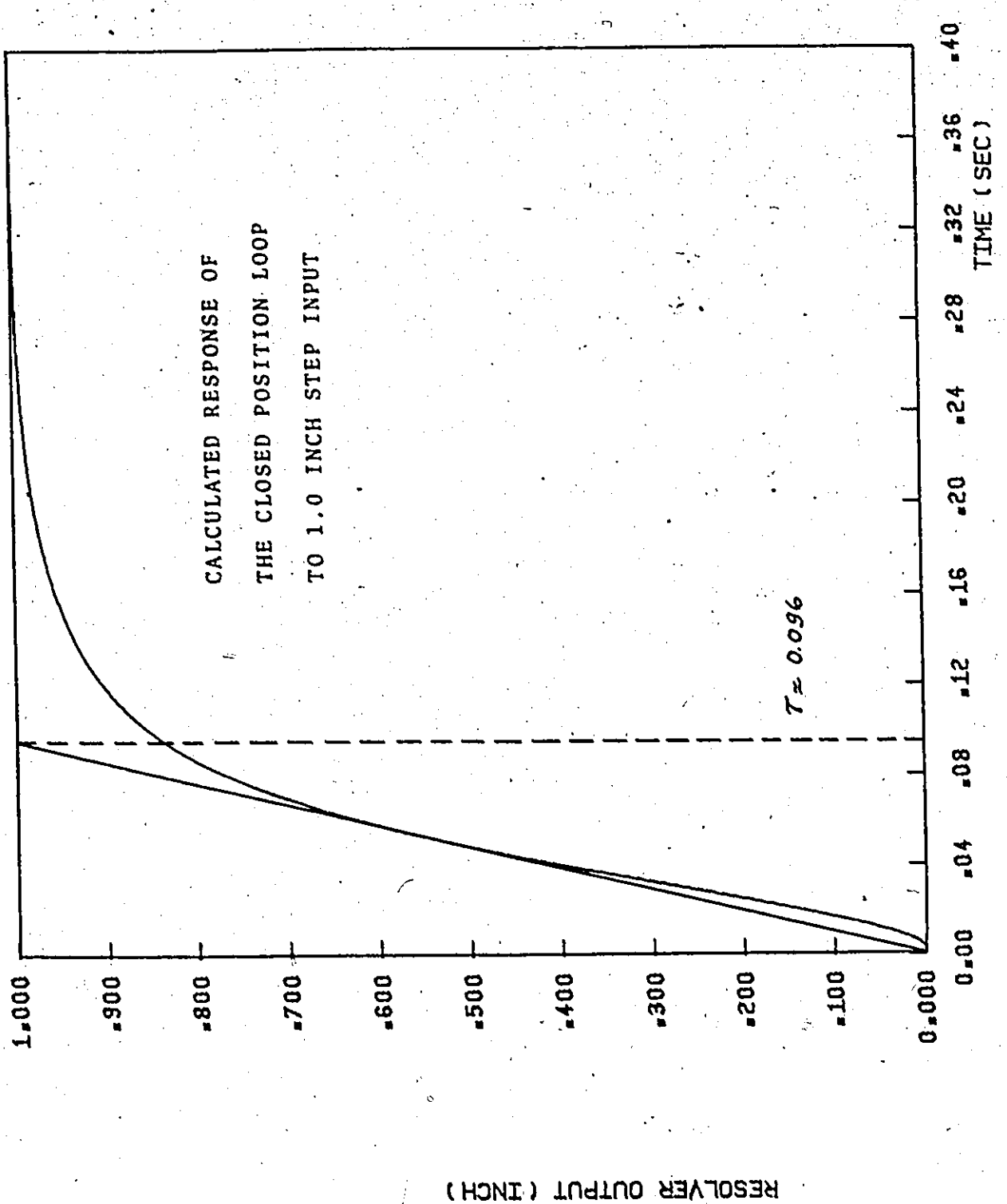
CALCULATED RESPONSE OF
THE CLOSED POSITION LOOP
TO 1.0 INCH STEP INPUT
T≈ 0.096
RESOLVER OUTPUT (INCH)
TIME (SEC)
1.000
.900
.800
.700
.600
.500
.400
.300
.200
.100
0.000
0.00
.04
.08
.12
.16
.20
.24
.28
.32
.36
.40

FIGURE 24

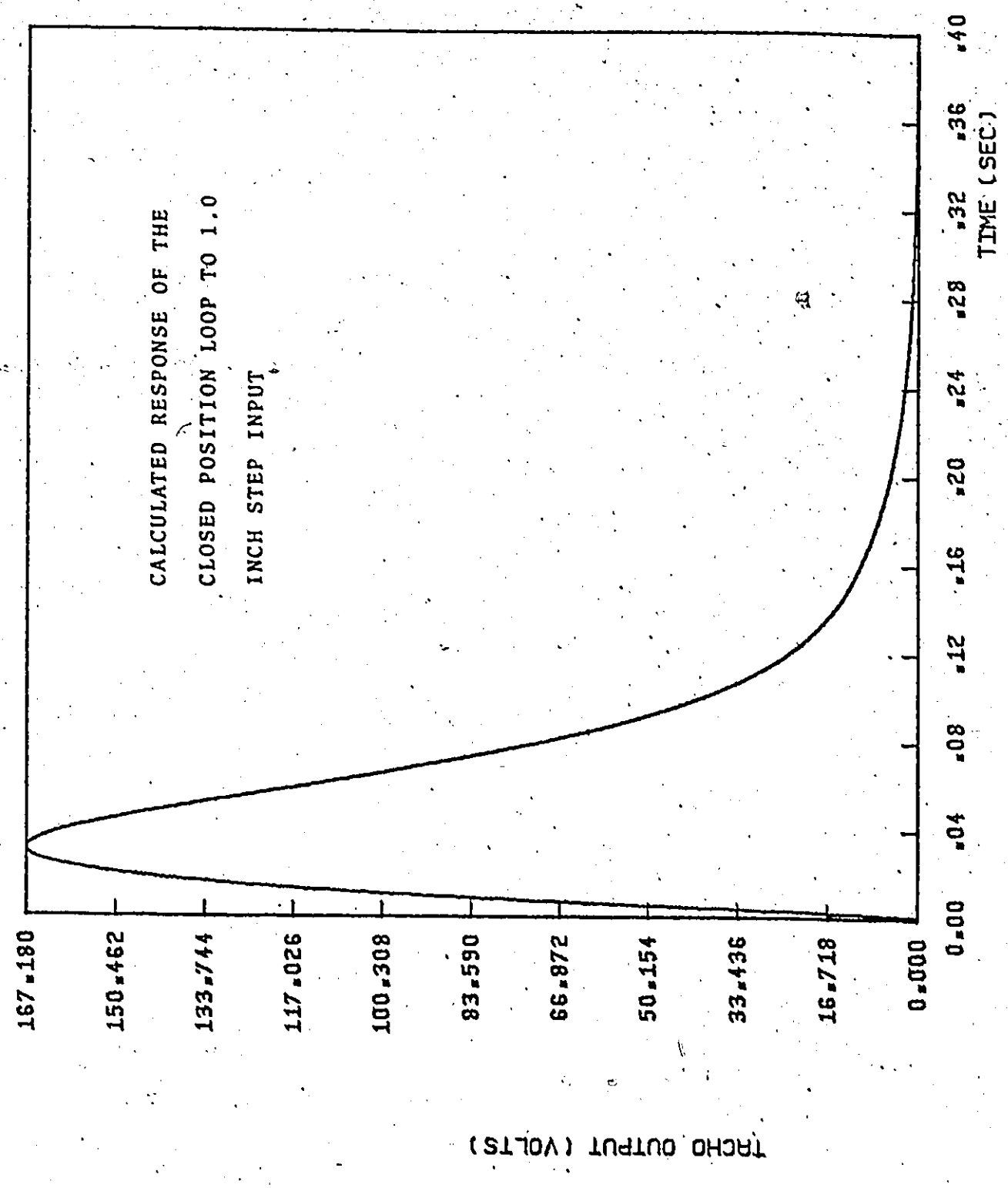
CALCULATED RESPONSE OF THE
CLOSED POSITION LOOP TO 1.0
INCH STEP INPUT
TACHO OUTPUT (VOLTS)
167.180
150.462
133.744
117.026
100.308
83.590
66.872
50.154
33.436
16.718
0.000
0.00
.04
.08
.12
.16
.20
.24
.28
.32
.36
.40
TIME (SEC)

FIGURE 25

strictly a positional step input. The actual N/C system can supply a distance command only over a finite time. Although a step input command equal to one basic length unit (0.0001 inch) which is the system resolution could be applied, but in such a case, factors not included in the model such as static friction in the guide ways and windup in the lead screw may easily distort the response. An input which the actual system is capable of supplying is a ramp input.

The response of the N/C loop to a ramp input shown in figure 26 and described by:

$f(t) = 0.5t$ inch for $0 < t < t_1$

and $f(t) = 0.01$ inch for $t_1 < t < \infty$

where $t_1 = 0.02$ sec

as seen from the tacho output is:

$$V_t(t) = 6.201 - 6.349\, e^{-t/0.0519} + 0.148\, e^{-t/0.026} \cos (32.537\, t) - 3.58\, e^{-t/0.026} \sin (32.537\, t) - \{6.201 - 6.349\, e^{-(t-0.02/0.0519} + 0.148\, e^{-(t-0.02)/0.026} \cos [32.537\,(t-0.02)] - 3.58\, e^{-(t-0.02)/0.026} \sin [32.537\,(t-0.02)]\} \qquad (3.3)$$

The derivation of the above response is discussed in appendix C. Figures 27 and 28 show the resolver and the tacho outputs for the above mentioned ramp input as calculated from equation (3.3). The response of the tacho to such a ramp input was also verified experimentally.

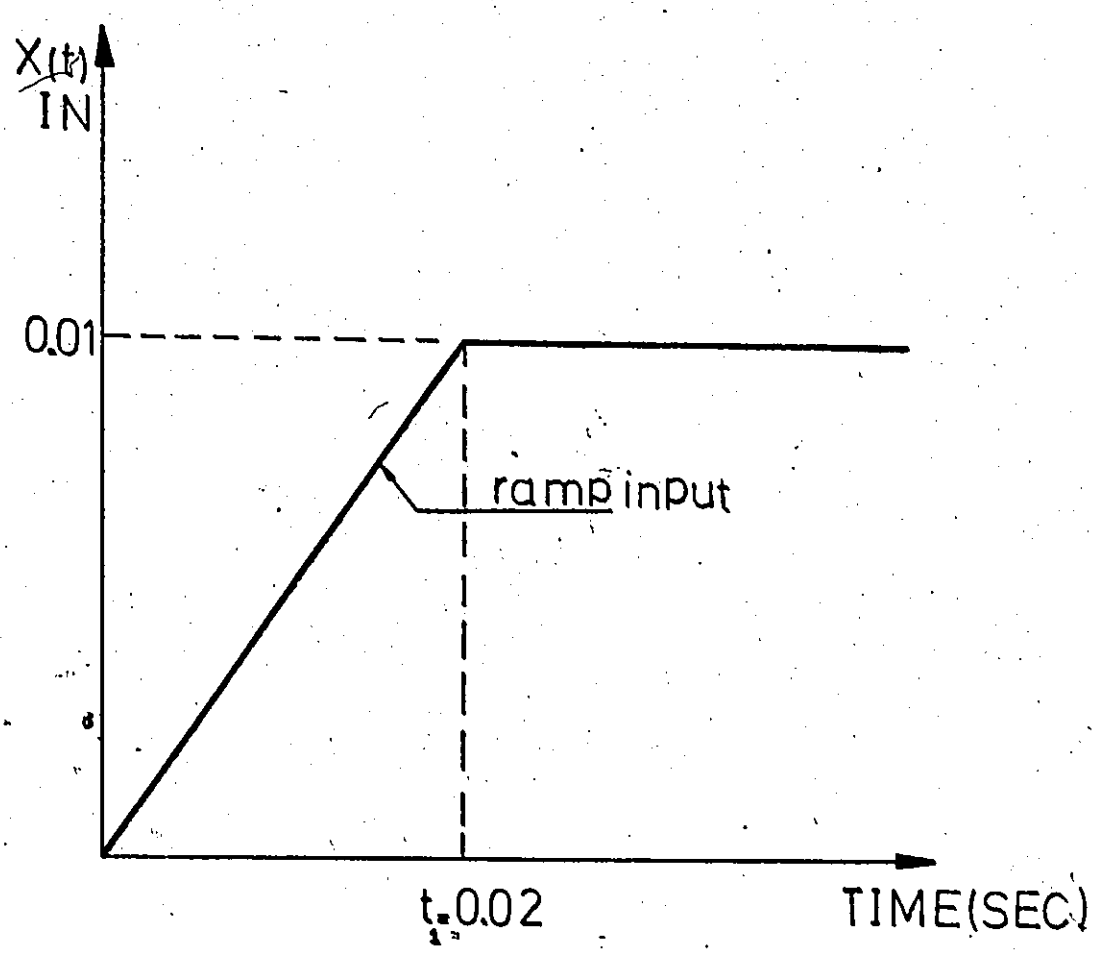

FIGURE 26

RAMP APPLIED TO THE CLOSED POSITION LOOP

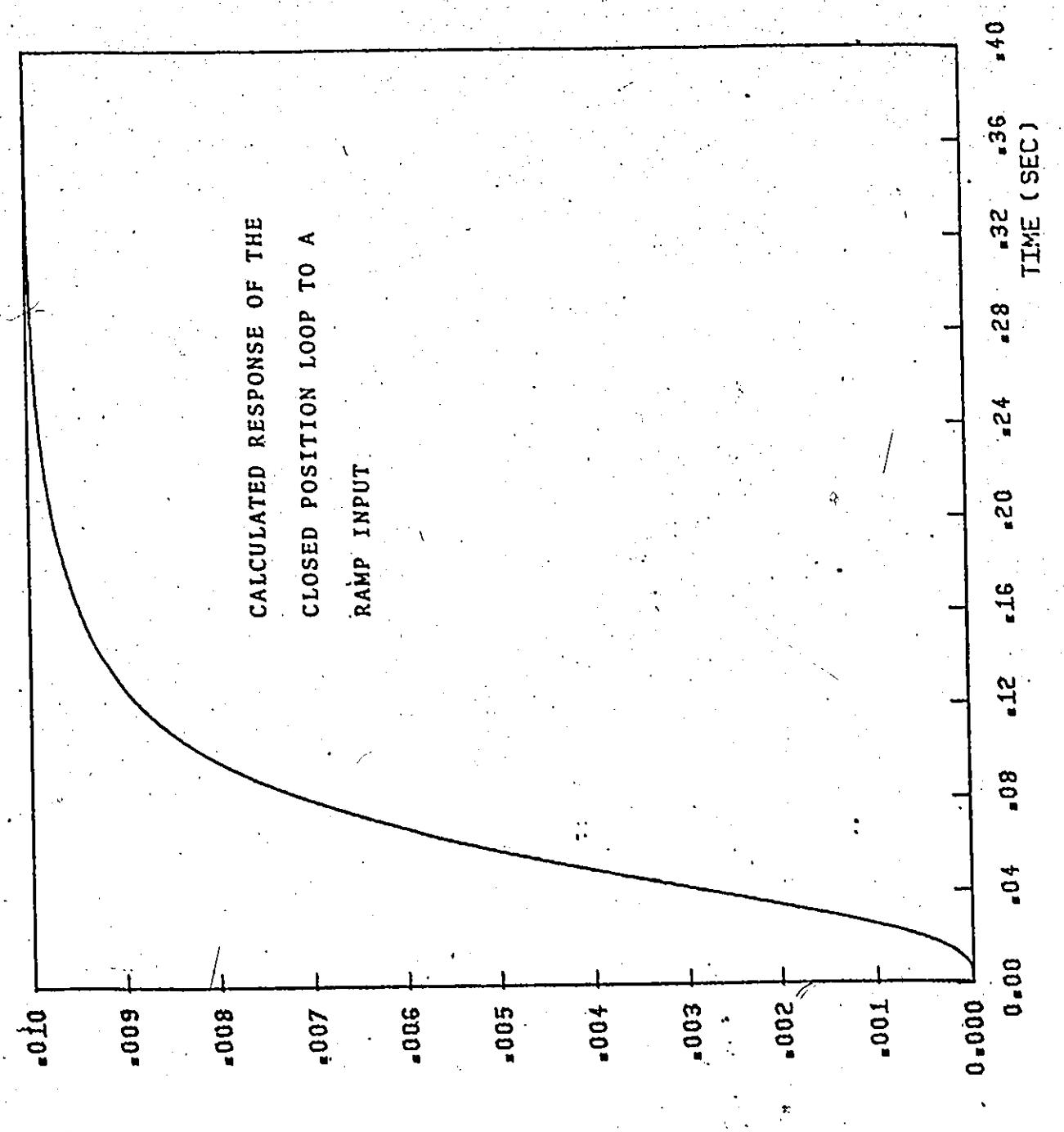
CALCULATED RESPONSE OF THE
CLOSED POSITION LOOP TO A
RAMP INPUT
RESOLVER OUTPUT (INCH)
TIME (SEC)
0.000
.001
.002
.003
.004
.005
.006
.007
.008
.009
.010
0.00
.04
.08
.12
.16
.20
.24
.28
.32
.36
.40

FIGURE 27

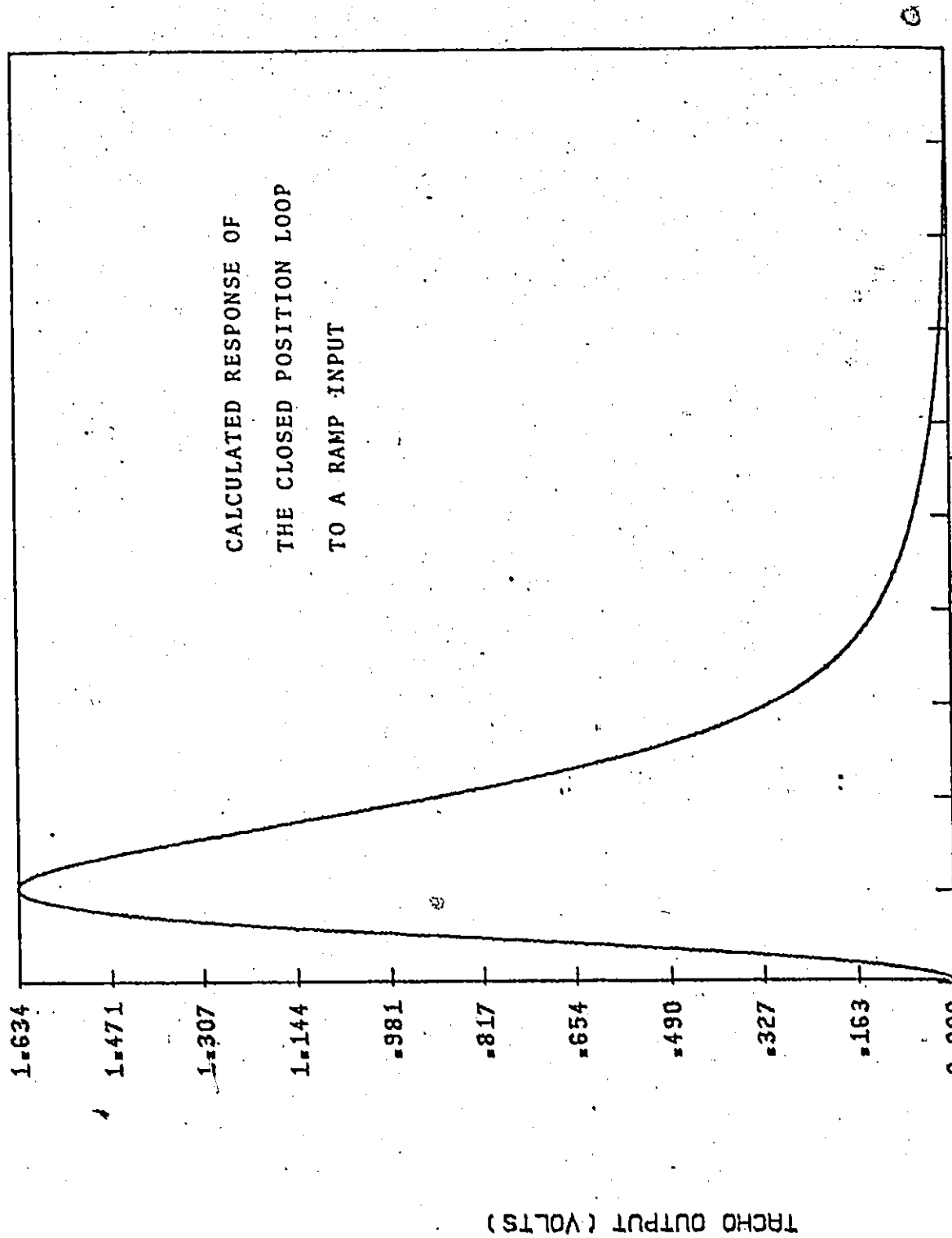
CALCULATED RESPONSE OF
THE CLOSED POSITION LOOP
TO A RAMP INPUT
TACHO OUTPUT (VOLTS)
TIME (SEC)
1.634
1.471
1.307
1.144
.981
.817
.654
.490
.327
.163
0.000
0.00
.04
.08
.12
.16
.20
.24
.28
.32
.36
.40

FIGURE 28

Programming a distance of 0.01 inch at a feed rate of 30 inch/min results in the ramp input described previously. The tacho output was recorded using a high speed U-V recorder. The result is shown in figure 29. The result of the measurement is seen to agree rather well with the computations. Both figures showed a peak voltage of approximately 1.6 volt reached after 60 milliseconds.

The frequency characteristics of the position loop were next investigated. Figure 30 shows the frequency response plot for the open position loop both as calculated and experimentally. In order to experimentally investigate the frequency characteristics of the open position loop, the loop was opened just before the correcting network (i.e. disconnecting point H of TB-107 in figure 9). A pulse input was supplied to the correcting network using a piezo-electric transducer in the manner described for the velocity loop measurements. Both the input signal and the output of the D/A convertor and filter measured at point H* on TB-107 were fed to the Fourier analyzer. It is immediately evident from the examination of the open loop frequency characteristics that the system is always stable since the phase shift never exceeds - 180^{o}.

It is of course, fair to comment that these calculations relate to a system which is idealized as compared

---

* Point H on TB-107 (figure 9) receives the output of the D/A convertor and filter located in the N/C controller and acts as an input to the velocity loop.

MEASURED RESPONSE OF THE POSITION LOOP TO A RAMP INPUT

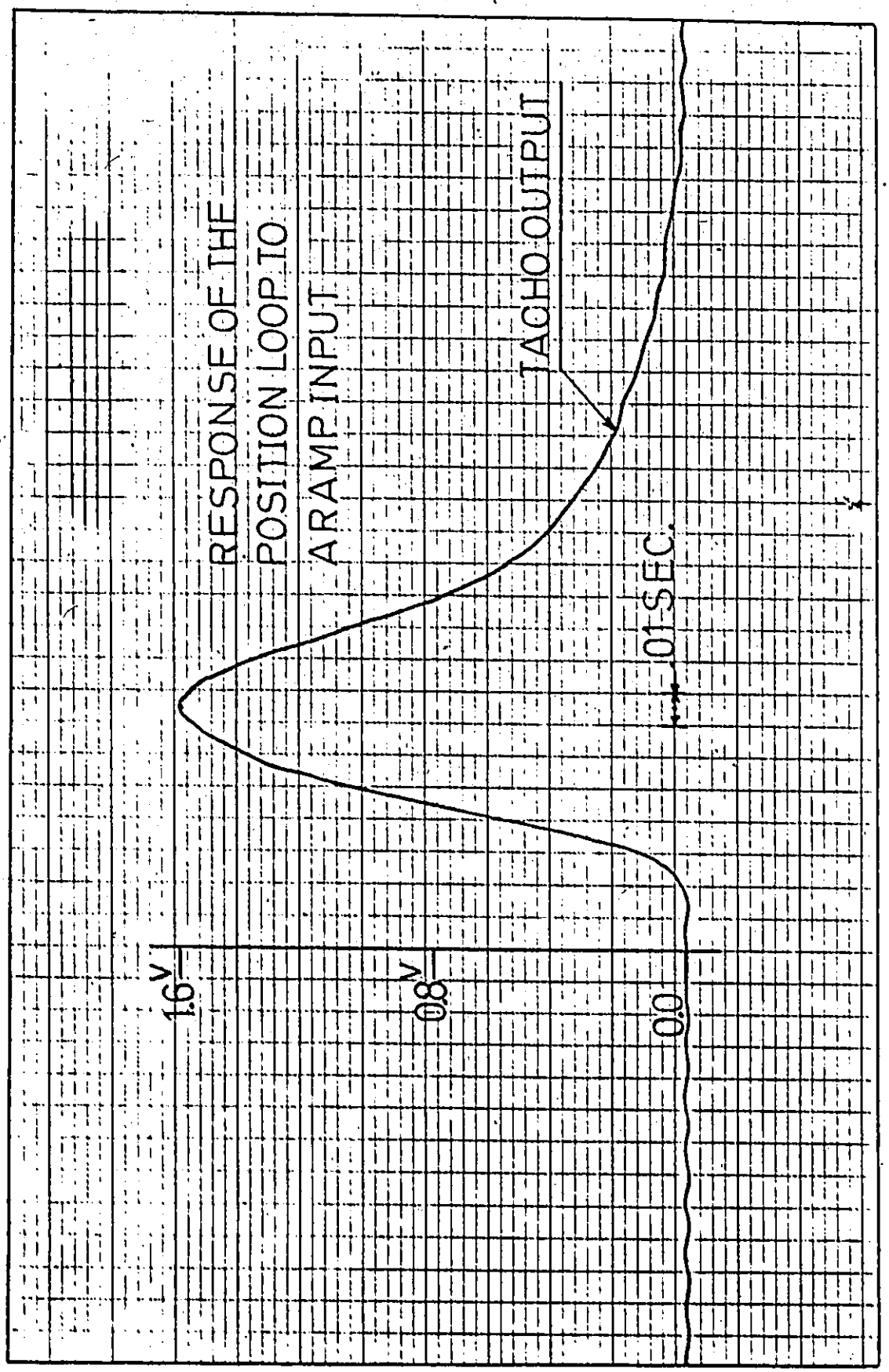

FIGURE 29

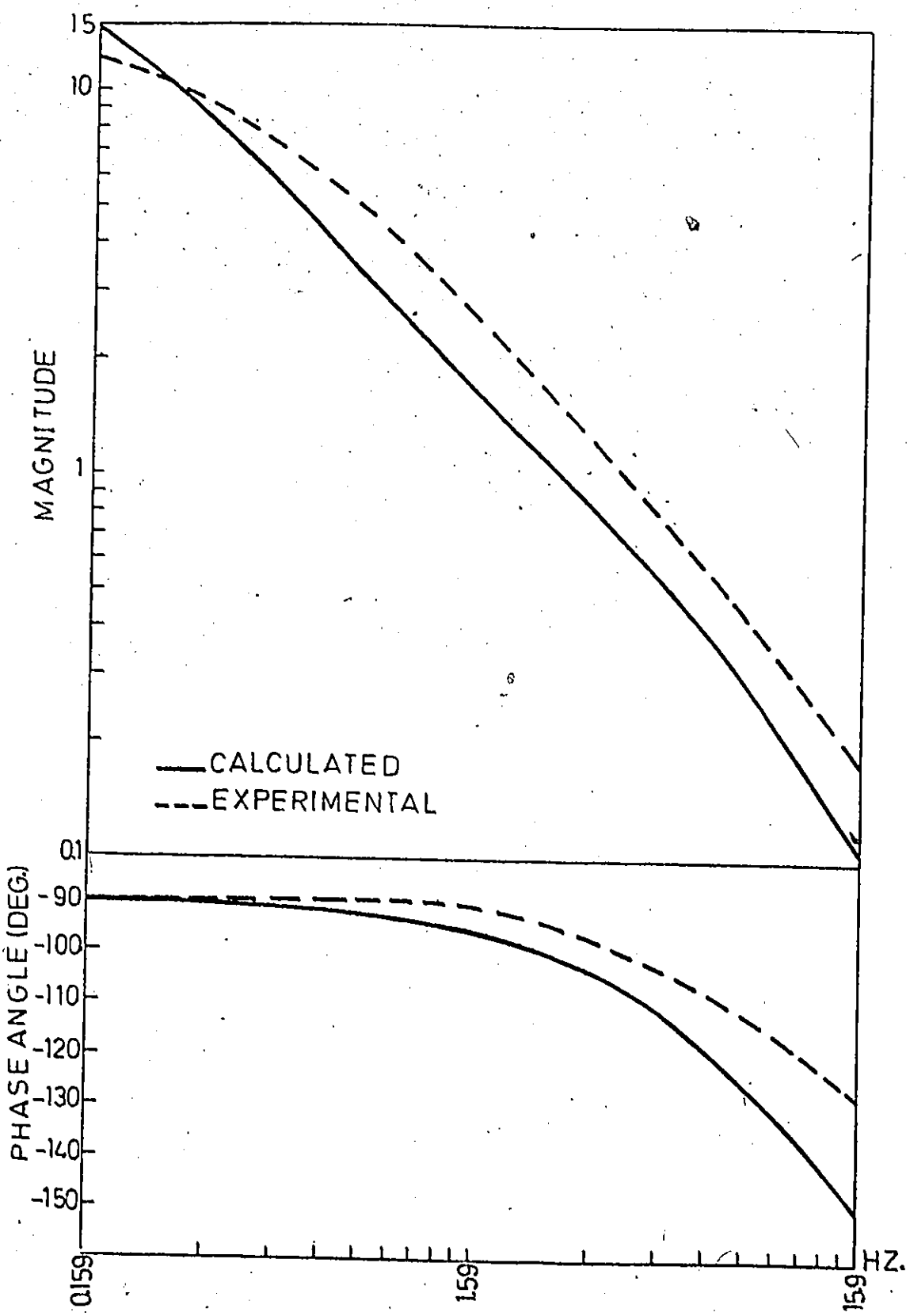

FREQUENCY CHARACTERISTICS OF THE OPEN POSITION LOOP

FIGURE 30

with reality. The real system contains flexibilities and inertias not considered here and it can become unstable if the gain is too high. In order to better study the effect of changing the system parameters on the behaviour of the position loop, the entire N/C loop was simulated by a digital computer program. The system was described by a set of first-order differential, or difference equations that describe its "state" variables. The solution to a set of first-order equations may be determined rather simply with the use of a digital computer. Figure 31 shows the state space system used for the entire N/C system.

Let the initial distance input to the N/C loop be labelled as x1. The input to both the D/A converter and filter x11 is calculated from the relationship:

$$x11 = x1 - x7$$

where x7 is the resolver output. Next, the output of the D/A converter and filter denoted x10 is obtained as:

$$x10 = K_p \cdot x11$$

where K_p is the gain in the D/A converter, usually set at 45.0 volts/inch. The input to the correcting network x2 is defined by the equation:

$$x2 = x10 - x9$$

where x9 is the velocity feedback defined as:

$$x9 = R_1/R_4 \cdot x8$$

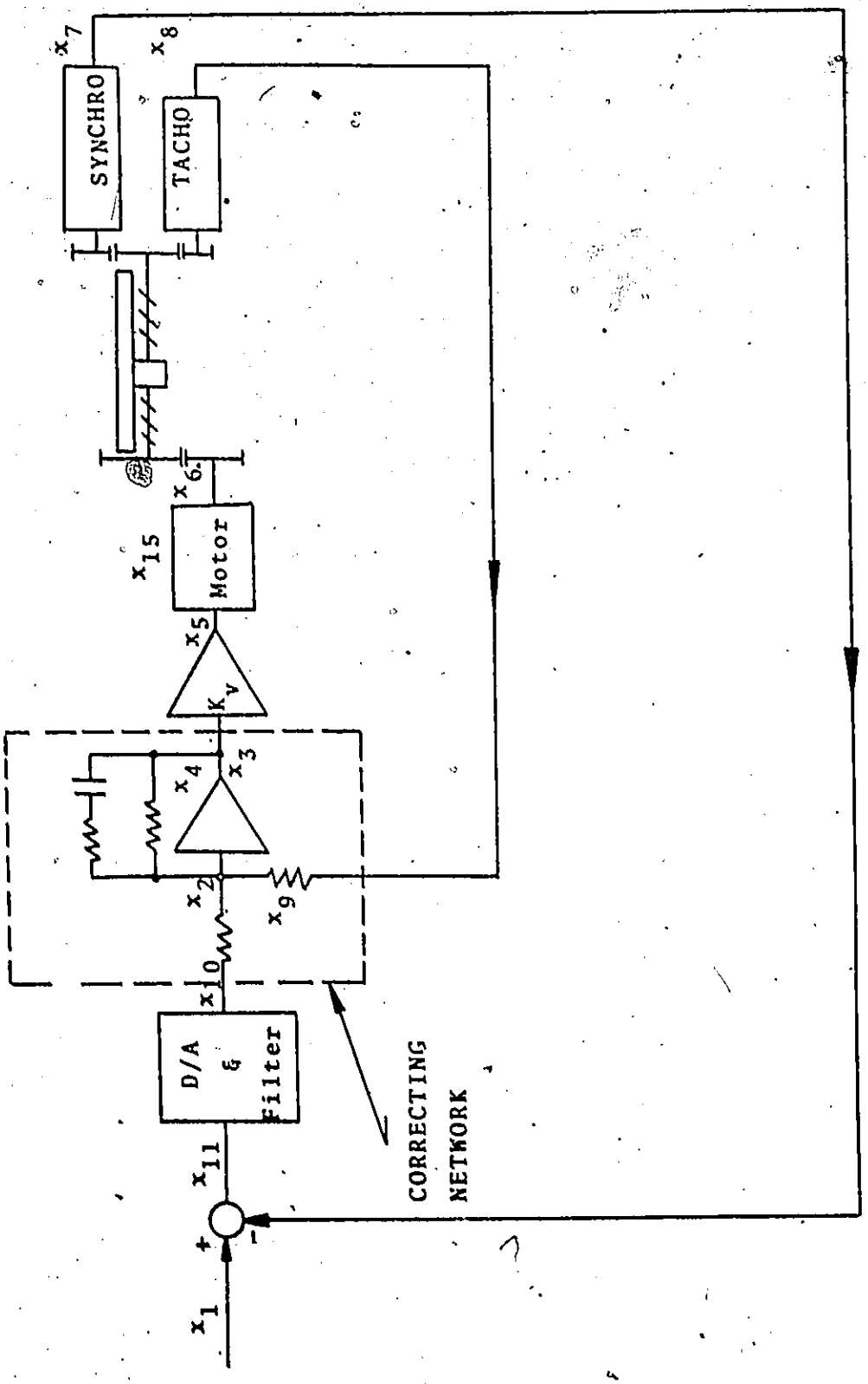

CLOSED POSITION LOOP
"THE STATE SPACE SYSTEM"

FIGURE 31

and x8 is the tacho output in volts.

The operation of the correcting network is next represented by the following equations:

$$\dot{x4} = x2 \frac{1}{(R_2+R_3)C} x4$$

and $$x3 = \frac{R_3 R_2}{R_1(R_2+R_3)} \left(x2 + \frac{1}{CR_2} x4\right)$$

where x4 is an intermediate state space variable used in the state space description of the network and x3 is the output of the correcting network.

The output of the power amplifier is denoted x5 where:

$$x5 = K_v \cdot x3$$

and K_v is the amplifier gain set at the value of 10.0. In order to represent the operation of the armature-controlled DC servomotor circuit shown in figure 32 while taking into consideration the current limitation phenomena discussed in section 3.3.1, the following equations are used: first the voltage equation of the armature circuit is defined as follows:

$$e_a(t) = Rm\ ia + Lm \frac{d\,ia}{dt} + e_m \qquad (3.4)$$

where $e_a(t)$ is the input voltage to the motor circuit,

i_a is the armature current

Rm and Lm represent the resistive and inductive components of the armature circuit

e_m is the induced armature voltage

i.e. $e_m = Ke \cdot n$

where K_e is the voltage constant of the motor having units

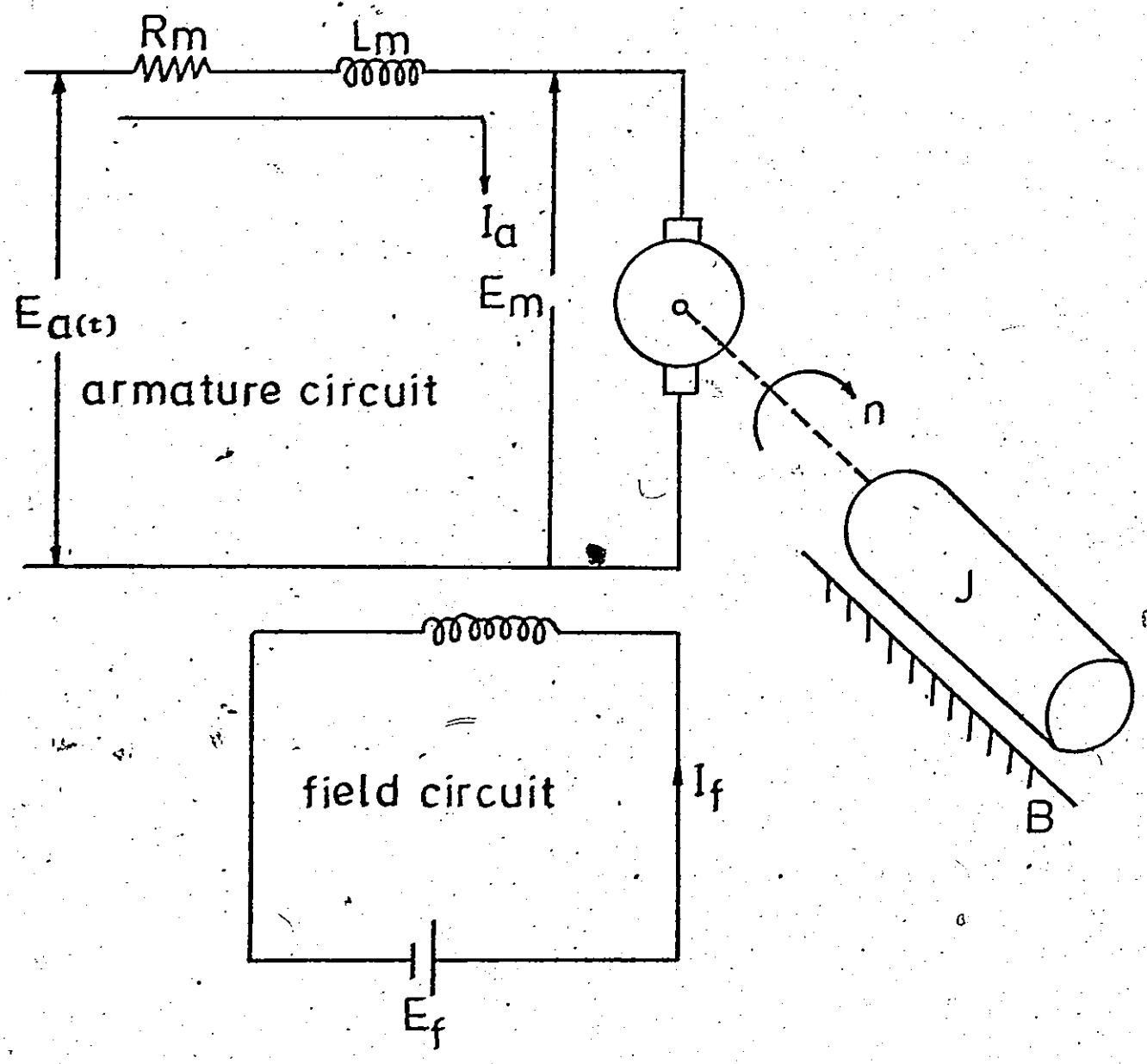

FIGURE 32

ARMATURE-CONTROLLED DC SERVOMOTOR SCHEMATIC DIAGRAM

volts/rev/sec.

n is the revolutions of the motor per second. Neglecting the armature inductance, the voltage equation of the armature circuit could be further rewritten in the following manner:

$$e_a(t) = Rm\ ia + Ke\ n \qquad (3.5)$$

Equation (3.5) is next further modified as:

$$e_a = PA_c + K_e\ n \qquad (3.6)$$

where P is a constant equal to $\frac{Rm}{K_i}$, K_i is another constant and A_c is the current analog signal i.e. $A_c = K_i \cdot i_a$

The developed torque of the motor T_D is given by:

$$T_D = 2\pi\ K_T \cdot i_a \qquad (3.7)$$

where K_T is the torque constant of the motor having units lb ft/A. The developed torque drives the mechanical load and the torque equation is:

$$\frac{T_D}{2\pi} = Jn' + Bn \qquad (3.8)$$

where J is the mass moment of inertia and B is the damping torque constant. Accordingly,

$$K_T\ i_a = Jn' + Bn \qquad (3.9)$$

Substituting in equation (3.5) twice using the data available from the measurements described in section 3.3.1 for a step of 200 millivolts and 1.6 volt respectively, the two constants P and K_e could be found. It should be noted here that these measurements were taken with the velocity loop closed

and the value of e_a should be modified accordingly. Therefore, in the steady state operation of the loop only 0.8333 of the step input is considered due to the effect of the feedback.

Accordingly,

P = 3.0112 and Ke = 2.86 volts/rev/sec

Having determined these constants and denoting Ac as x15, e_a ad x5 and n as x6, equation (3.6) could be written in the following way:

$$x15 = \frac{x5 - K_e\, x6}{P} \qquad (3.10)$$

In order to simulate the current limitation phenomena, x15 should not exceed the value of 3.49

Substituting the value of i_a in equation (3.9) from equation (3.5) it follows that:

$$\frac{K_T}{Rm}\, x5 = J\, \dot{x6} + \left(B + \frac{K_T K_e}{Rm}\right) x6 \qquad (3.11)$$

Equation (3.11) could be also rewritten as:

$$KT/Rm(P.\ x15 + Ke\ x6) = J\ x'6 + (B + KT\ Ke/Rm)\ x6$$

$$Km[P\ x15 + Ke\ x6] = \tau_m\, x'6 + x6 \qquad (3.12)$$

where $Km = \frac{KT}{BRm + K_T K_e}$

Km is the motor gain measured 0.35 volt/rev/sec. and τ_m is the motor time constant measured 32 milliseconds. Equations (3.10) and (3.12) thus describe the operation of the armature-controlled DC servo motor.

Proceeding with the state space description of the system, the tacho output denoted x8 is expressed as:

$$x8 = K_{ta} \cdot x6$$

where K_{ta} is the gain of the tacho stated by the manufacturer as 1.24 volt/rev/sec. Taking into account the transmission ratio in the mechanical drive, the resolver output x7 is obtained from the expression:

$$x'7 = \frac{x6}{10}$$

The closed velocity loop response is then quite simply represented by the following equations:

$$x'4 = x2 - \frac{1}{(R^2+R^3)C} \; x4$$

$$x'6 = \frac{Km}{\tau m} [P \; x15 + Ko \; x6] - \frac{x6}{\tau m}$$

$$x2 = x10 - x9$$

$$x9 = \frac{R1}{R4} \cdot x8$$

$$x3 = \frac{R2 \; R3}{R1(R2 + R3)} [x2 + \frac{1}{CR2} \; x4]$$

$$x8 = K_{ta} \cdot x6$$

$$x5 = K_v \cdot x3$$

$$x15 = \frac{x5 - Ke \; x6}{p}$$

Using Euler's method the integration of the above equations was evaluated as follows:

$$x'(t) = \lim_{\Delta t \to o} \frac{x(t+\Delta t) - x(t)}{\Delta t} = \frac{x(t+T) - x(t)}{T}$$

for a small increment of time $\Delta t = T$
Accordingly, the required set of equations thus becomes:

$$x4\ (t+T) = T\ x2(t) - \left[1 - \frac{T}{(R2+R3)\ C}\right] x4\ (t)$$

$$x6\ (t+T) = x6(t) + P.T.Km.x15\ (t)/\tau m$$

$$x2 = x10 - x9$$

$$29 = \frac{R1}{R4}\ x8$$

$$x3 = \frac{R2\ R3}{R1(R2+R3)}\ \left[x2 + \frac{1}{CR2}\ x4\right]$$

$$x8 = K_{ta}\ .\ x6$$

$$x5 = K_{v}\ .\ x3$$

$$x15 = x5 - K_{e}\ x6/P$$

Again the response of any $x_i(t)$ to any arbitrary chosen input $x7 = f(t)$ may be observed by sequential application of the entire set of equations. The time increment used was equal to 1 millisecond. Figures 33 and 34 show the computed current analog signal and tacho output for two different step inputs of 0.2 and 1.3 volt respectively. In both case the capacitance of the correcting network is assumed short circuited in order to simulate the cases previously measured and presented in section 3.3.1. The effect of the current limitation phenomena is clearly pronounced in figure 33, where the current analog signal calculated for a step of 1.3 volt applied to the closed velocity loop is held constant at its maximum value for a longer period of time than the case presented for a step of 0.2 volt. Obviously, the acceleration resulted for the case of 1.3 volt step input as shown in figure 34 is higher than the second investigated case due

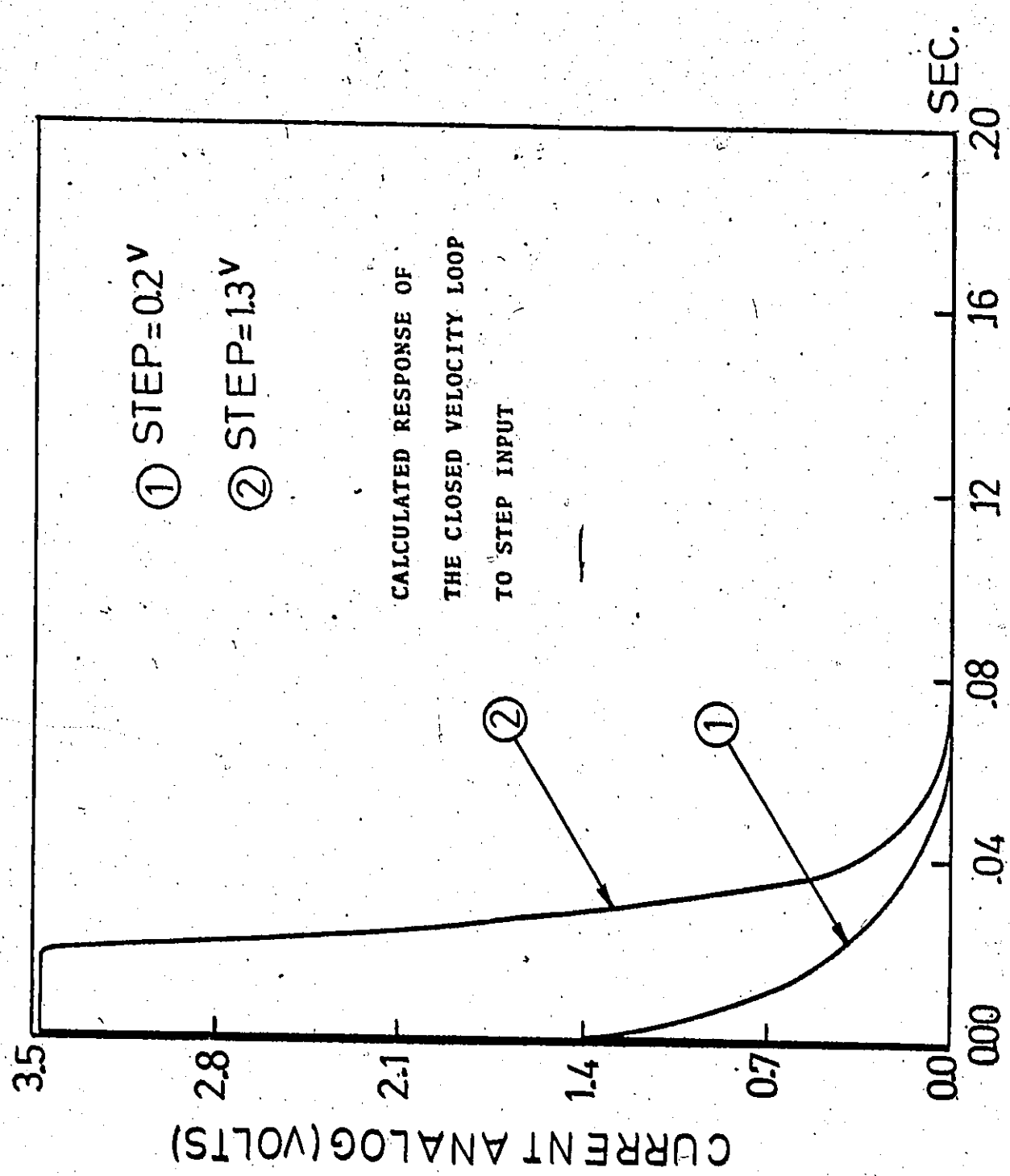
CURRENT ANALOG (VOLTS)
3.5
2.8
2.1
1.4
0.7
0.0
.00
.04
.08
.12
.16
.20
SEC.
① STEP=0.2V
② STEP=1.3V
CALCULATED RESPONSE OF
THE CLOSED VELOCITY LOOP
TO STEP INPUT
②
①

FIGURE 33

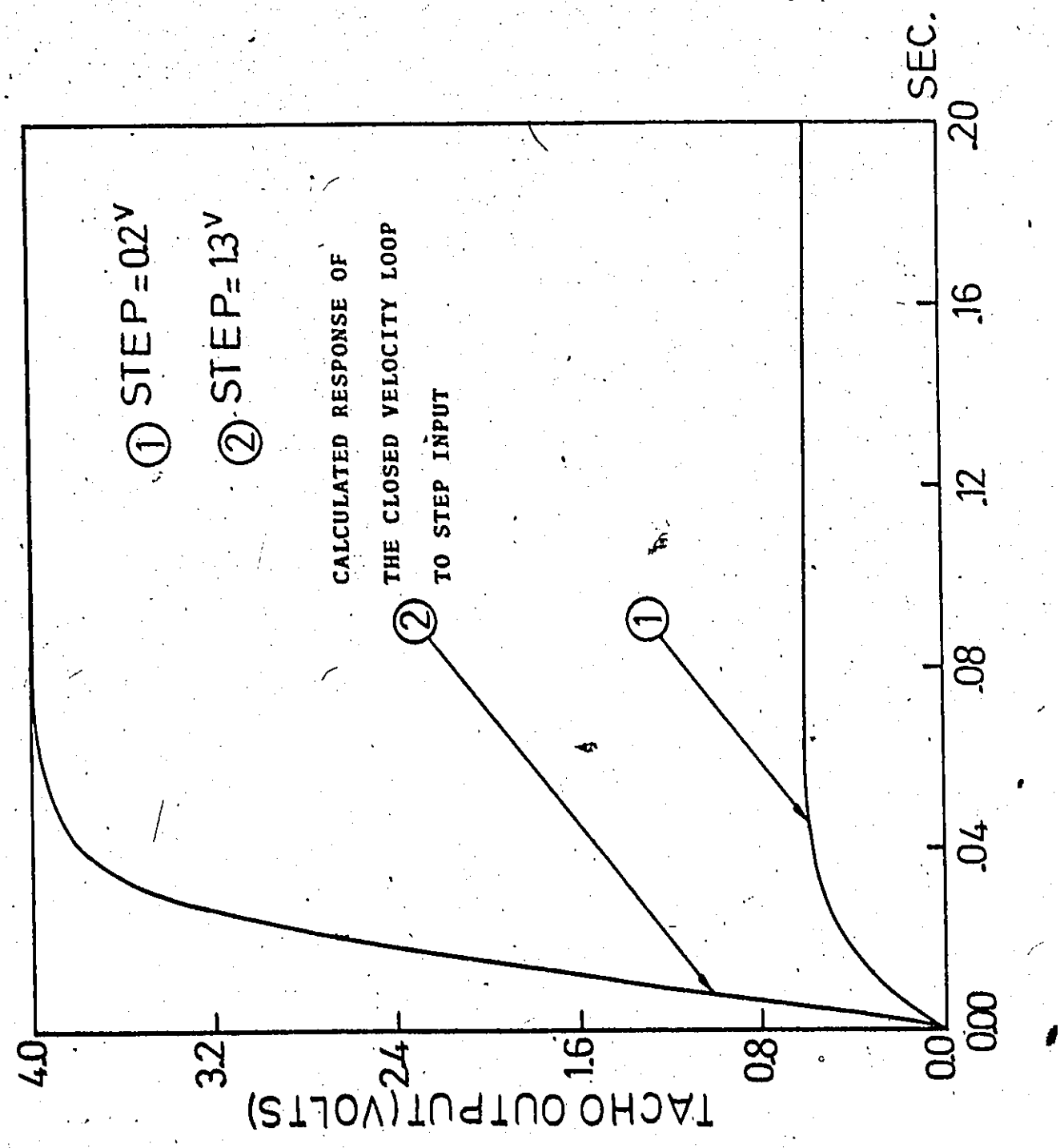
TACHO OUTPUT (VOLTS)
4.0
3.2
2.4
1.6
0.8
0.0
0.00
.04
.08
.12
.16
.20
SEC.
① STEP=.02V
② STEP=.13V
CALCULATED RESPONSE OF
THE CLOSED VELOCITY LOOP
TO STEP INPUT
①
②

FIGURE 34

to the higher value of armature current in the motor circuit.

To describe the position loop closed, only the following equations have to be added to the previous ones:

$$x7(t+T) = 0.1T \cdot x6(t) + x7(t)$$

$$x11(t) = x1(t) - x7(t)$$

$$x10(t) = Kp \cdot x11(t)$$

A step input of 1.0 inch was next supplied to the closed position loop, and the resolver output was plotted in each case simulated. The gain in the D/A converter "Kp" was first increased to 100 volts/inch. Figure 35 shows the resolver output. The prevalent time constant observed was 54 milliseconds, however overshoot started occurring. A further increase of the D/A gain "Kp" up to 500 volts/inch yields the response shown in figure 36. The main time constant computed was 26 milliseconds, however the amount of overshoot in the system, certainly, became unacceptable. The cases simulated so far showed that increasing the position loop gain certainly results in a faster response of the entire system, but on the other hand decreases the amount of damping in the system. The same conclusion could be verified by investigating the root locus plot of the position loop shown in figure 37.

As seen three roots govern the transient behaviour of this loop. The dominant one is the real root which

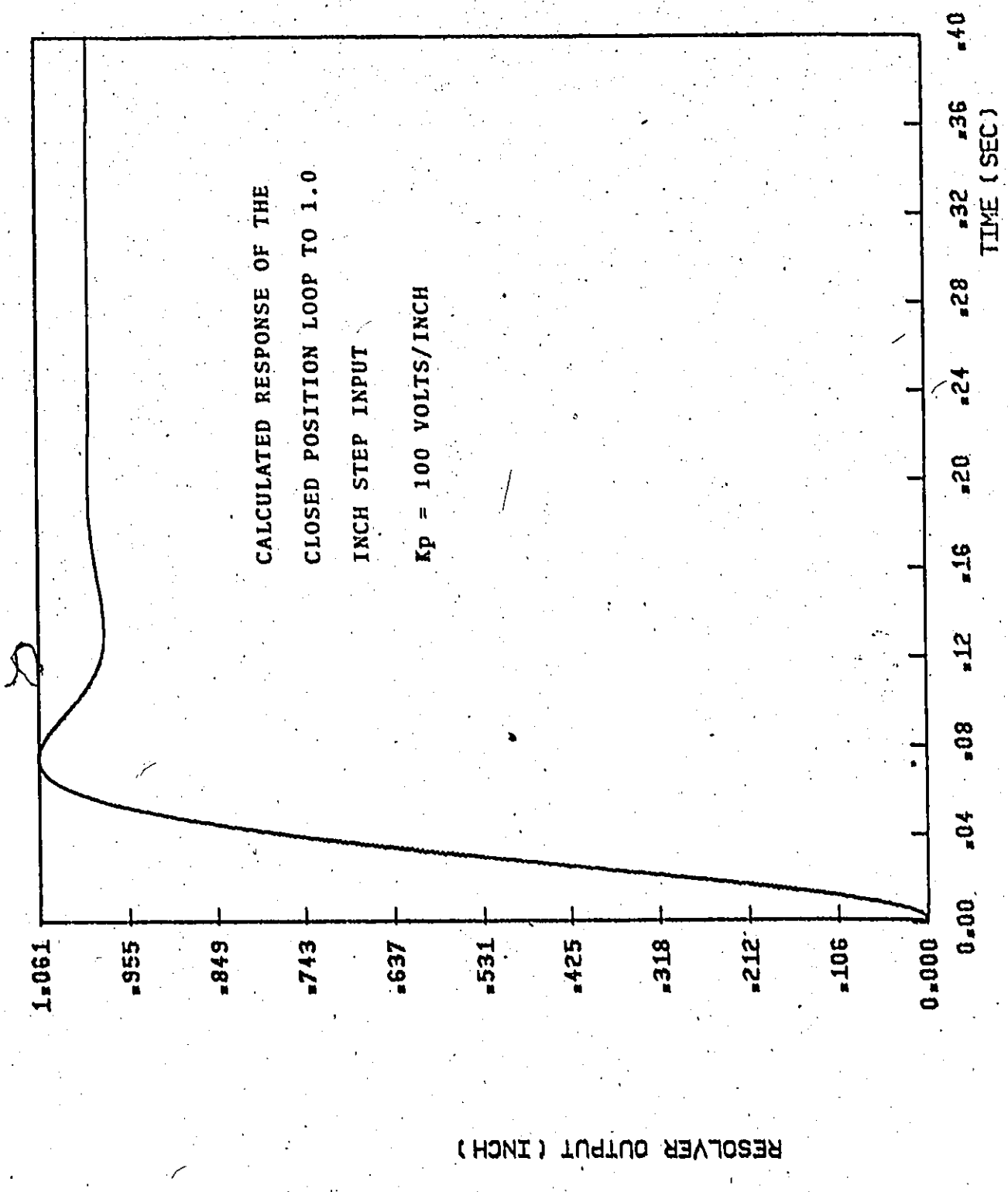
CALCULATED RESPONSE OF THE
CLOSED POSITION LOOP TO 1.0
INCH STEP INPUT
Kp = 100 VOLTS/INCH
1.061
.955
.849
.743
.637
.531
.425
.318
.212
.106
0.000
0.00
.04
.08
.12
.16
.20
.24
.28
.32
.36
.40
TIME (SEC)
RESOLVER OUTPUT (INCH)

FIGURE 35

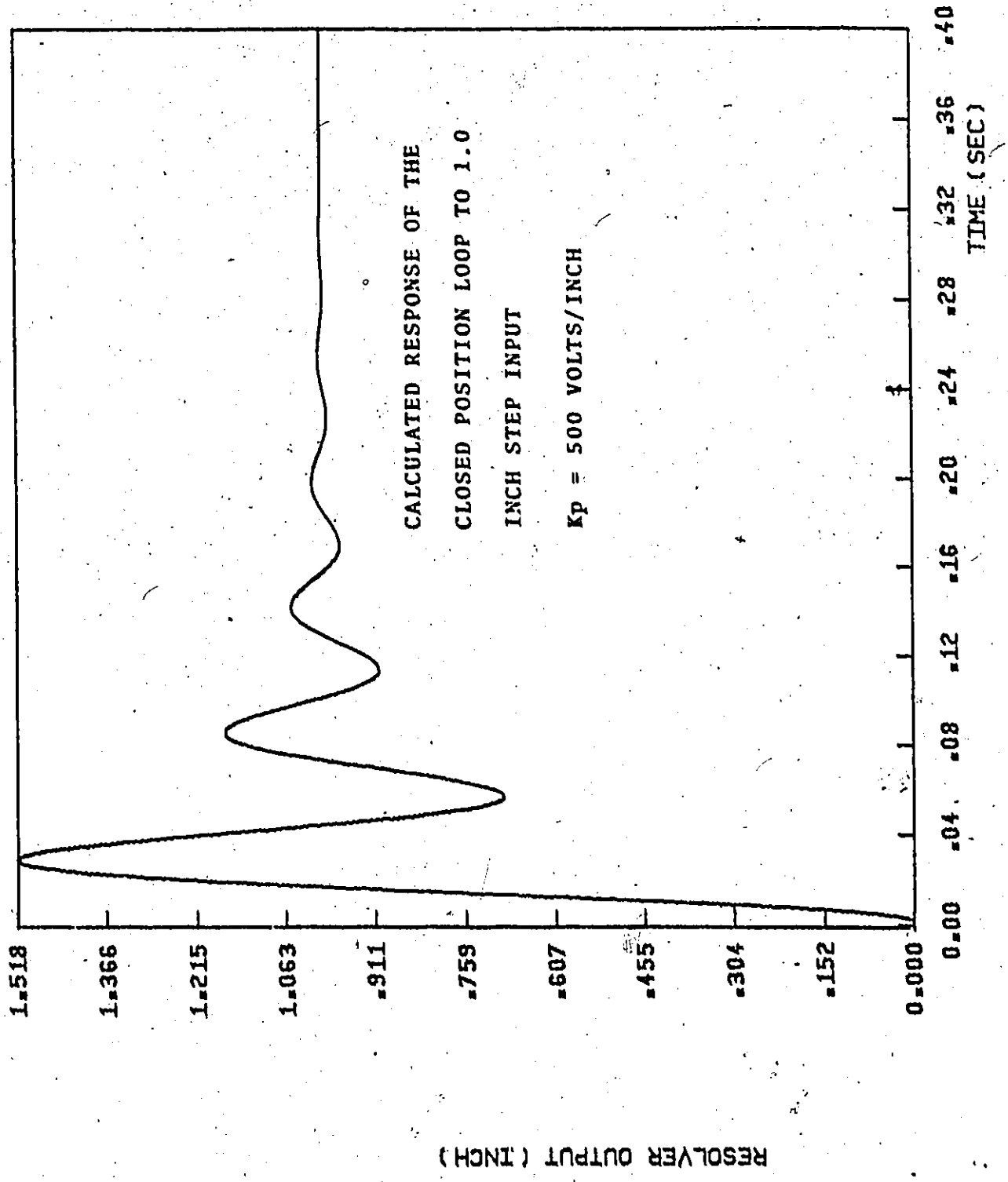
CALCULATED RESPONSE OF THE
CLOSED POSITION LOOP TO 1.0
INCH STEP INPUT
Kp = 500 VOLTS/INCH
RESOLVER OUTPUT (INCH)
TIME (SEC)
1.518
1.366
1.215
1.063
.911
.759
.607
.455
.304
.152
0.000
0.00
.04
.08
.12
.16
.20
.24
.28
.32
.36
.40

FIGURE 36

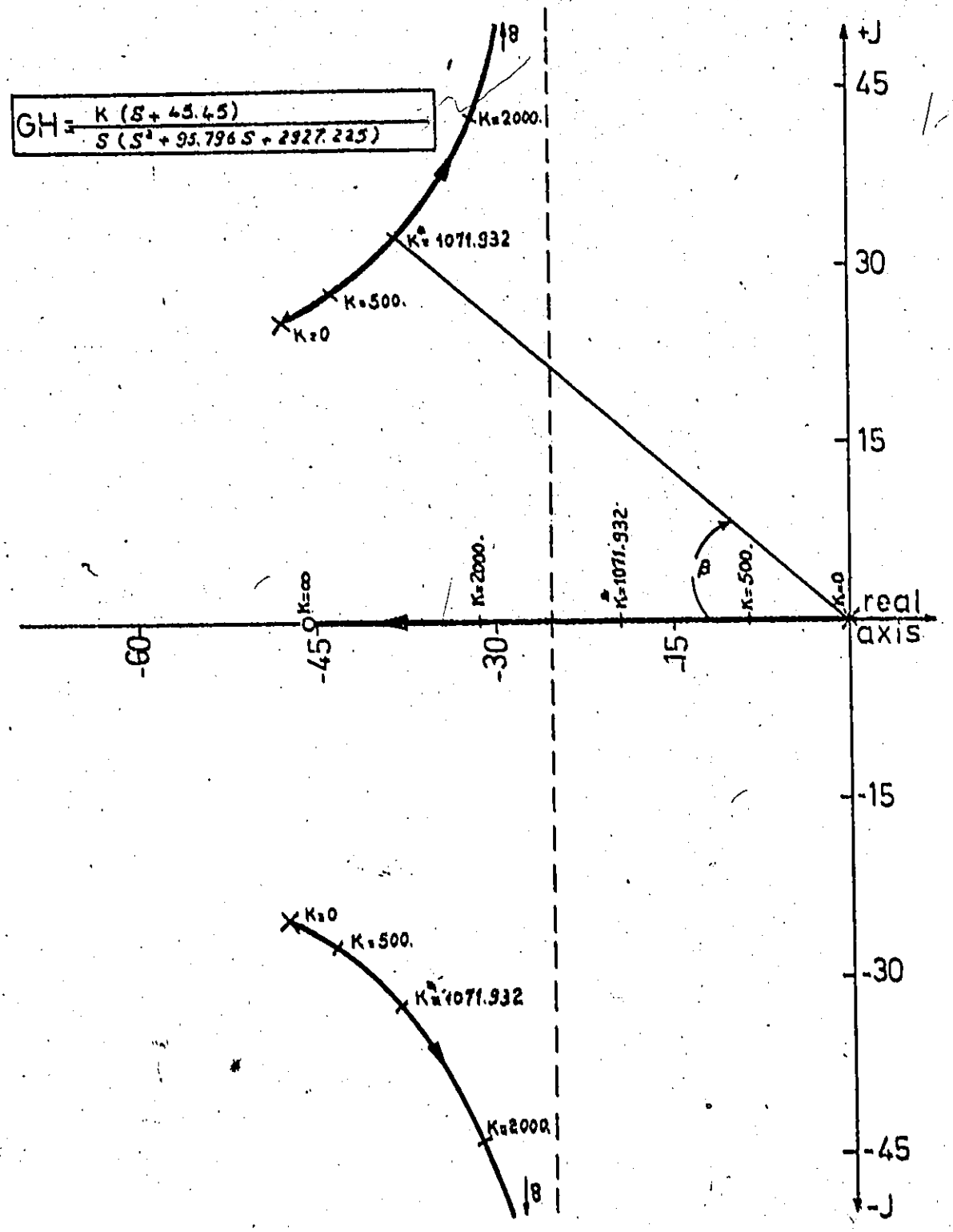

ROOT LOCUS PLOT OF THE POSITION LOOP

FIGURE 37

yields an exponentially decaying term in the time domain. The two complex and conjugate roots yield sinusoidal and exponentially decaying terms in the time domain. The influence of a particular pole (or pair of complex poles) on the response is mainly determined by the real part σ of the pole $p = \sigma + jw$, which determines the rate at which the transient term due to that pole decays; the larger σ, the faster the rate of decay. This fact then explains the faster response observed when increasing the gain in figures 35 and 36. Aslo, it is seen from the root locus plot that increasing the gain results in a smaller value of the real part σ of the two complex roots. Their influence on the response is then increased, and as a result the amount of oscillations increased too in the loop response. The faster response observed when increasing the open loop gain is also due to the increase in the natural frequency of the system w_n. Figure 38 illustrates the effect of increasing the open loop gain on the frequency characteristics of the system. Adjustment of the gain does not affect the phase angle plot. Thus, only the magnitude had to be adjusted. The next task was then to investigate the possible means of increasing the damping in the N/C system. One possible mean was to increase the gain in the internal velocity loop.

Two different methods were used to increase the gain of the velocity loop, that is increasing the value

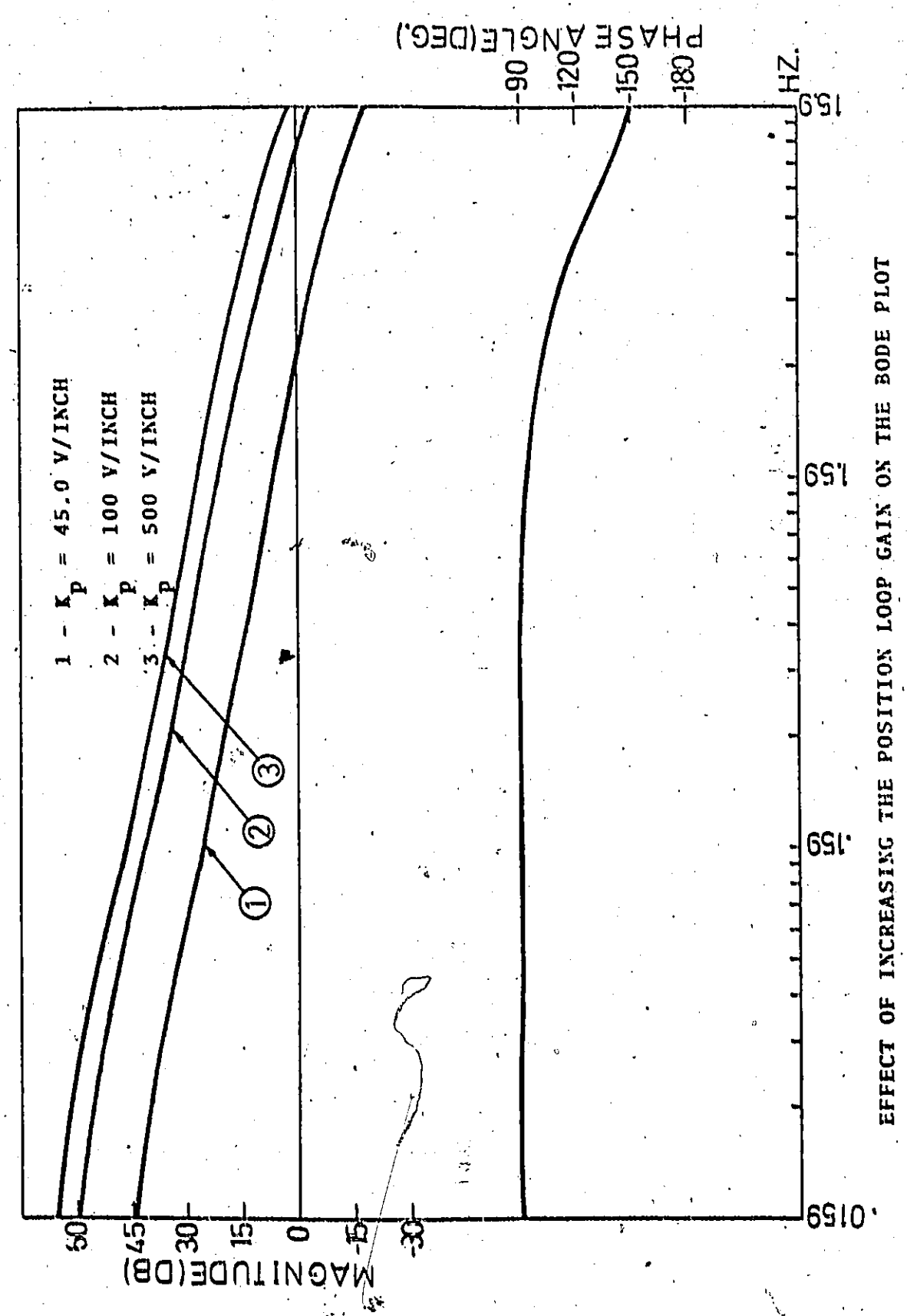

EFFECT OF INCREASING THE POSITION LOOP GAIN ON THE BODE PLOT

FIGURE 38

R2 or decreasing R4 of the correcting network. The response of the closed position loop to different ramp inputs using different values of R2 and R4 was next investigated. The effect of the current limitation phenomena will be first neglected in the following cases and investigated later on in this chapter. A ramp input described by a ramp height of 0.01 inch at a ramp speed of 5 inch/min was first applied to the N/C loop with the original gain to provide a base of camparison for the cases discussed later on. Figure 39 shows the tacho output to such a ramp input. Next, increasing the gain in the D/A converter "Kp" to 180 volts/inch taht is increasing the position loop gain 4 times yields the response shown in figure 40. Oscillations of considerable magnitude are clearly shown in the tacho output. Increasing the value of R2 from 22K to 33K yields the response shown in figure 41. The previously mentioned oscillations decreased considerably. The result of a further increase in the value of R2 to 47 is shown in figure 42. The resolver outputs to the above described four cases are shown in figure 43. The system is seen to be quite stable in the fourth case and the time needed for the resolver output to reach its steady state is found equal to 160 milliseconds as compared with 370 milliseconds required in the case of the original gain in the system (case I). The case where the positional loop gain was increased four times and the value of R2 increased to 47K was further investigated. Figure 44

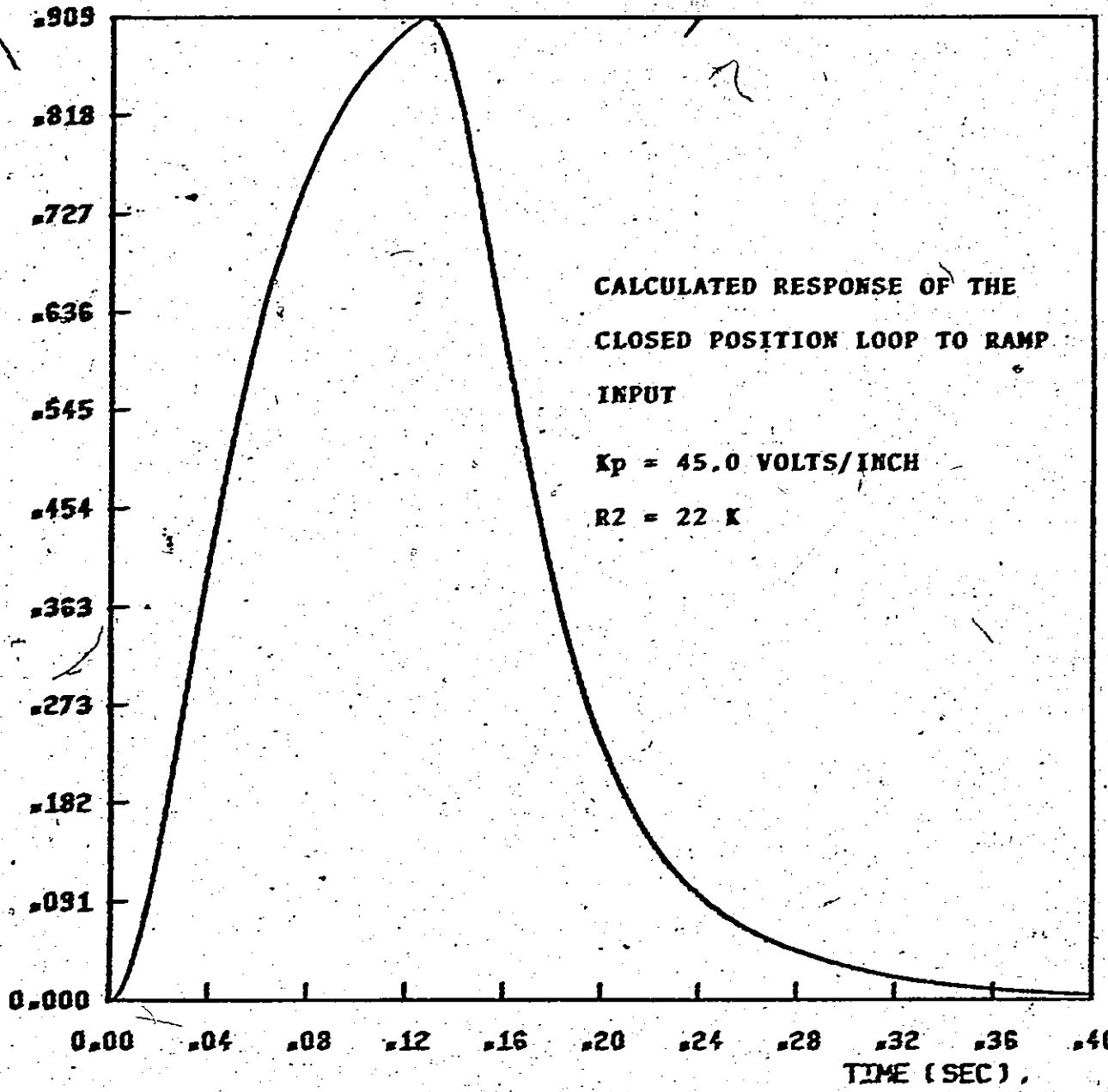
.909
.818
.727
.636
.545
.454
.363
.273
.182
.091
0.000
TACHO OUTPUT (VOLTS)
0.00
.04
.08
.12
.16
.20
.24
.28
.32
.36
.40
TIME (SEC).
CALCULATED RESPONSE OF THE
CLOSED POSITION LOOP TO RAMP
INPUT
Kp = 45.0 VOLTS/INCH
R2 = 22 K

FIGURE 39

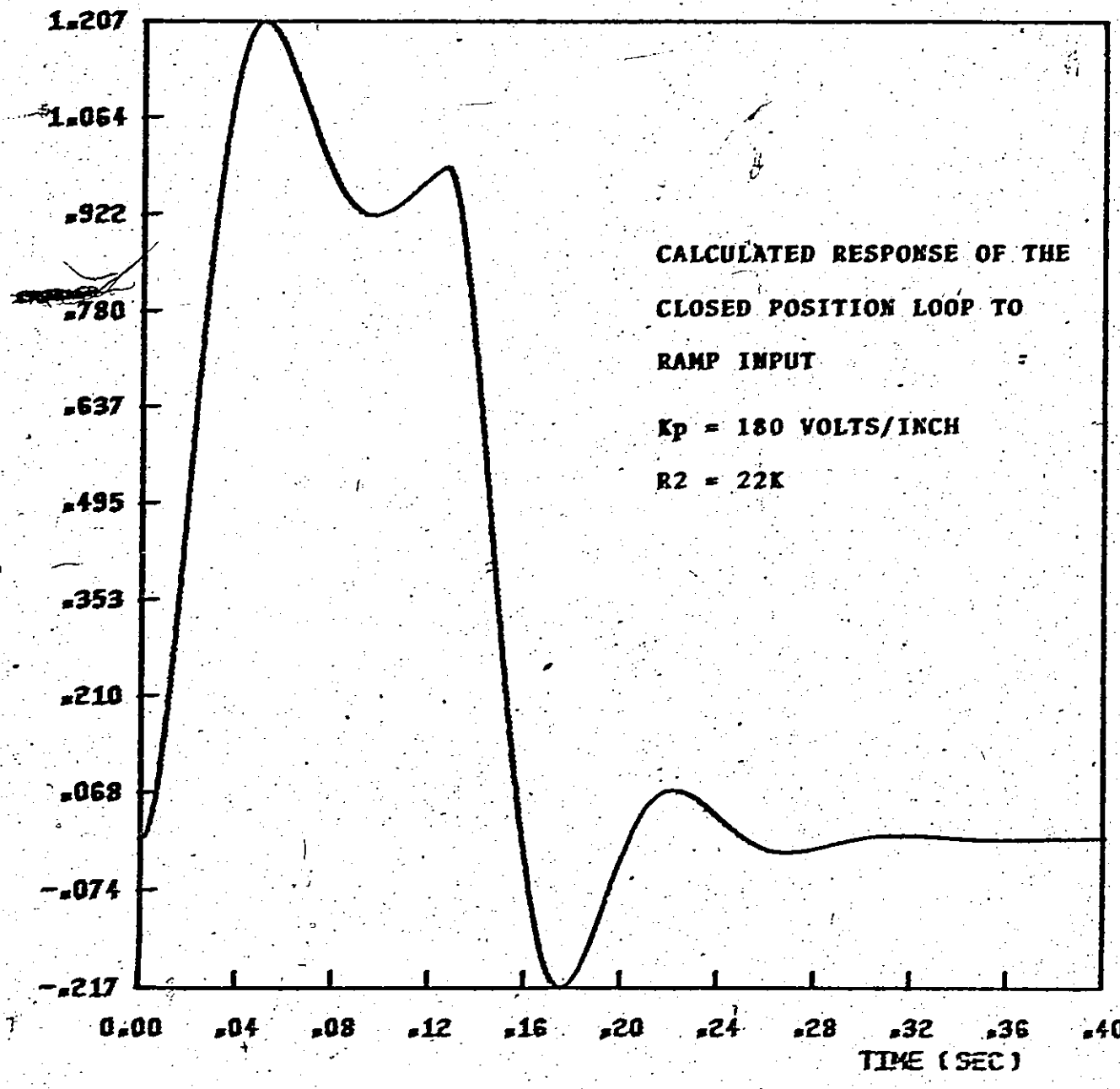
1.207
1.064
.922
.780
.637
.495
.353
.210
.068
-.074
-.217
0.00
.04
.08
.12
.16
.20
.24
.28
.32
.36
.40
TIME (SEC)
TACHO OUTPUT (VOLTS)
CALCULATED RESPONSE OF THE
CLOSED POSITION LOOP TO
RAMP INPUT
Kp = 180 VOLTS/INCH
R2 = 22K

FIGURE 40

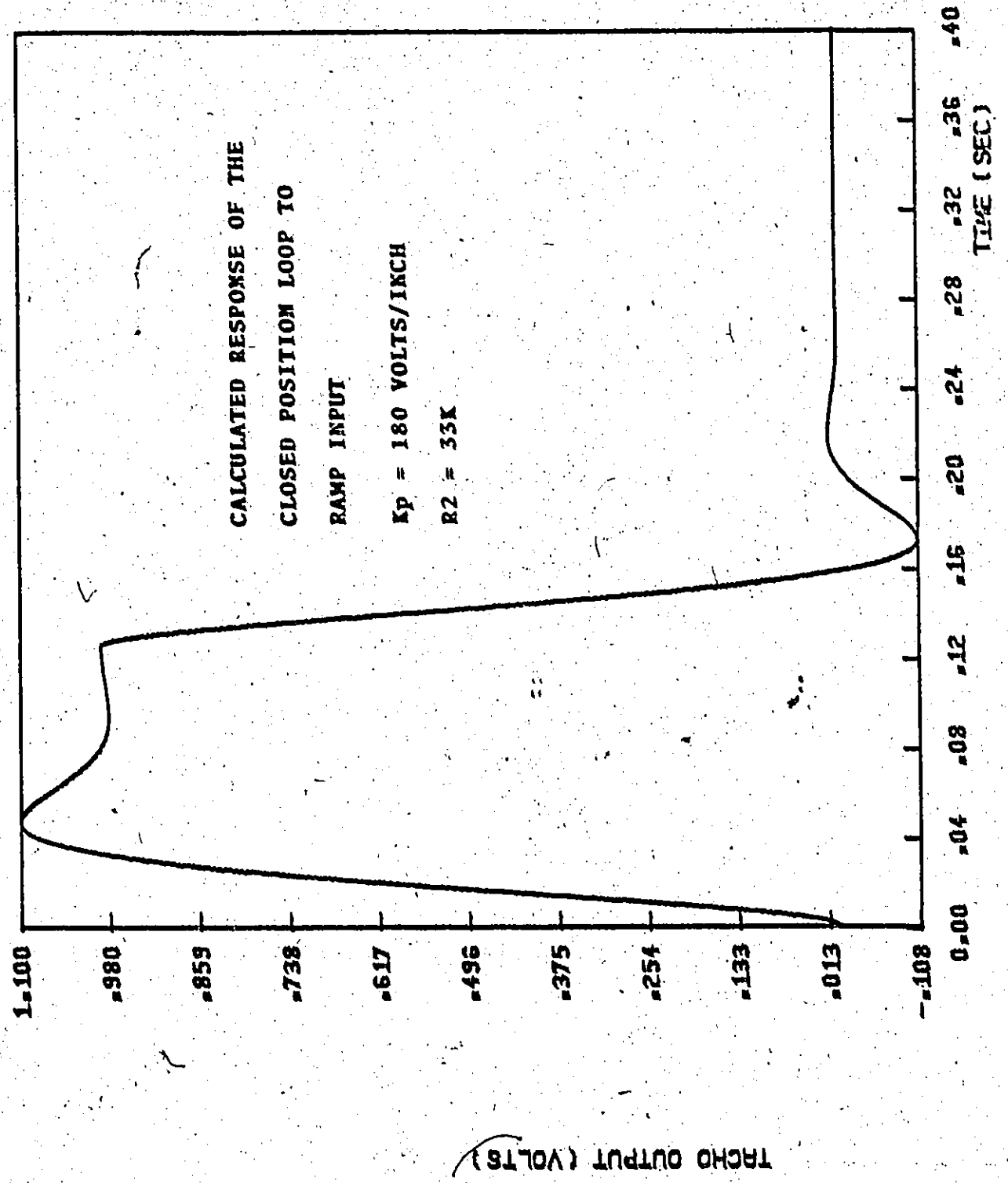
CALCULATED RESPONSE OF THE
CLOSED POSITION LOOP TO
RAMP INPUT
Kp = 180 VOLTS/INCH
R2 = 33K
1.100
.980
.859
.738
.617
.496
.375
.254
.133
.013
-.108
0.00
.04
.08
.12
.16
.20
.24
.28
.32
.36
.40
TIME (SEC)
TACHO OUTPUT (VOLTS)

FIGURE 41

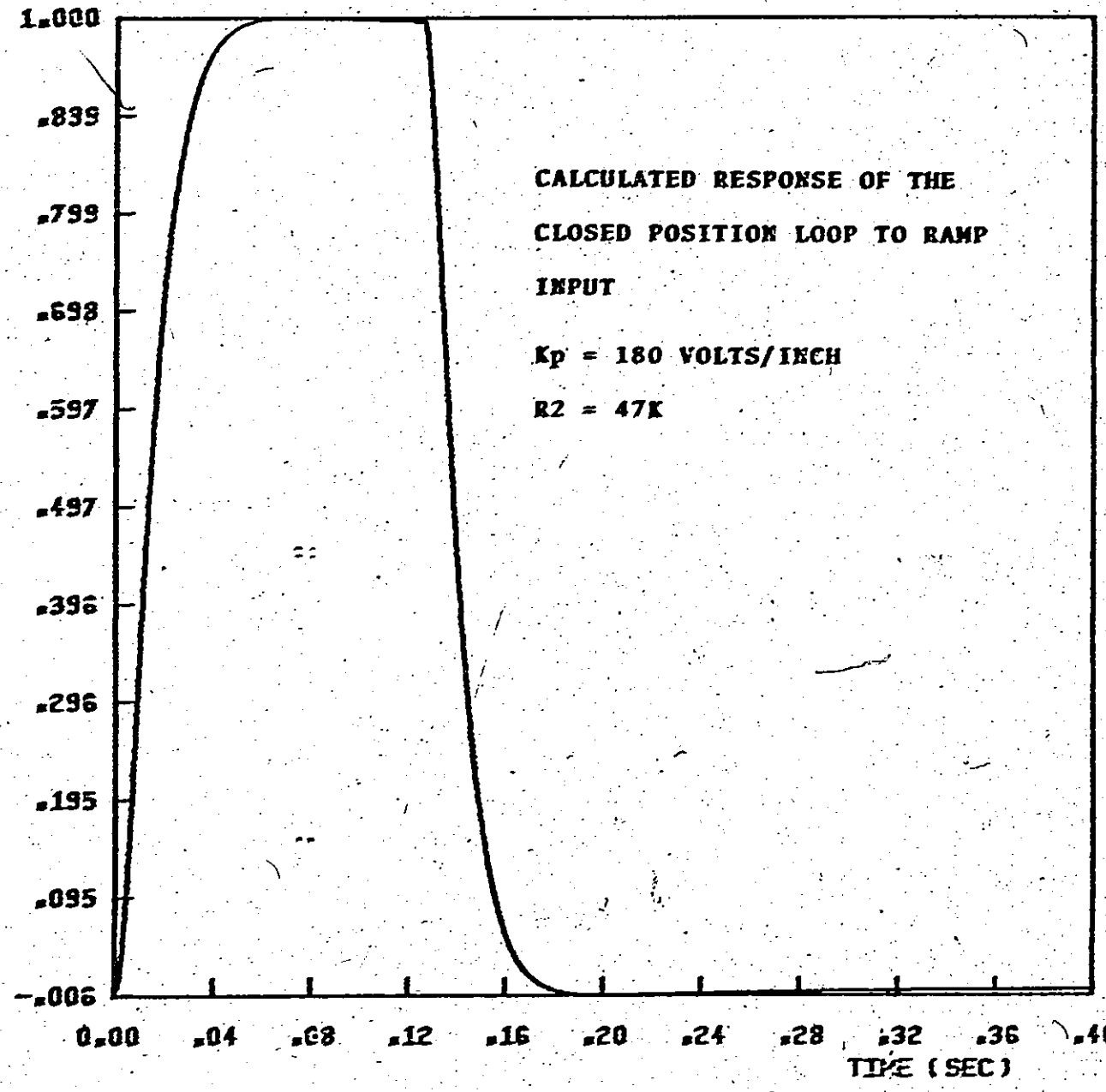
1.000
.839
.799
.698
.597
.497
.396
.296
.195
.095
-.006
0.00
.04
.08
.12
.16
.20
.24
.28
.32
.36
.40
TIME (SEC)
TACHO OUTPUT (VOLTS)
CALCULATED RESPONSE OF THE
CLOSED POSITION LOOP TO RAMP
INPUT
Kp = 180 VOLTS/INCH
R2 = 47K

FIGURE 42

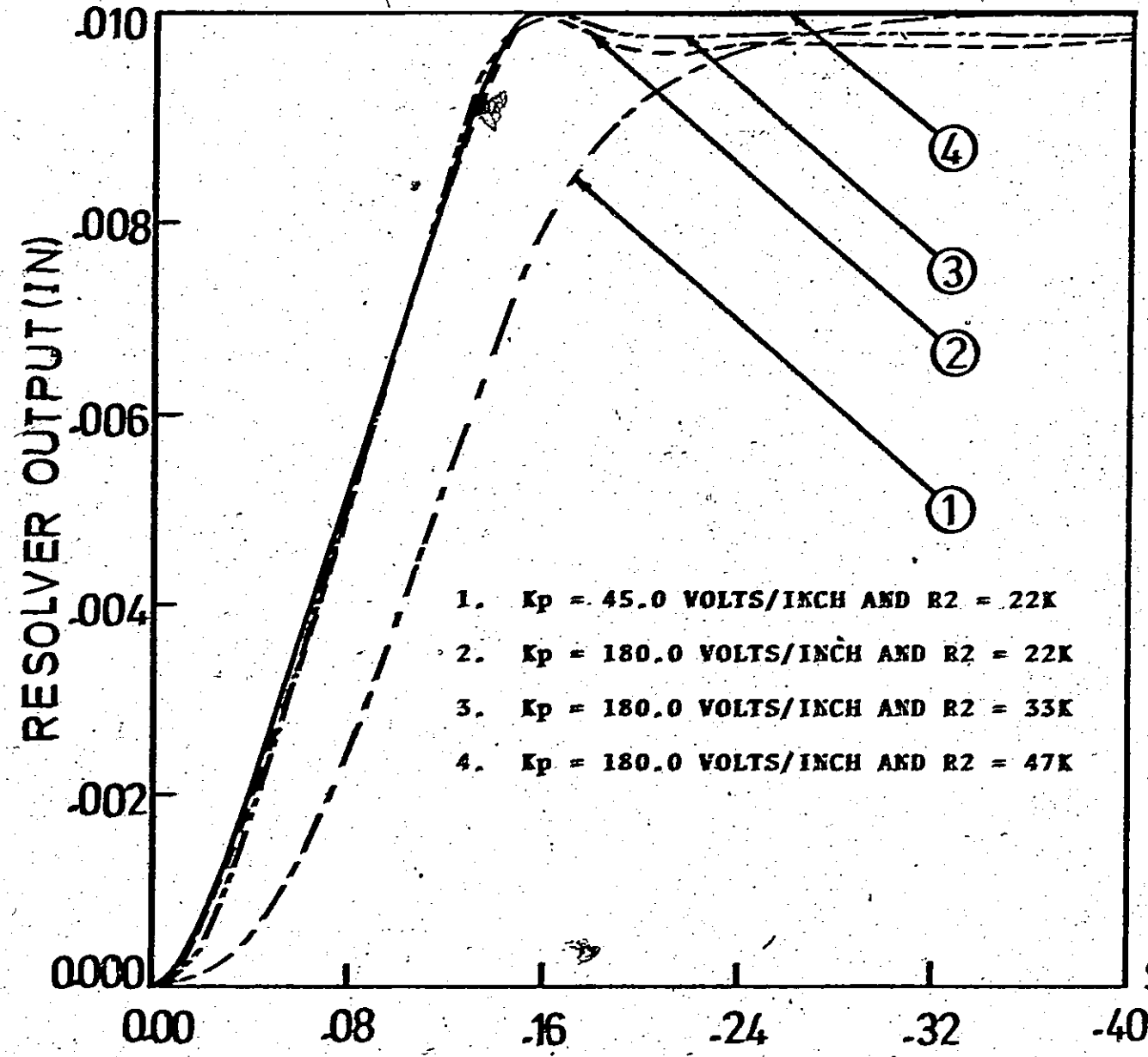

FIGURE 43

CALCULATED RESPONSE OF THE CLOSED POSITION LOOP TO RAMP INPUT

shows the corresponding Bode plot of the above mentioned case. The system as shown in quite stable having a gain cross-over frequency at 9.55 Hz, which also means an increase in the band width over the case of original gain in the system (the system with the original gain has a gain cross-over frequency at 2.86 Hz).

As previously mentioned a second method of increasing the gain in the velocity loop is to decrease the value of R4. Keeping the gain in the position loop increased 4 times from its original value and decreasing the value of R4 from 46 K to 10K yields the response shown in figures 45 and 46 for the resolver and tacho outputs respectively. Almost the same effect of increasing R2 on the damping of the system could be achieved by decreasing R4.

It is by now obviously seen that in order to obtain a faster response of the system and in the meantime ensure its stability, that is to ensure the safety of machining itself, both the position and velocity gains had to be increased. The important restriction which has to be considered here is the current limitation phenomena. The influence of the current limitation on the system response is next investigated.

3.4.1 Influence of Current Limitation on the Behaviour of the Closed Position Loop

As previously mentioned the current limitation

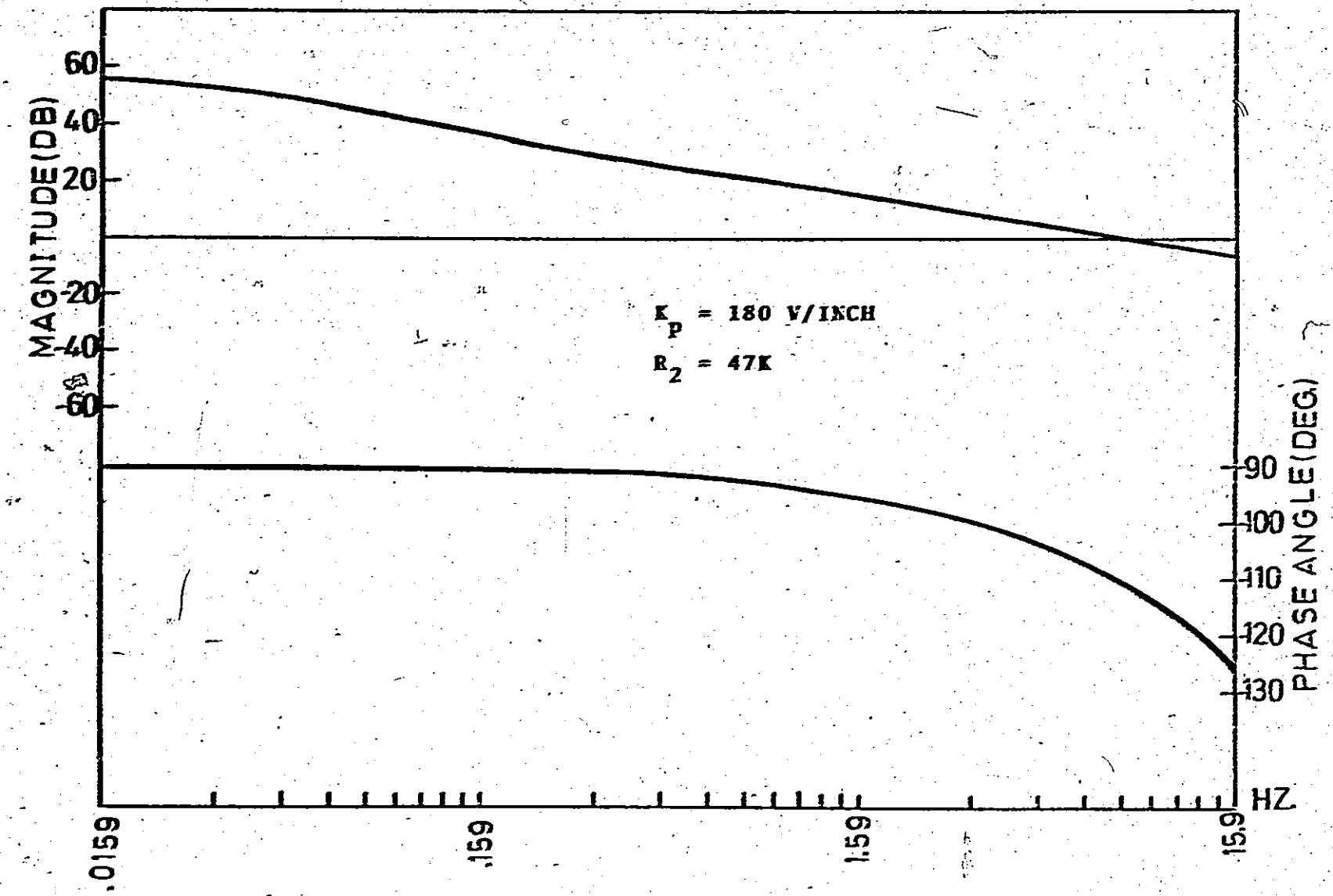

FIGURE 44

BODE PLOT OF THE OPEN POSITION LOOP

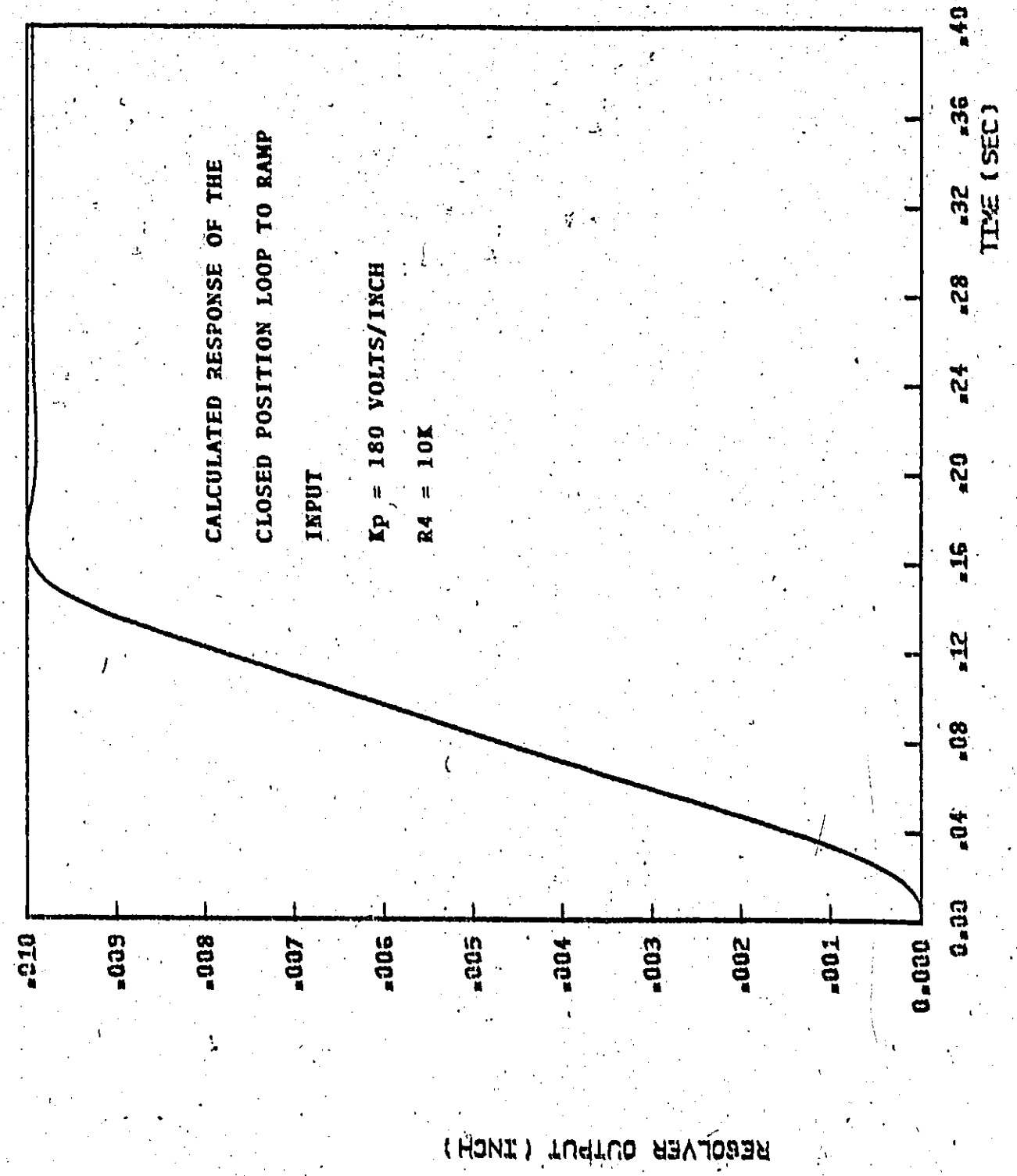
CALCULATED RESPONSE OF THE
CLOSED POSITION LOOP TO RAMP
INPUT
Kp = 189 VOLTS/INCH
R4 = 10K
.010
.009
.008
.007
.006
.005
.004
.003
.002
.001
0.000
0.00
.04
.08
.12
.16
.20
.24
.28
.32
.36
.40
TIME (SEC)
RESOLVER OUTPUT (INCH)

FIGURE 45

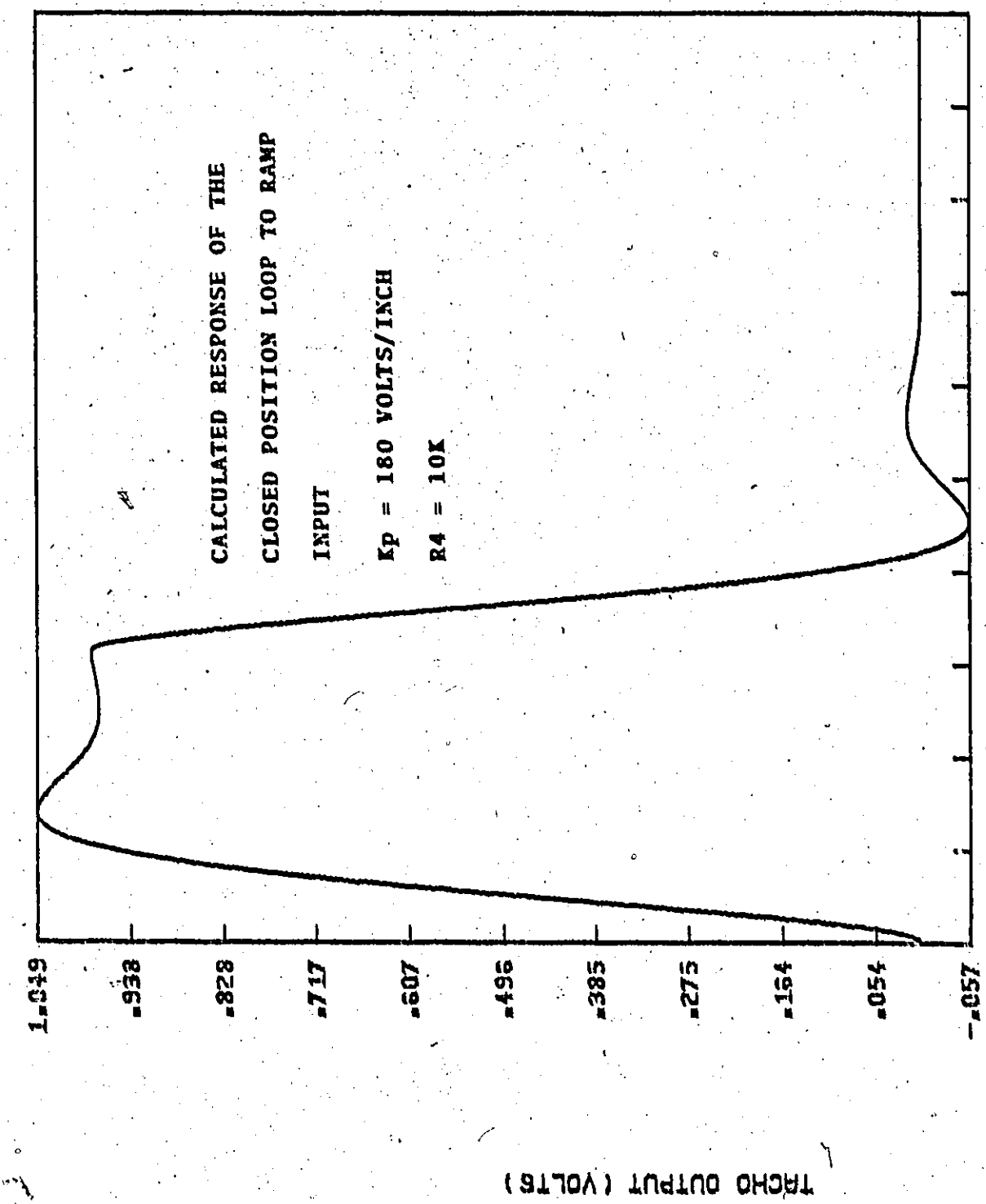
CALCULATED RESPONSE OF THE
CLOSED POSITION LOOP TO RAMP
INPUT
Kp = 180 VOLTS/INCH
R4 = 10K
1.049
.938
.828
.717
.607
.496
.385
.275
.164
.054
-.057
0.00
.04
.08
.12
.16
.20
.24
.28
.32
.36
.40
TIME (SEC)
TACHO OUTPUT (VOLTS)

FIGURE 46

phenomena was neglected in the cases simulated so far. In order to better understand its influence on the system, the cases discussed in the previous section was again investigated with the current limit constraint imposed. It was found that at 5 inch/min ramp speed the new constraint does not affect the system response in the cases considered previously and the same results wereobtained again. However increasing the ramp speed to 30 ipm showed a difference in both the resolver and tacho outputs. Typical results are presented in the following. Figures 47 and 48 show the resolver and tacho outputs respectively with and without current limitation imposed on the armature current for the case where the positional loop gain was increased four times as well as R2 to 47K. The output voltage of the tacho decreases with the presence of the current limitation constraint and accordingly the acceleration of the feed drives decreases too. Also the time needed to reach the steady state is increased. A second case where the position loop gain is assumed increased 10 times, and R2 increased to 470 K is also investigated. The results obtained are shown in figures 49 and 50 for the resolver and tacho outputs respectively. It is noticed that in the latter case, the resulting acceleration with current limitation is almost the same of the previous case where the position loop gain was increased only 4 times.

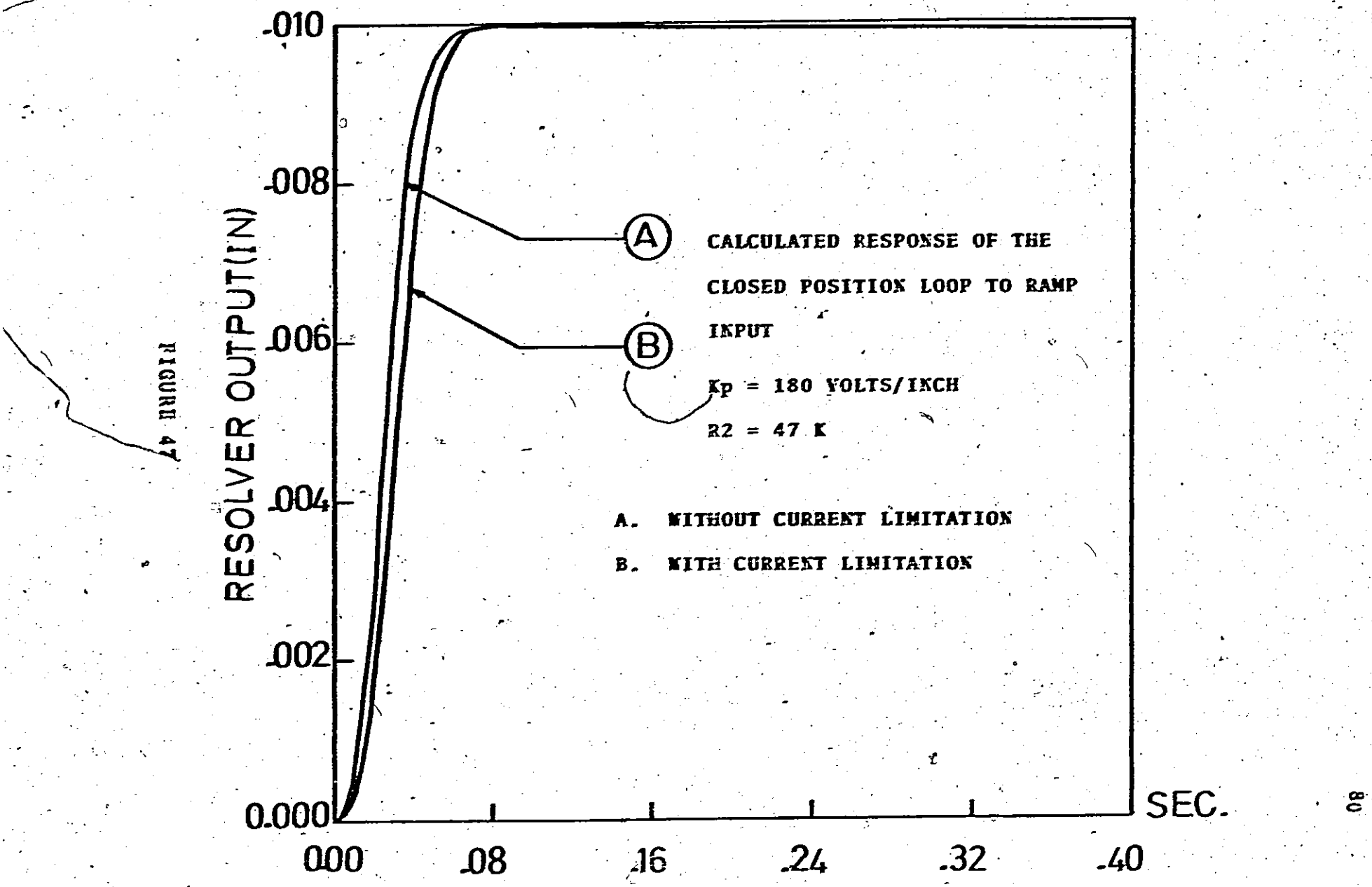
.010
.008
.006
.004
.002
0.000
RESOLVER OUTPUT(IN)
A
B
CALCULATED RESPONSE OF THE CLOSED POSITION LOOP TO RAMP INPUT
Kp = 180 VOLTS/INCH
R2 = 47 K
A. WITHOUT CURRENT LIMITATION
B. WITH CURRENT LIMITATION
SEC.
000
.08
.16
.24
.32
.40

FIGURE 47

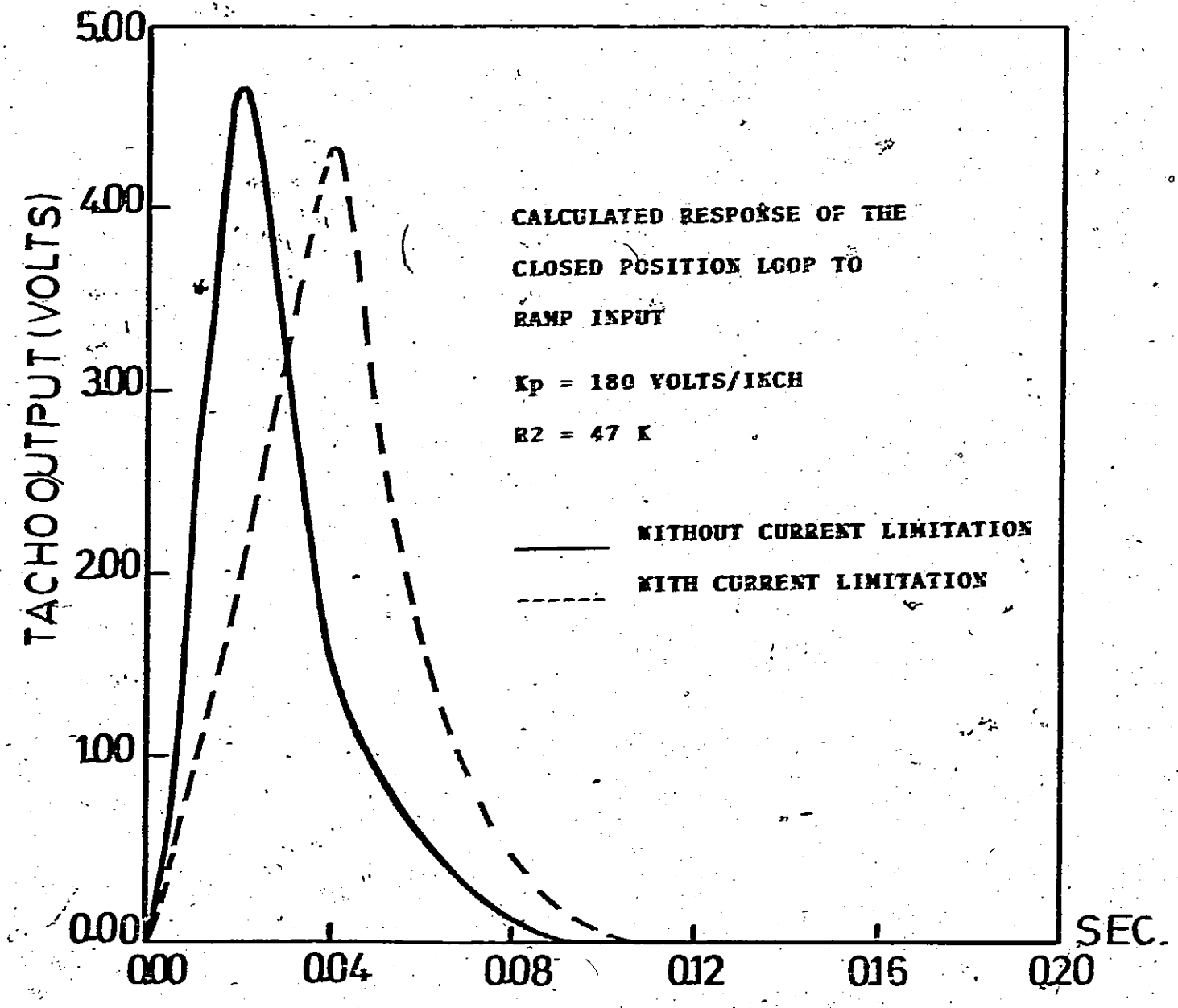
5.00
4.00
3.00
2.00
1.00
0.00
TACHO OUTPUT (VOLTS)
0.00
0.04
0.08
0.12
0.16
0.20
SEC.
CALCULATED RESPONSE OF THE
CLOSED POSITION LOOP TO
RAMP INPUT
Kp = 180 VOLTS/INCH
R2 = 47 K
WITHOUT CURRENT LIMITATION
WITH CURRENT LIMITATION

FIGURE 4B

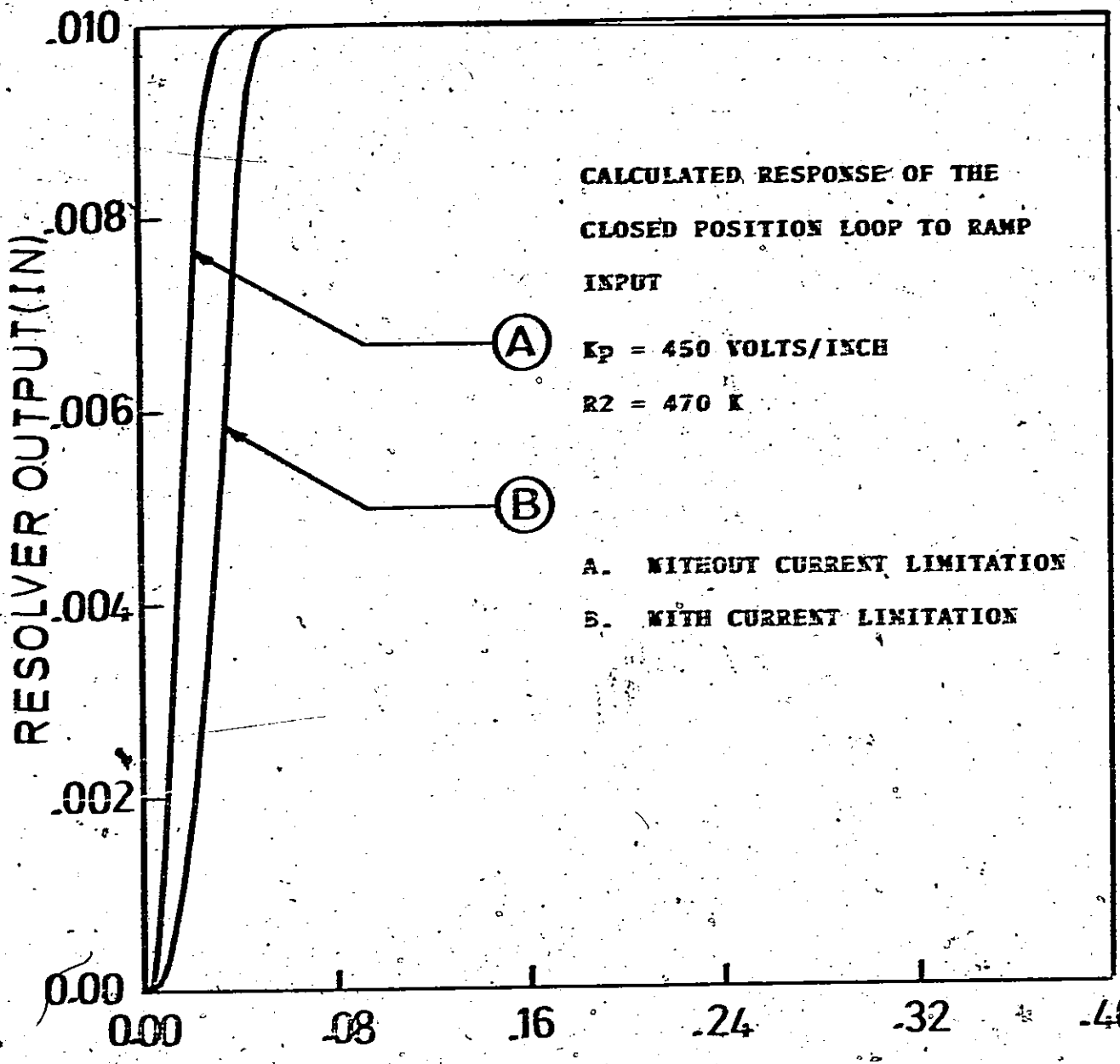
.010
.008
.006
.004
.002
0.00
RESOLVER OUTPUT(IN)
0.00
.08
.16
.24
.32
.40
SEC.
CALCULATED RESPONSE OF THE CLOSED POSITION LOOP TO RAMP INPUT
K_P = 450 VOLTS/INCH
R2 = 470 K
A
B
A. WITHOUT CURRENT LIMITATION
B. WITH CURRENT LIMITATION

FIGURE 49

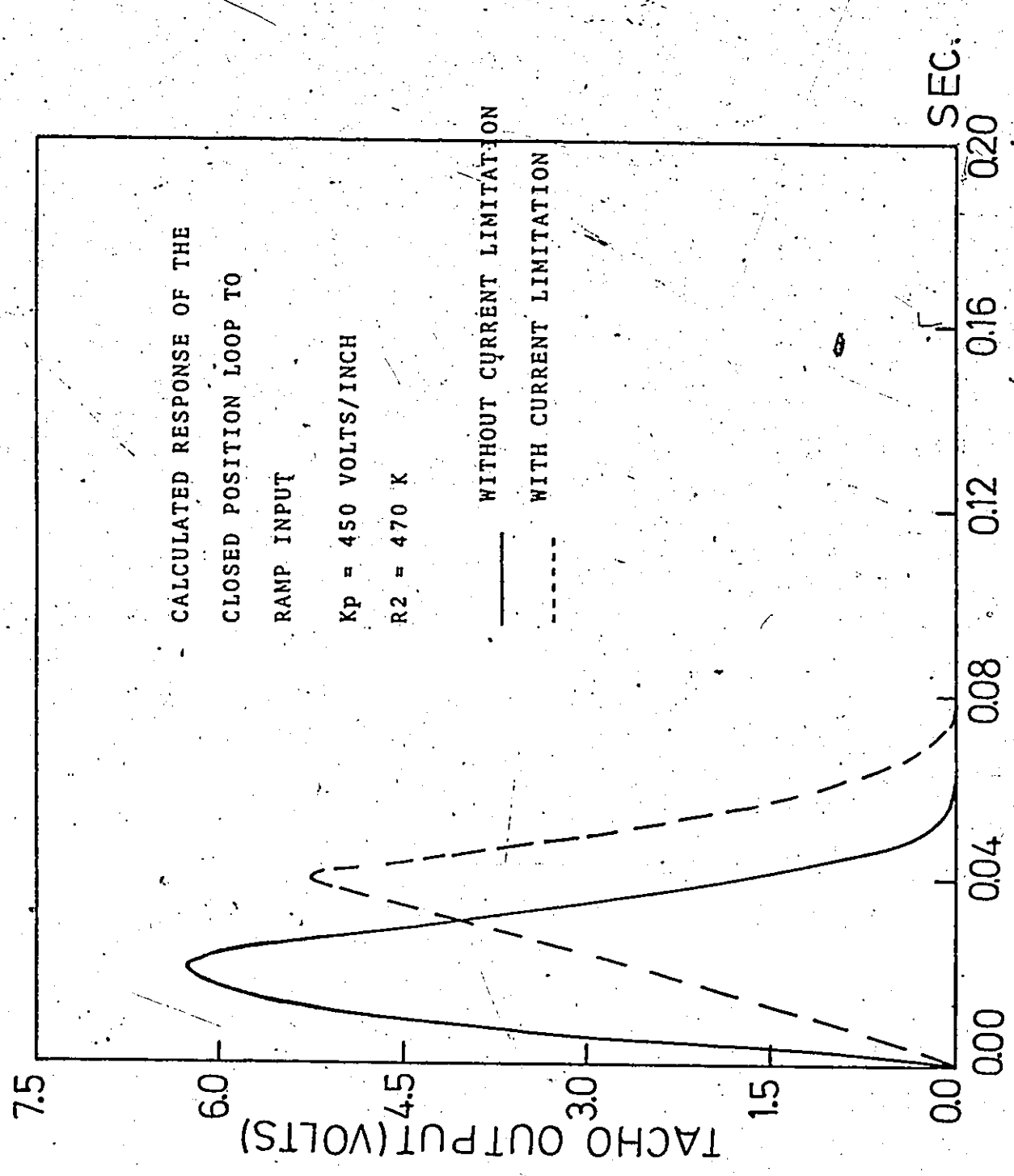
CALCULATED RESPONSE OF THE
CLOSED POSITION LOOP TO
RAMP INPUT
Kp = 450 VOLTS/INCH
R2 = 470 K
WITHOUT CURRENT LIMITATION
WITH CURRENT LIMITATION
TACHO OUTPUT (VOLTS)
7.5
6.0
4.5
3.0
1.5
0.0
0.00
0.04
0.08
0.12
0.16
0.20
SEC.

FIGURE 50

3.5 Measurements of the Closed Position Loop

The results obtained so far were verified experimentally. Figure 51 shows the response of the tacho to a ramp input described by a ramp height of 0.01 inch at a ramp speed of 5 inch/min. The gain in the position loop was next increased four times in order to compare the results with the ones obtained previously from the theoretical analysis. Figure 52 shows a schematic diagram of the low pass filter used to smooth the signal coming from the D/A converter. It was judjed, that by changing the gain of the filter one is able to increase the overall gain in the position loop. The transfer function of the filter is:

$$T_f(s) = -\frac{R}{R1}\left[\frac{1}{1 + jwRC}\right]$$

In order to increase the gain both R and C had to be changed. The frequency characteristics of this network is shown in figure 53. The voltage gain decreases rapidly above $\frac{1}{RC}$ and this obviously serves as a low pass filter.

The response of the tacho to the previously mentioned ramp input with a four times increase in the position loop gain is next shown in figure 54. As expected the system suffered oscillations of considerable magnitude. This agrees rather well with the results obtained from using the simulation technique. Figures 55 and 56 show the tacho output for values of R2 = 33K and 47K respectively. The time required to reach the steady state as measured

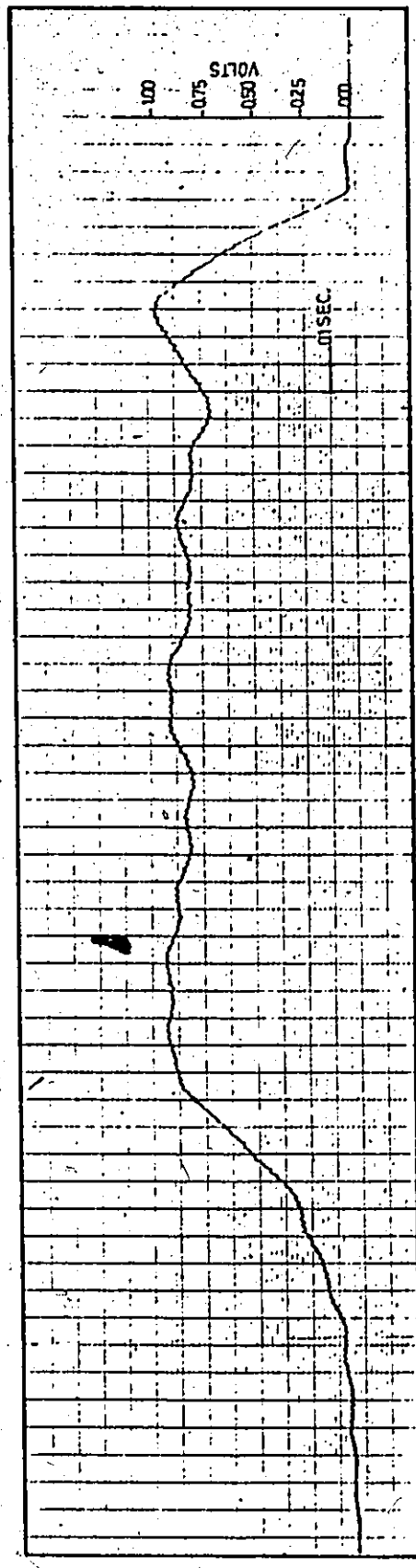

MEASURED RESPONSE OF THE N/C LOOP TO A RAMP INPUT

(Tacho Output)

K_p = 45.0 V/INCH

R_2 = 22K

R_4 = 46K

FIGURE 51

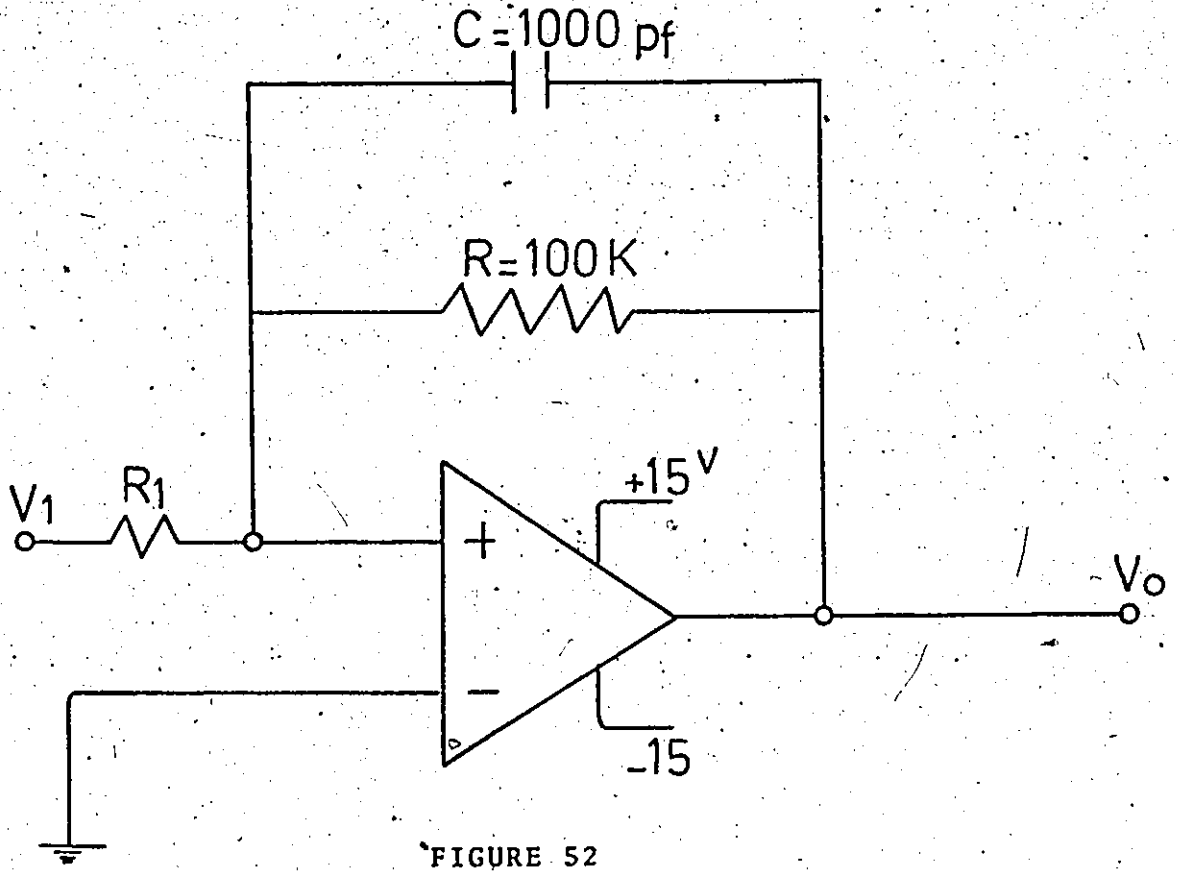

FIGURE 52

LOW PASS FILTER SCHEMATIC DIAGRAM

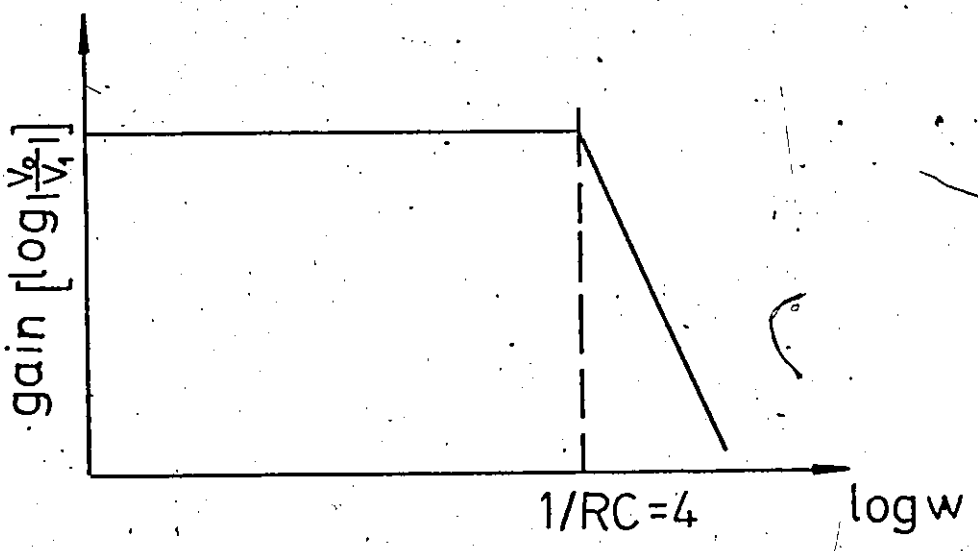

FIGURE 53

FREQUENCY RESPONSE OF THE LOW PASS FILTER

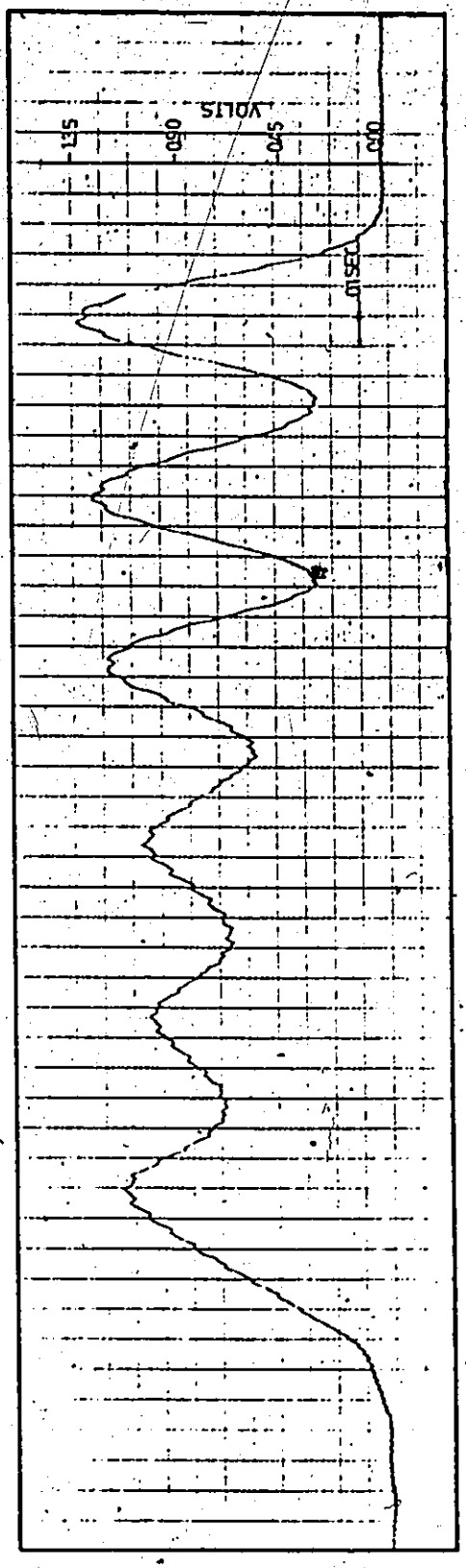

MEASURED RESPONSE OF THE N/C LOOP TO A RAMP INPUT
(Tacho Output).

K_p = 180 V/INCH
R_2 = .22K
R_4 = 46K

FIGURE 54

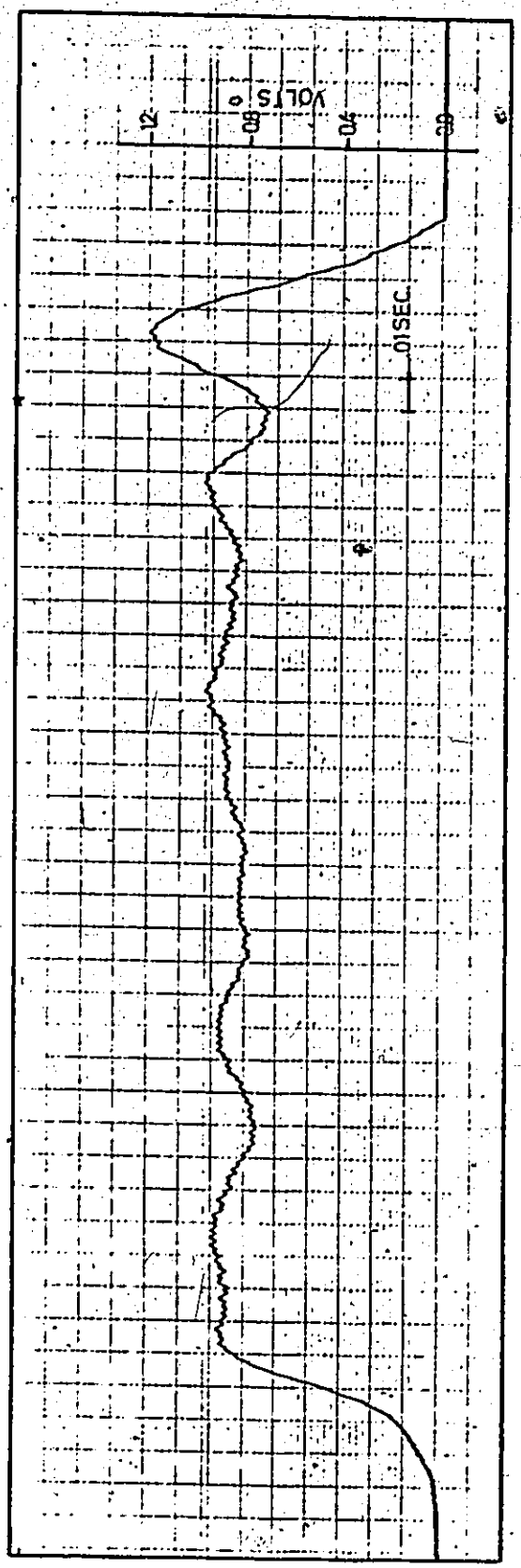

MEASURED RESPONSE OF THE N/C LOOP TO A RAMP INPUT
(Tacho Output)

K_p = 180 V/INCH

R_2 = 33K

R_4 = 46K

FIGURE 55

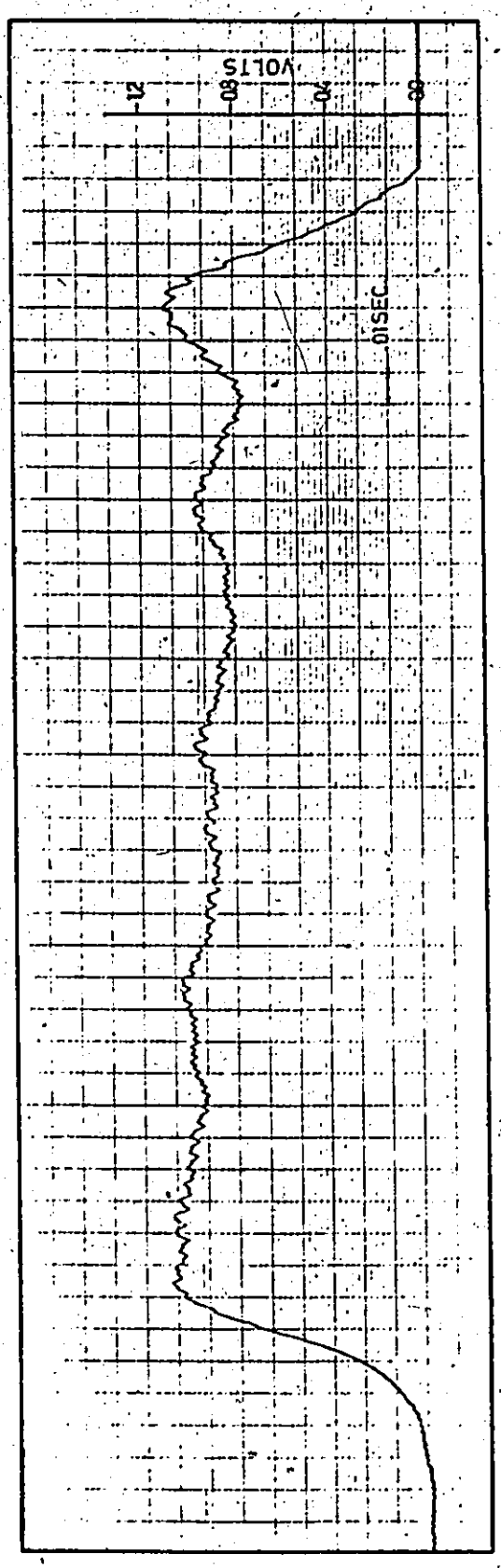

MEASURED RESPONSE OF THE N/C LOOP TO A RAMP INPUT
(Tacho Output)

K_p = 180 V/INCH
R_2 = 47K
R_4 = 46K

FIGURE 56

from figure 56 is 28 milliseconds as compared with 42 milliseconds measured in figure 51 for the system with the original gain. The later two cases also showed considerable decrease in the magnitude of oscillations observed in the case presented in figure 54.

The tacho output for a positional gain increased four times and R4 decreased to 10K while R2 is left unaltered i.e. equal to 22 K is next shown in figure 57. Almost the same response obtained from increasing R2 could be obtained also from decreasing R4.

Finally, a case where the positional gain is increased 4 times its original value along with R2 increased to 33K and R4 decreased to 10K is presented in figure 58. The time required to reach the steady state is measured equal to 35 milliseconds. The amount of damping in the later case was considered quite satisfactory. These tests thus agreed rather well with the results obtained from the theoretical analysis and certainly gave some insight about the nature of the system behaviour for higher values of gains which could be used in order to improve its response.

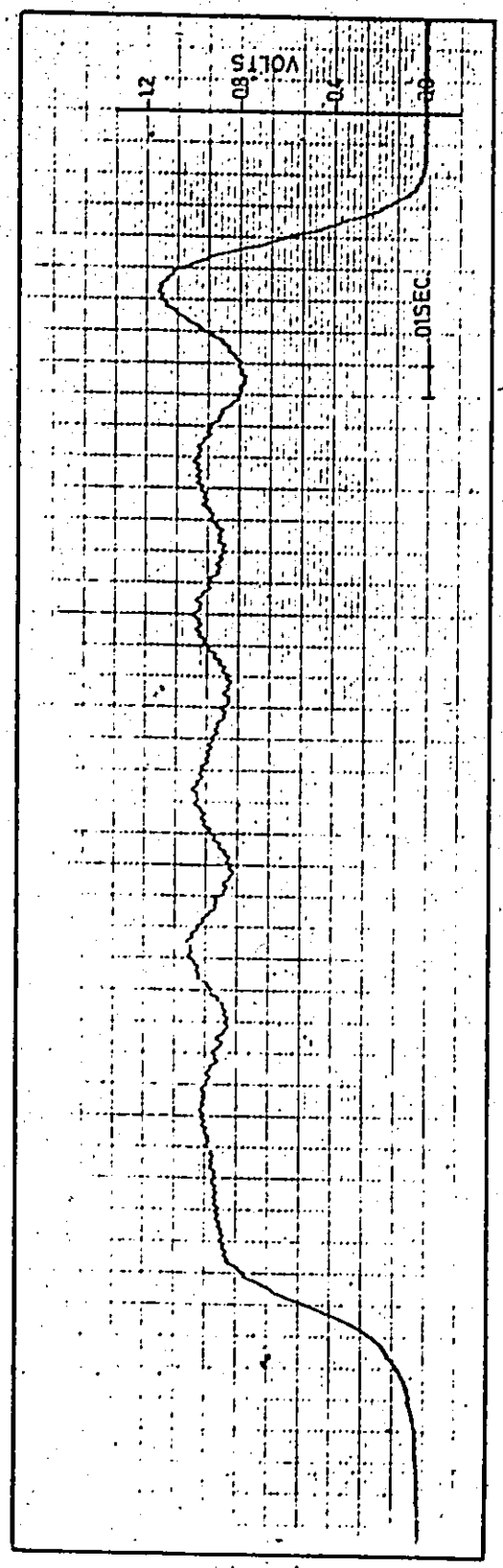

MEASURED RESPONSE OF THE N/C LOOP TO A RAMP INPUT

(Tacho Output)

K_p = 180 V/INCH

R_2 = 22K

R_4 = 10K

FIGURE 57

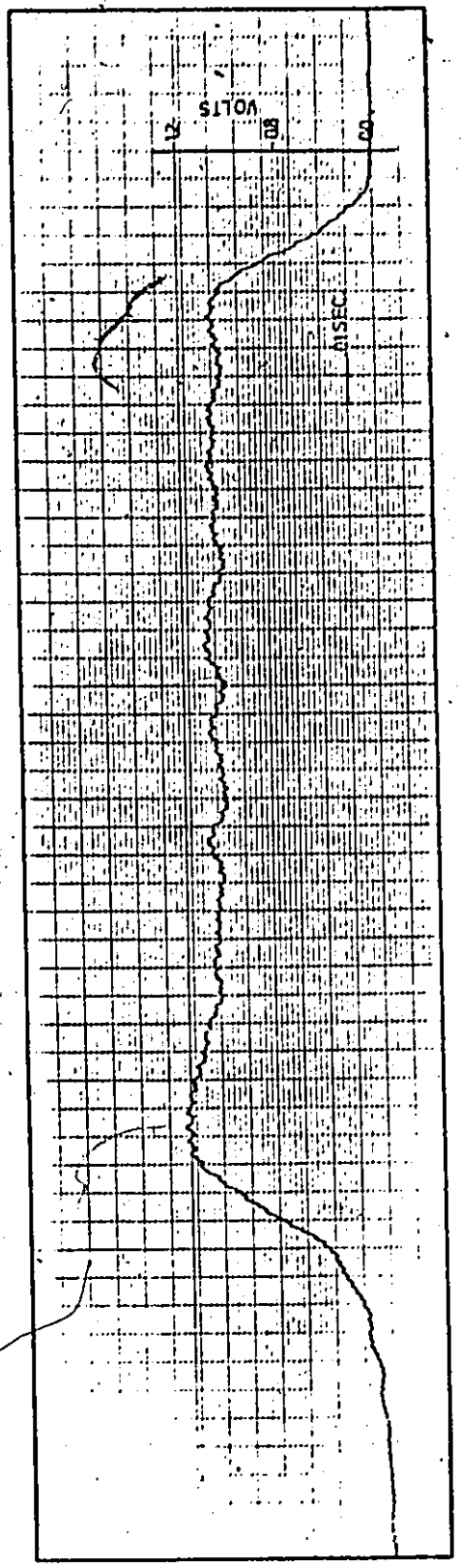

MEASURED RESPONSE OF THE N/C LOOP TO A RAMP INPUT

(Tacho Output)

K_p = 180 V/INCH

R_2 = 33K

R_4 = 10K

FIGURE 58

CHAPTER 4

THE ADAPTIVE CONTROL SYSTEM

4.1 Introduction

The development of an adaptive control (AC) system for an NC milling machine was described in references 7, 8 and 10. The system has four major components; a milling machine, a mini computer, an instrumentation system for the AC and a device which interfaces the computer and the milling machine termed as a controller. A block diagram representation of the CNC/AC system, including its three main functions: measurement, decision and implementation is shown in figure 59. In the system, two components of cutting force are measured by means of a transducer attached to the spindle of the milling machine. The sensor outputs (F1 and F2) are fed through an analog-to-digital processor (ADP) to the computer, where a resultant force in the plane of the table is calculated from the relationship:

$$\text{FORCE} = \sqrt{F_1^2 + F_2^2}$$

The computer handles two programs: NC and AC programs.[7,8] The interrupt system of the computer takes care of the simultaneous running of both programs. The AC program

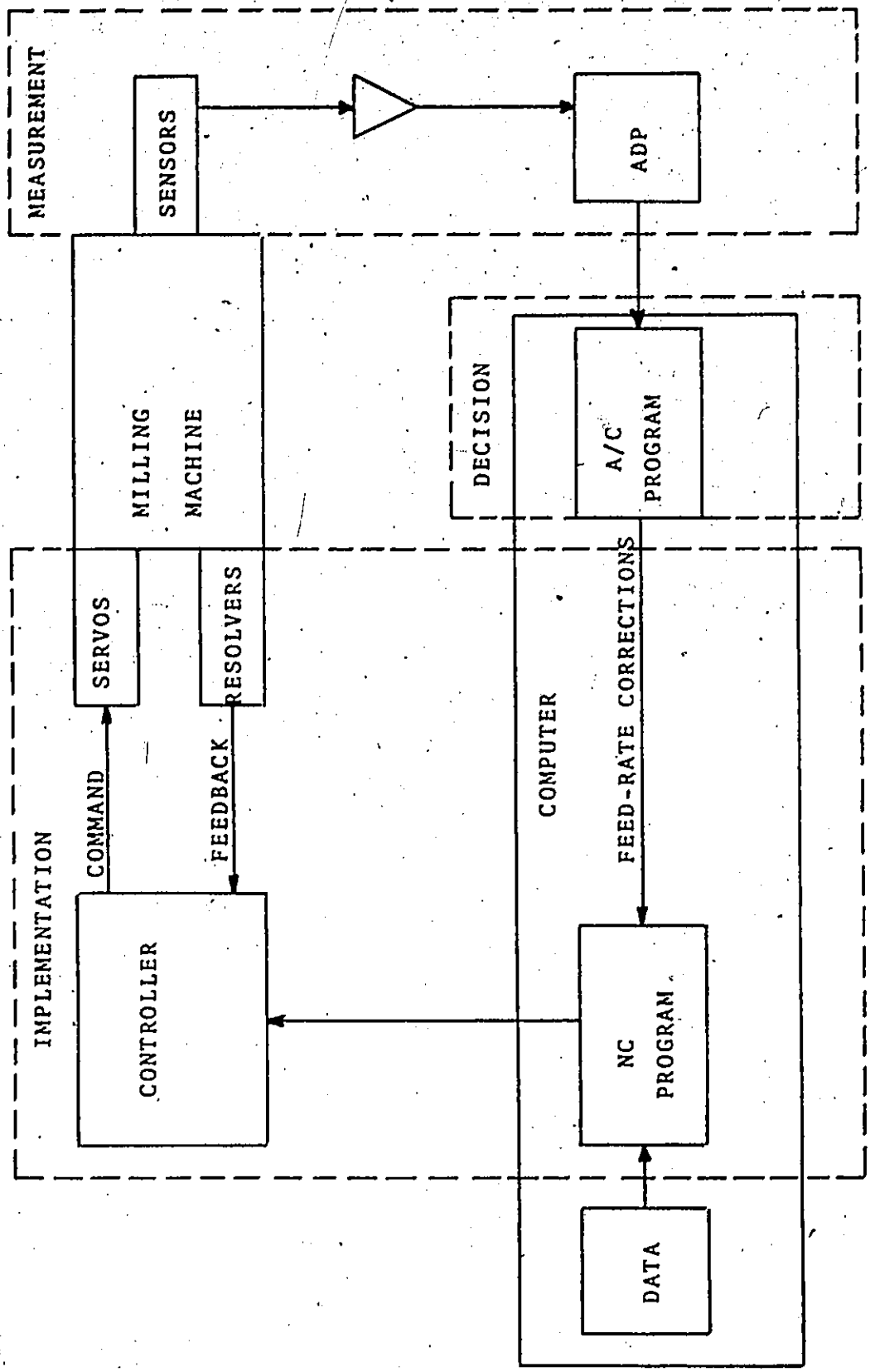

BLOCK DIAGRAM OF THE A/C SYSTEM

FIGURE 59

accepts the sensor outputs and uses them to calculate a feed-rate correction which is supplied to the NC program.

First, the value of the actual force is compared with a proselected nominal force to determine a relative error

$$\text{ERROR} = \frac{F_{nominal} - F_{actual}}{F_{nominal}}$$

The new commanded feed rate is then based on the previous one according to the equation:

$$f_{new} = f_{old} + K_{ac} \cdot \Psi\,(\text{ERROR})$$

where

f_{new} is the new commanded feed rate

f_{old} is the previous commanded feed rate

K_{ac} is the AC gain

Ψ is a function of the error

The corrections are provided continuously throughout the cutting process in order to maintain a maximum permissible feed rate compatible with the limitations imposed by the strength of the cutter, despite unpredictable variations in machining conditions.

The actual force is sampled in intervals, approximately every 10 msec. The number 10 msec was arrived at by assuming that the maximum spindle speed which would be used (for steel machining) is 600 rpm and at least 10 samples of measurements would be required per evolution

of the spindle.

The complete CNC/AC system is first analysed using various techniques of the classical linear control theory. The simulation technique is also used in order to explore ways of how to improve the performance of the system. Two different strategies are investigated, and the system response is computer plotted in each case simulated.

4.2 Mathematical Analysis of the Loop

Figure 60 shows a simplified block diagram of the complete CNC/AC system. It can be seen that the AC loop represents another feedback loop in the system. Within the new loop are three elements. The first element is the cutting process which produces a cutting force dependent upon the cutting conditions. The dynamics of the transfer function between table velocity (feed rate) and the cutting force F seriously affects the behaviour of the system. "There are three aspects of this dynamics: the variation of the cutting force in a steady state of constant depth and width of cut, in the transients (e.g. entry of the cutter into the workpiece) and the time delay included in this transfer function." [26]

However, in the analysis that follows, it is assumed that for a given depth of cut a, width of cut b (Figure 61) and spindle speed n, the cutting force is

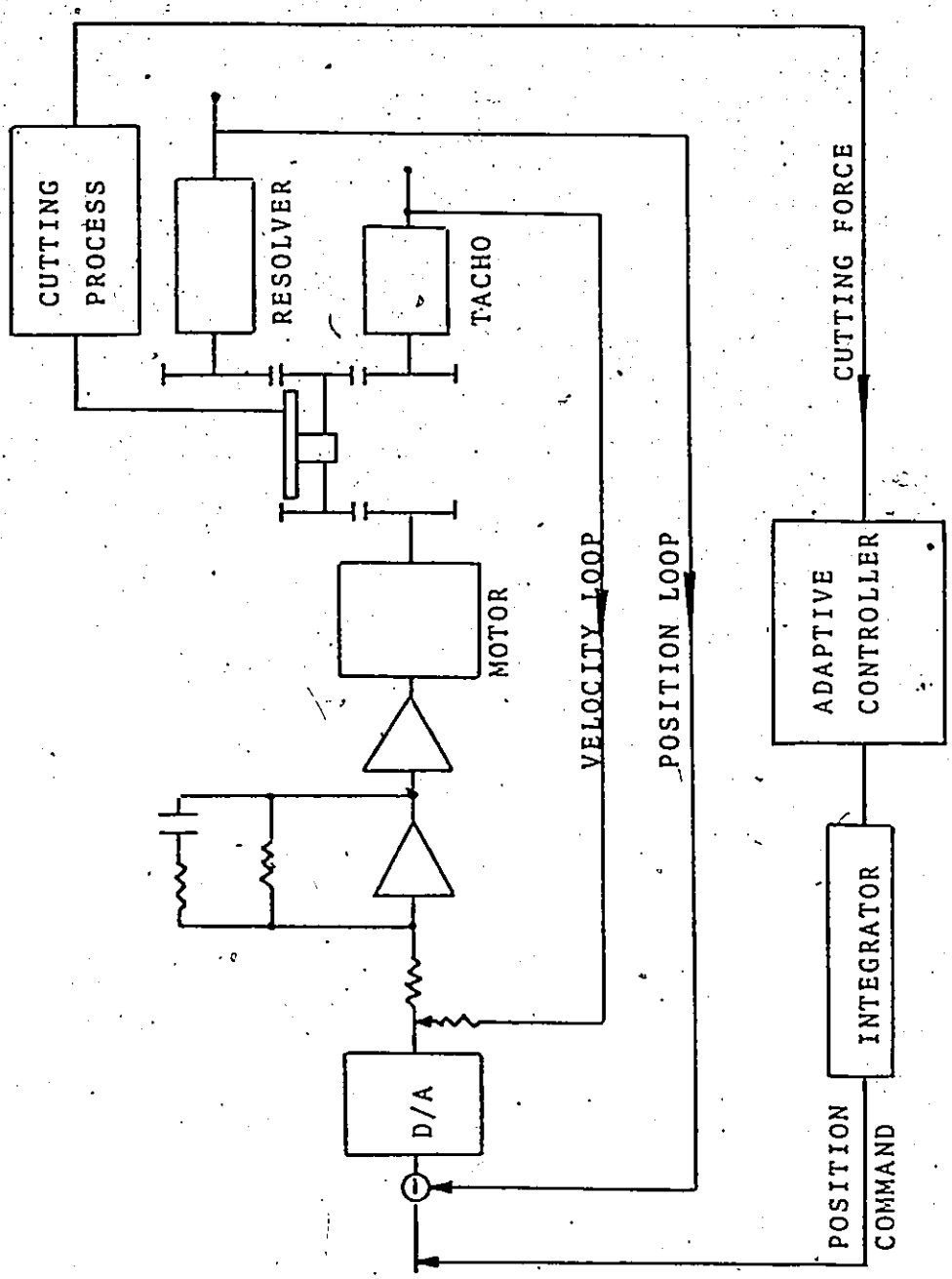
CUTTING PROCESS
RESOLVER
TACHO
MOTOR
VELOCITY LOOP
POSITION LOOP
CUTTING FORCE
ADAPTIVE CONTROLLER
INTEGRATOR
D/A
POSITION COMMAND
ADAPTIVE CONTROL LOOP

FIGURE 60

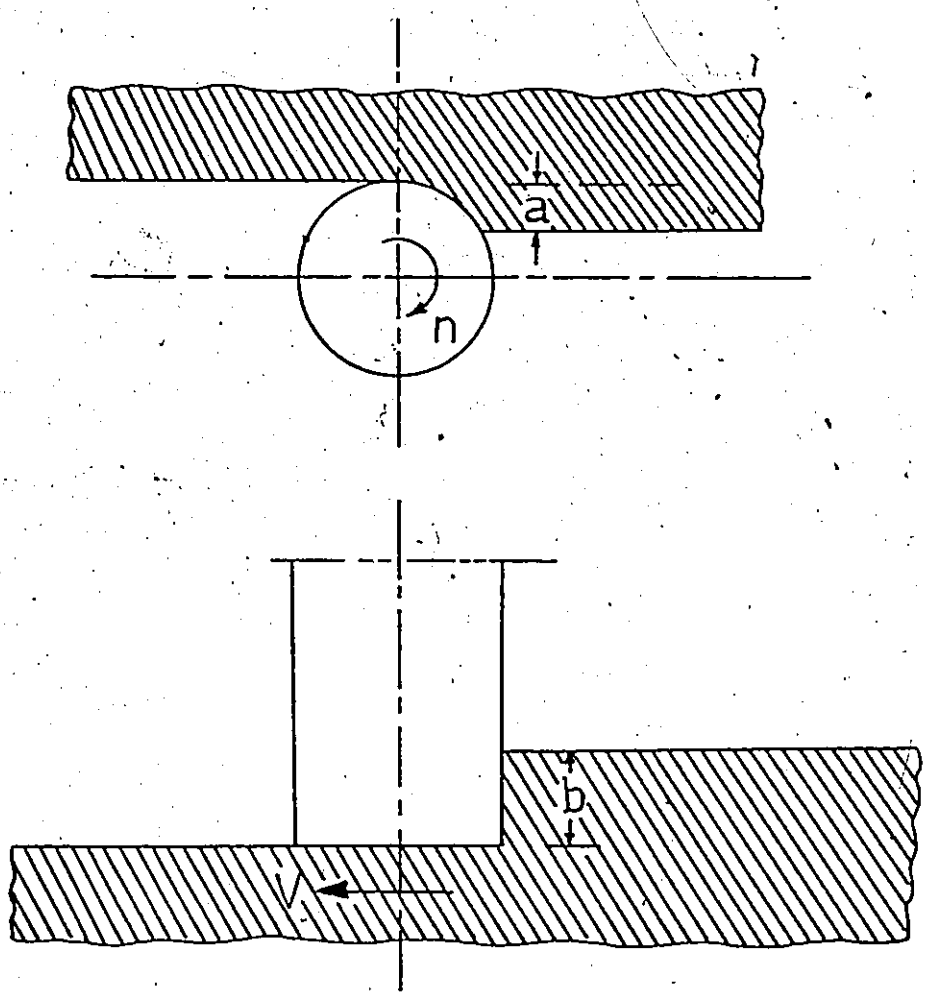

MILLING CONFIGURATION

FIGURE 61

proportional to the feed per tooth S_t, which itself is obtained as:

$$S_t = \frac{v}{n \times Z}$$

where v is the table velocity (feed rate), n/min is spindle speed and Z is the number of teeth of the cutter. Accordingly, in the simplest case:

$$F = c.v$$

where c is a constant. Furthermore, it may be shown that there is a time delay included in this relationship.

Figure 62 illustrates what happens in the case of a two flutted cutter milling with full diameter (slotting). For simplification, the sinusoidal variation of the chip thickness is neglected, and every tooth is assumed moving along a straight line across the machined surface while it simultaneously moves with constant feed velocity. As spon as one tooth left the cut at the bottom the next tooth starts to cut at the top at the same x-position. At the beginning the feed per tooth is S_{t_1}. From point M on the feed velocity is doubled so that the new established feed per tooth $S_{t_2} = 2S_{t_1}$. From point M on the chip thickness (shown dashed) starts to increase until in point N, one tooth period later, it reaches fully the new value S_{t_2}. Thus, it is obvious that a sudden increase in table velocity produces a corresponding change in the resulting force fully after a delay of one tooth period. Figure 63

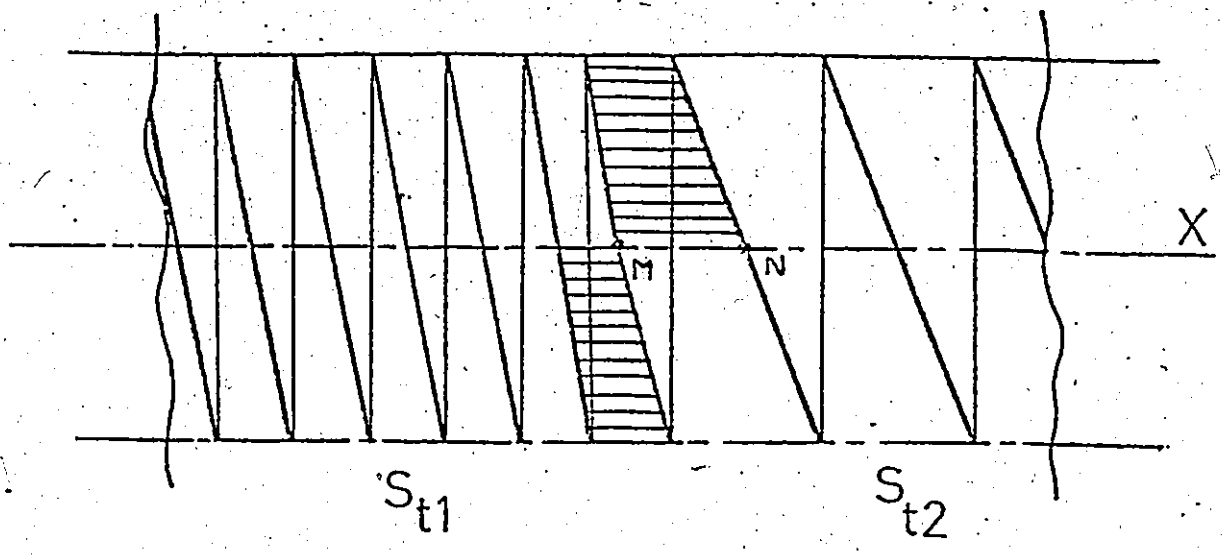

VARIATION OF CHIP THICKNESS DUE TO SUDDEN CHANGE IN FEED RATE (Case A)

FIGURE 62

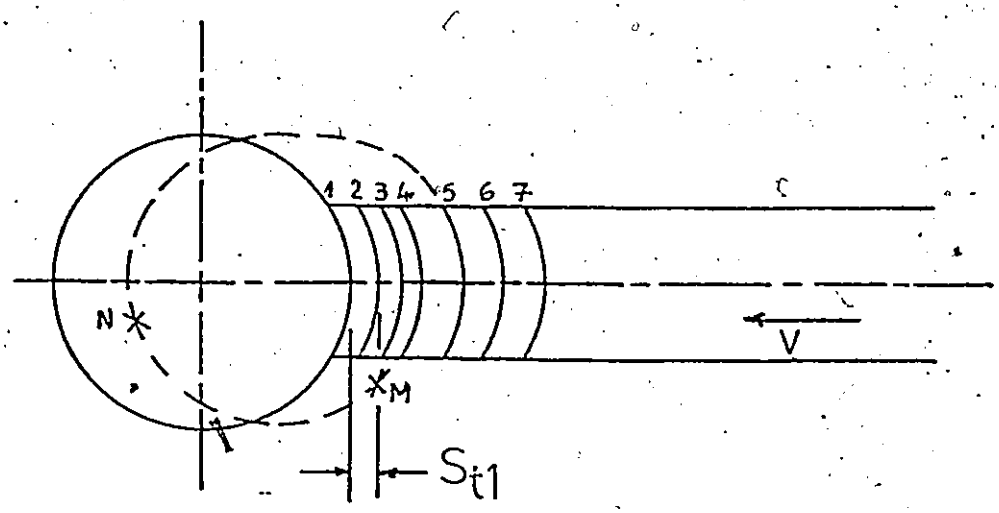

VARIATION OF CHIP THICKNESS DUE TO SUDDEN CHANGE IN FEED RATE (Case B)

FIGURE 63

illustrates a case where the corresponding change in the resulting force occurs after a delay of one and half tooth period. To conclude the relationship between the cutting force and the table velocity may be more correctly written in the form

$$F(t) = c.v(t-\tau_L)$$

where τ_L is the time lag between the cutting force F and the table velocity v.

The second element of the A/C loop may be termed the adaptive controller. This function is performed by the adaptive control algorithm in the HP-2100 mini-computer. As previously discussed, it determines the error between the actual and desired forces and calculates a corrected feed rate command based upon this error. In the analysis that follows it was assumed that the correction factor is linearly dependent on the error.

i.e. $$f_{new} = f_{old} + K_{ac} \cdot error$$

The third element of the AC loop was added to convert the feed rate command into a distance command, thus it is basically an integrator. In order to be able to apply the classical control theory in the analysis, the system is first assumed linear, i.e. the sampling interval in the A/C loop and the time lag between the force and feed rate were neglected. Secondly, the cutting force produced during the cutting process was assumed directly

proportional to the feed rate while the constant of proportionality was always assumed fixed.

For the purpose of analysing the system using various techniques of the classical control theory, the block diagram of figure 60 was altered in the manner shown in figure 64. In the latter case the open loop transfer function written as a function of the A/C gain K_{ac} and neglecting the time lag between the cutting force and the table velocity is:

$$G(S) = 7977.15\ K_{ac}\ \frac{(S+45.45)}{S(S+23.45)(S^2+72.34\ S+2560.38)}$$

The system has a unity feedback element. The root locus plot shown in figure 65 is next used to investigate the transient behaviour of this loop. Assuming first that K_{ac} is equal to unity in the expression of the open loop transfer function; the marginal gain found was 95725.80 which corresponds to an A/C gain $K_{ac} = 12.0$. Further investigation of the root locus plot showed that starting with $K_{ac} = 1.0$, four complex and conjugate roots govern the transient behaviour of the system, yielding sinusoidal exponentially decaying terms in the time domain. Increasing the A/C gain should obviously result in a faster response, however, at the expense of the amount of damping in the system.

At this point of the analysis, it is worthwhile to investigate the frequency characteristics of the system. Figure 66 shows the Bode plot of the open loop where K_{ac}

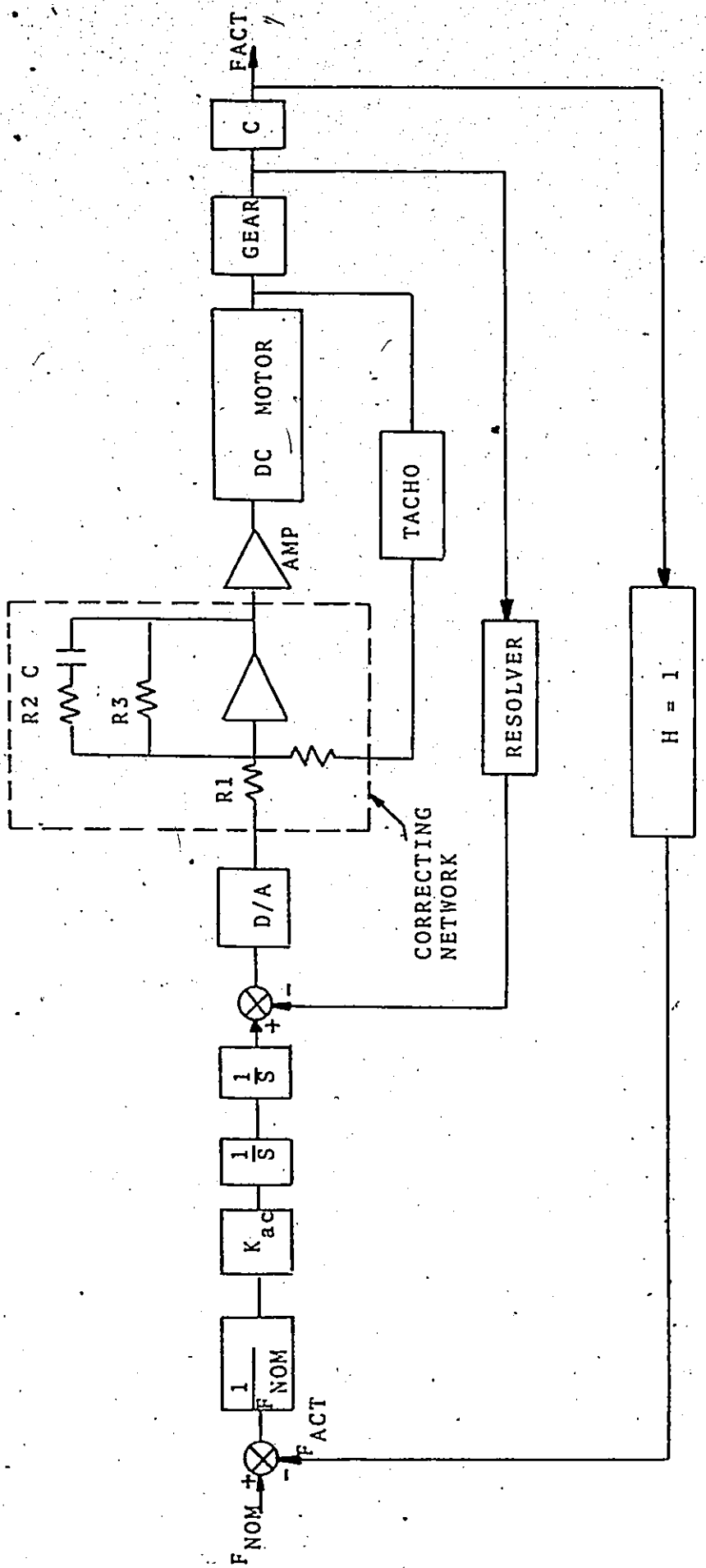

FIGURE 64

ALTERATION TO THE BLOCK DIAGRAM OF THE CNC-AC SYSTEM

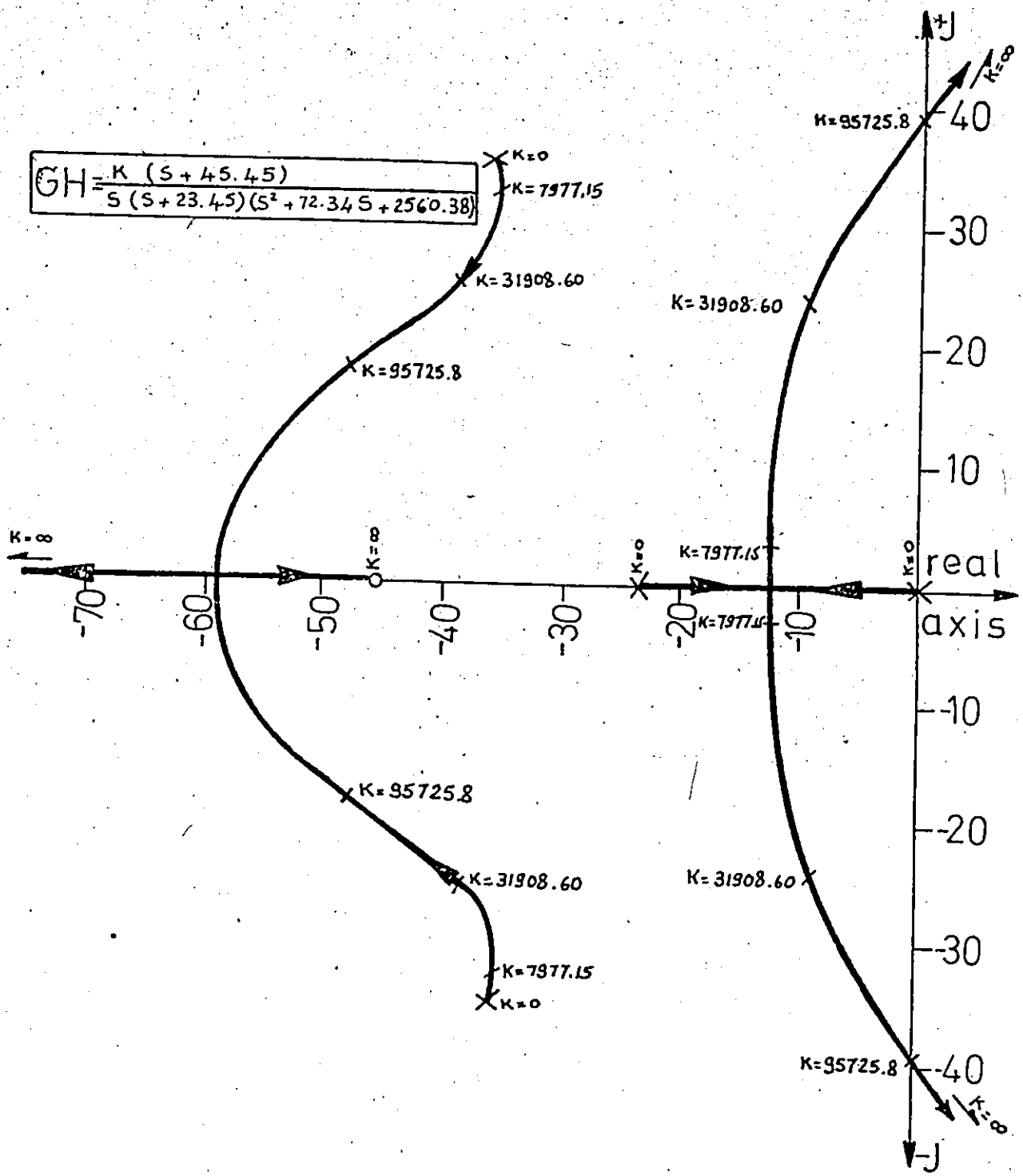

ROOT LOCUS PLOT OF THE LINEARIZED A/C SYSTEM

FIGURE 65

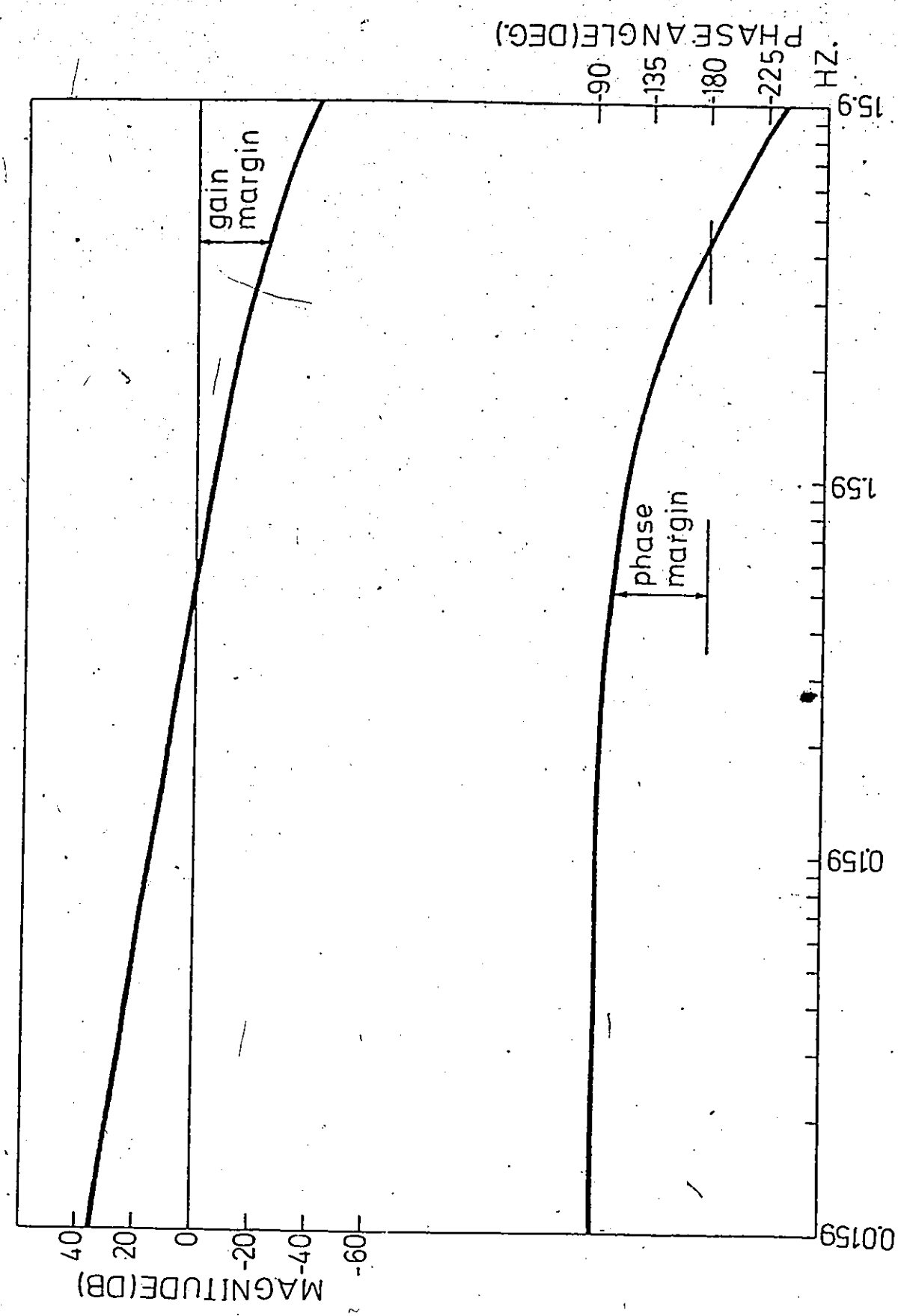

BODE PLOT OF THE LINEARIZED A/C SYSTEM

FIGURE 66

is again considered equal to unity. Obviously, adjustment of the gain does not affect the phase angle plot, thus only the magnitude will be adjusted.

Figure 67 shows a stability analysis using a log-modulus plot. The A/C gain margin (K_M) is seen to be equal again to 12.0 and the phase margin "γ" to 74 degrees. The system has a gain cross-over frequency of 5.0 rad/sec. The effect of time-lag on the frequency response of the system was next investigated:

the transfer function of a pure time-lag factor is given by:

$$G(jw) = e^{-jw\tau_L}$$

The time-lag factor $e^{-jw\tau_L}$ results in a phase shift,

$$\phi\ (w) = -\ w\ \tau_L \text{ rad}$$

which has to be added to the phase shift resulting from the rest of the system. The magnitude of the time-lag factor is always unity and, therefore, does not affect the magnitude characteristics, however the time-lag factor produces a phase-lag and decreases the phase margin.

With a four-fluted cutter rotating at 500 rpm, a time-lag of 30 milliseconds is typical, while a time lag of 60 milliseconds may be caused by a two-fluted cutter rotating at 500 rpm.

The frequency response of the system when introducing these two values of time-lag was compared with the hypothetical case of no time lag in figure 68.

The following table shows the effect of the time lag

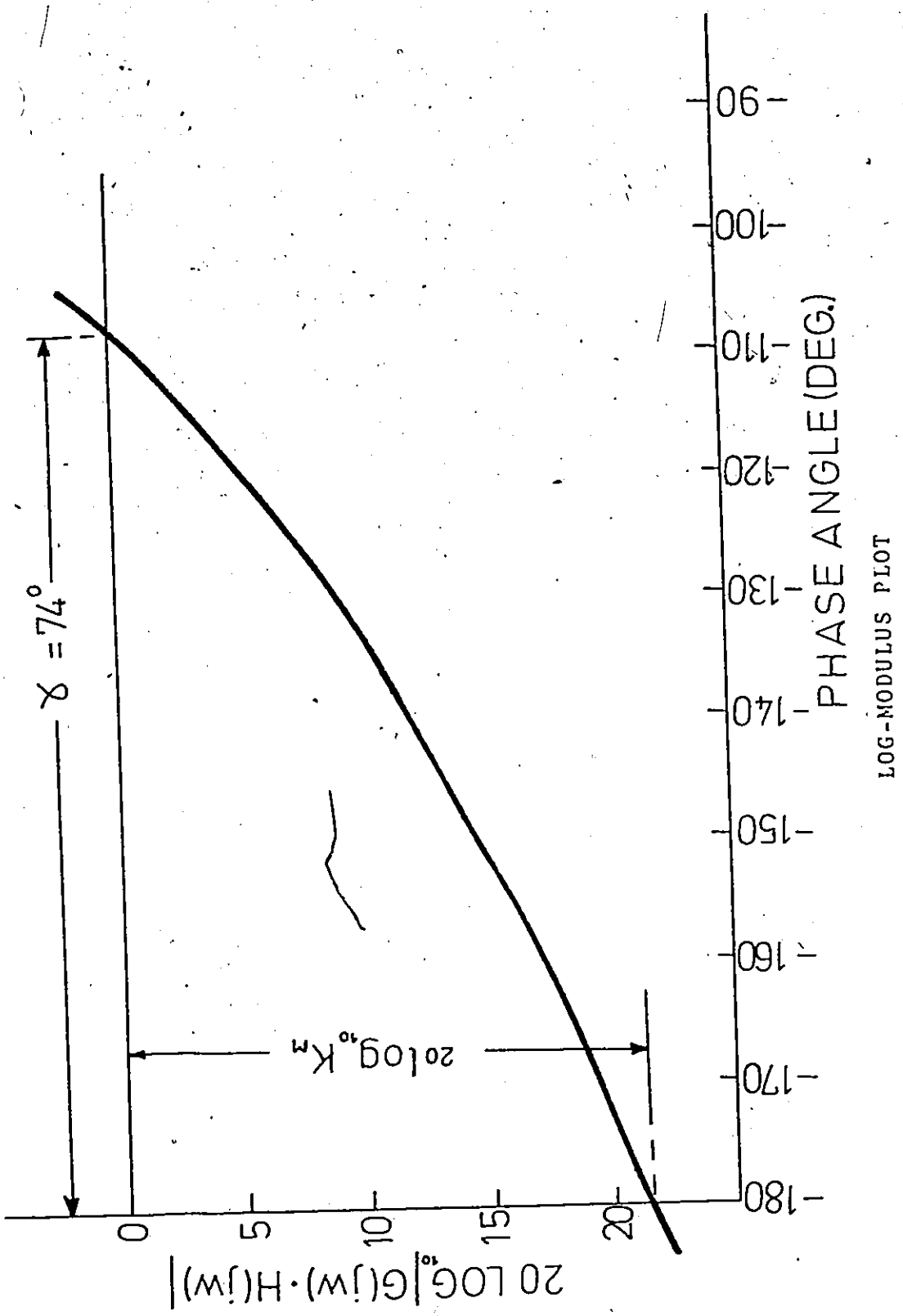
20 LOG10|G(jw)·H(jw)|
0
5
10
15
20
20log10Km
γ = 74°
-180
-170
-160
-150
-140
-130
-120
-110
-100
-90
PHASE ANGLE(DEG.)
LOG-MODULUS PLOT

FIGURE 67

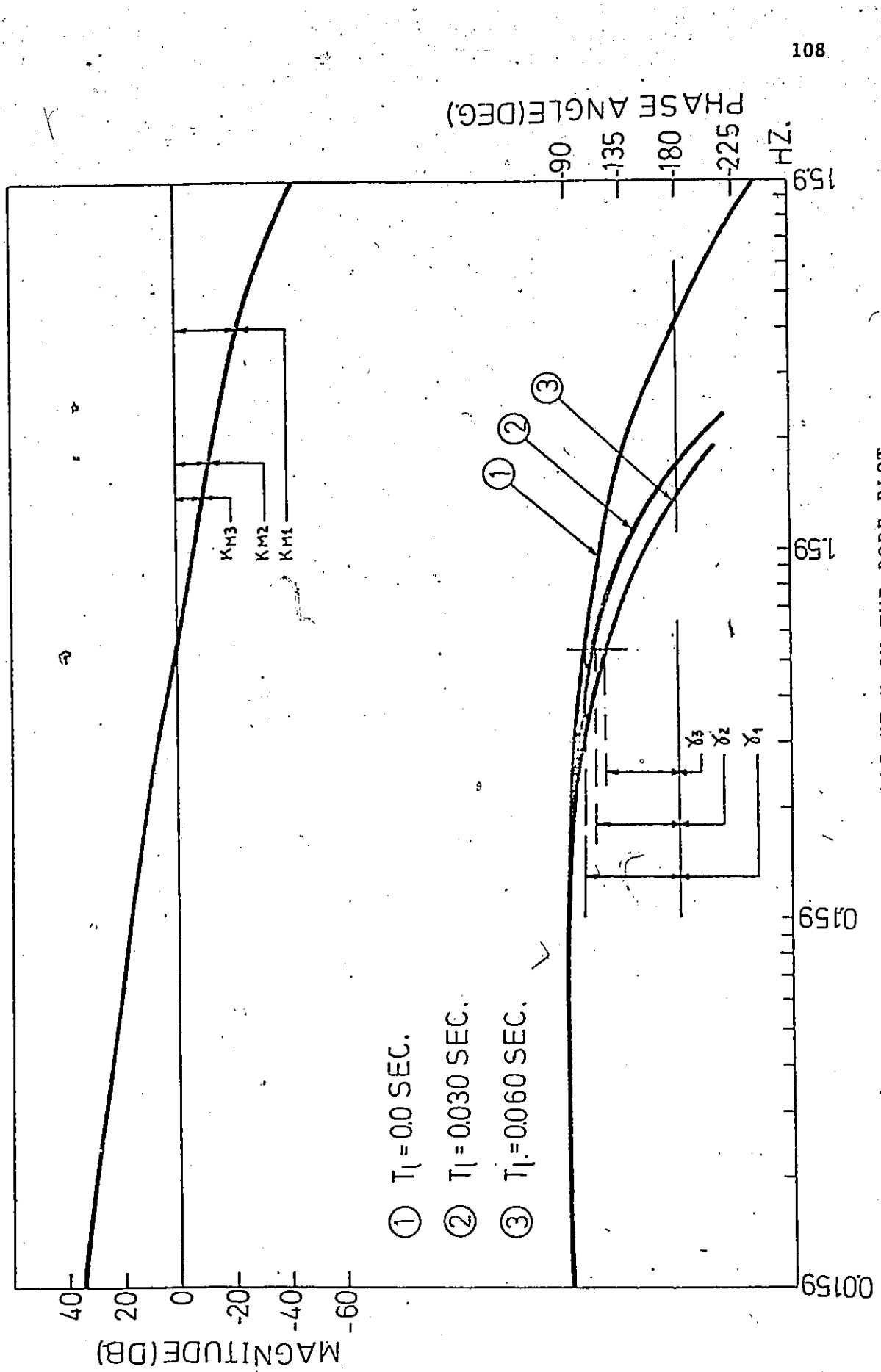

EFFECT OF THE TIME LAG "T_L" ON THE BODE PLOT

FIGURE 68

"τ_L" in the loop on both the A/C gain margin and the phase margin.

Time lag in Milliseconds	A/C Gain Margin K_M	Phase Margin γ
0.0	12.00	74^o
30	5.80	62^o
60	3.16	58^o

4.3. A/C Simulation

Figure 69 shows the block diagram of the entire CNC/AC system, where the new variables belonging to the AC loop were added in order to provide a complete set of variables for the purpose of simulation.

These variables are defined as follows:

1. x1 is the distance command in inches
2. x2 is the input to the correcting network in volts
3. x3 is the output of the correcting network in volts
4. x4 is an intermediate state space variable used in the correcting network state space representation
5. x5 is the output of the power amplifier in volts
6. x6 is the motor speed in rev/sec
7. x7 is the output of the resolver in inches
8. x8 is the output of the tacho in volts
9. x9 is the velocity feedback in volts
10. x10 is the output from the D/A converter and filter
11. x11 is the input to the D/A and filter

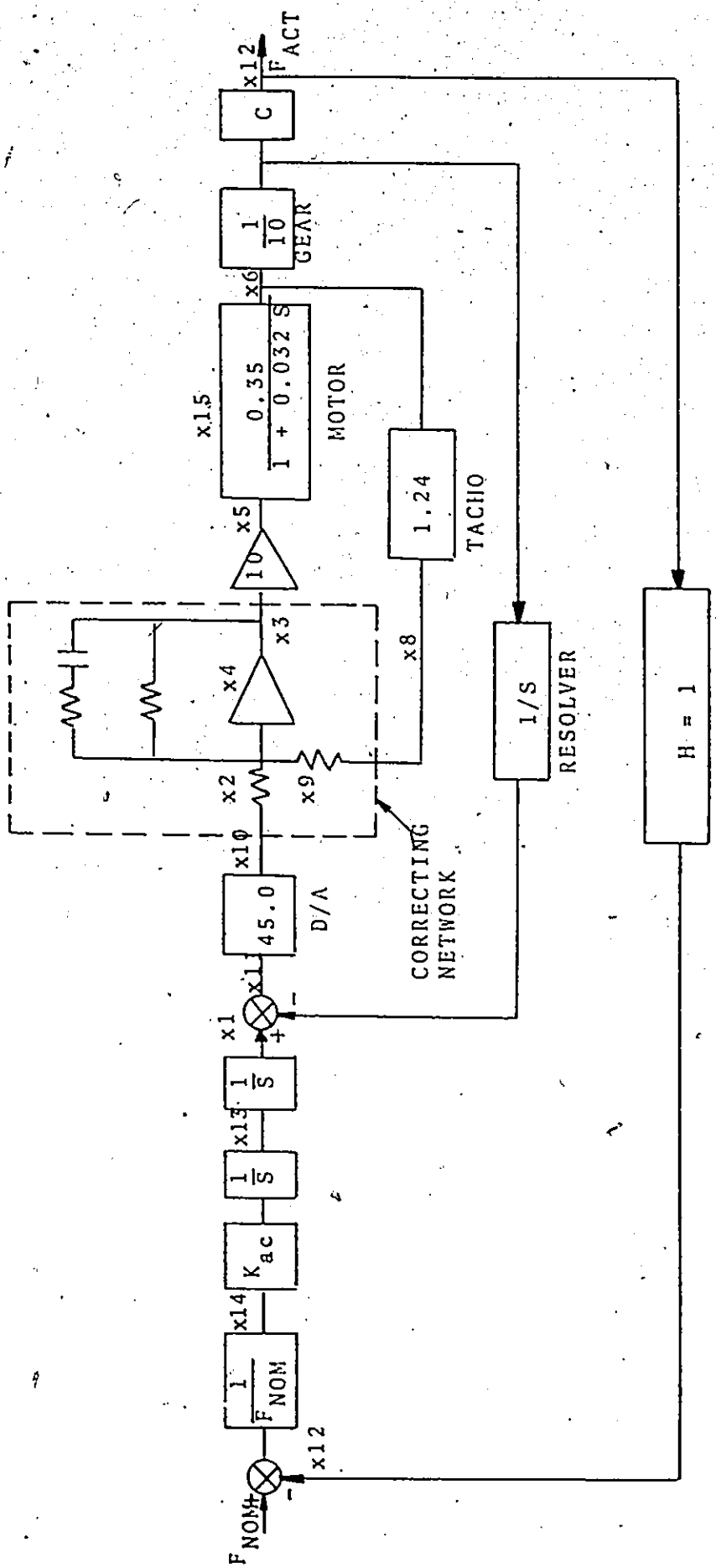

FIGURE 69

BLOCK DIAGRAM OF THE CNC-A/C SYSTEM "THE STATE-SPACE 'SYSTEM

12. x12 is the cutting force in pounds
13. x13 is the new commanded feed rate in inches/sec
14. x14 is the error
15. x15 is the current analog signal in volts

For the purpose of simulation of the complete control function, a set of initial conditions were first generated. This set represents the steady-state operation of the NC loop alone as determined by the NC simulation.

The actual table velocity resulting from the steady-state operation of the NC loop causes a case of excessive cutting force. This is further explained as follows:
Let the actual velocity resulting from the NC simulation be:

x6/10 = 0.8531 inches/sec

For simplicity, the cutting force is assumed directly proportional to the feed rate; i.e.:

x12 = c. x6/10

where c is a constant arbitrary chosen 1200 lb/inch/sec
Accordingly, x12 = 1023.72 lbs.
A nominal or optimal force "FNOM" is again arbitrary taken as:

FNOM = 200 lbs.

Practically, in the adaptive control mode of operation of the milling machine, an AC auxilliary routine "initialization routine)[7] is used to determine the "optimal" force. The formula used for calculating the "optimal" force is based on the assumption that a circular cylinder may be a crude

approximation to the shape of an end mill.[7,8]

The equation used is:

$$F_{max} = \frac{\sigma_{ys} \cdot \pi \cdot D^3}{32 \cdot L} \qquad (1b)$$

where σ_{ys} = yield strength of high speed steel

D = diameter of cutter

L = length of cutter

using,

$$\sigma_{ys} = 1.2 \times 10^5 \text{ lb/in}^2$$

Accordingly,

$$F_{max} = 1.178.10^4 \frac{D^3}{L} \qquad (1b)$$

Also, there exists a constraint equation governing the maximum force, the milling machine can apply:

$$F_{MACH} = 2560 \text{ lbs.}$$

The smaller of the two calculated forces is then considered as the optimum force. However, only 80% of the calculated "optimum" is used in the AC routine.

The AC loop is then suddenly attached to the NC loop, which in other words also means a step input in FNOM. The complete CNC-AC system is then allowed to react to the initial error x14. Referring to Figure 69, the following formulae are used to simulate the entire operation of the system:

the cutting process is described by

$$x12(t) = 0.1c \cdot x6(t - \tau_L)$$

where τ_L is the force time lag

Accordingly,

$$x14 = 1 - \frac{x12}{FNOM}$$

Next, an acceleration command "ACC" or a (correction factor) directly proportional to the force error is generated;

$$ACC = K_{ac} \cdot x14$$

where K_{ac} is the proportionality constant or the A/C gain.

The A/C algorithm calculates a new feed rate approximately every 10.5 milliseconds. The time delay between feed rate corrections "$\tau\alpha$" is measured by a software counter which counts the number of assembly language instructions which have been executed; each instruction requiring approximately 2 microseconds. When the software counter indicates that a feed rate correction is required, the resultant force and force error are calculated. A change in feed rate which is proportional to the force error is then calculated.

Accordingly, the new feed command is:

$$x13(t) = x13(t-\tau_d) + ACC * \tau_d$$

It should be noted here that τ_d also represents the force sampling intervals.

The commanded feed rate must be between the limits of a maximum and a minimum value of the allowable feed rate of the milling machine. The obtained feed rate is checked to see whether it exceeds the extreme limits. If it does,

the limit which was exceeded will be used as the new feed rate. These limits are 30 and 0.3 ipm for maximum and minimum allowable feed rates respectively.

A new element in the AC loop must be added to convert the feed rate command into a distance command added to x1. Thus, it is an integrator, determining the addition to x1 over each basic time increment.
The expression for this is:

$$x1(t) = x1(t - T) + x13(t) \cdot T$$

where T is the basic time increment in the state-space analysis.

This integrator is actually resident within the CNC computer routine. The basic time increment in the system T was taken equal to an integer fraction of the forc sampling interval (2.1 milliseconds). The set of equations describing the operation of the NC loop is next added to the previous ones describing the A/C policy. Both of them simulate the entire operation of the complete CNC-AC system. The computer simulation routine used generates a plot of the resultant cutting force versus time.

At this point of the discussion, it is worthwhile to note that the cutting force is first assumed directly proportional to the table velocity. Also, the system is allowed to react to the initial error without imposing any constraints on the new commanded feed rate, accordingly the CNC — AC control system is once again considered basically

a linear system.

The results of simulating a set of hypothetical cases where no time lag is assumed between the cutting force and the commanded feed rate and in the meantime the time delay between feed rate corrections "τ_d" is neglected, are next discussed. Figures 70, 71 and 72 illustrate plots of the resultant cutting force for an A/C gain of 4.0, 6.0 and 12.0 respectively. As shown in figure 72, instability starts occurring at K_{ac} = 12.0 which agrees rather well with the results obtained from investigating the root locus and Bode plots of the system as discussed in section 4.2. However, even for K_{ac} = 4.0, a considerable amount of overshoot occured when a time lag in the cutting force formula τ_L = 30 milliseconds was considered, the system turned unstable for K_{ac} = 6.0. For a time lag τ_L = 60 milliseconds instability occured at K_{ac} = 4.0 as shown in figures 73 and 74. This certainly gave some insight into the effect of this time lag on the overall performance of the system.

In the following simulated cases, the sampling interval of 10.5 milliseconds between feed rate corrections is introduced in the model along with two constraints of minimum and maximum allowable feed rates as well as the constraint on maximum current which was discussed previously in Chapter 3. In attempting to decrease the amount of overshoot in the system with the time lag in the cutting force formula, the A/C gain was reduced down to 0.8. Figure 75

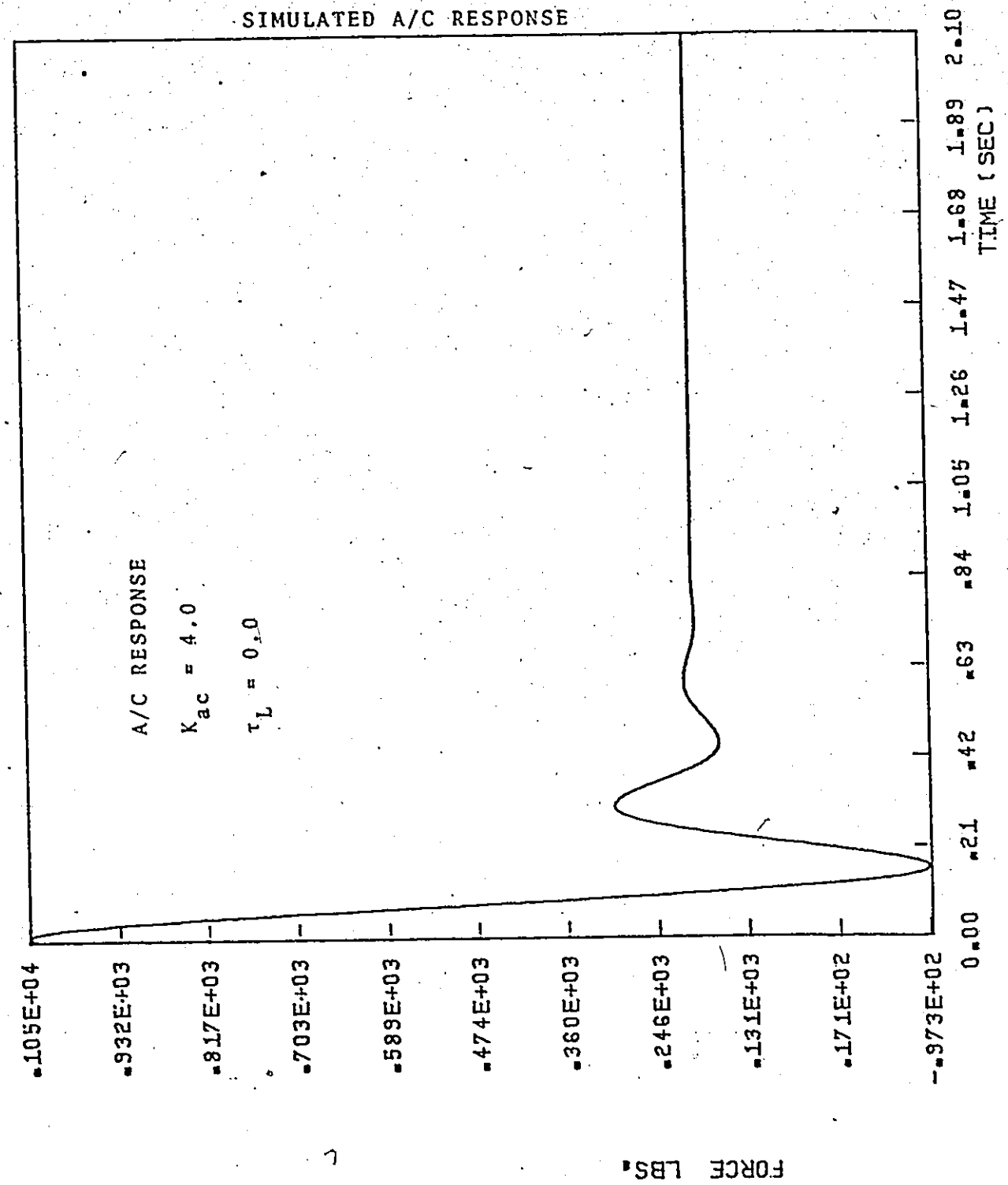
SIMULATED A/C RESPONSE
A/C RESPONSE
K_{ac} = 4.0
τ_L = 0.0
.105E+04
.932E+03
.817E+03
.703E+03
.589E+03
.474E+03
.360E+03
.246E+03
.131E+03
.171E+02
-.973E+02
FORCE LBS.
0.00
.21
.42
.63
.84
1.05
1.26
1.47
1.68
1.89
2.10
TIME (SEC)

FIGURE 70

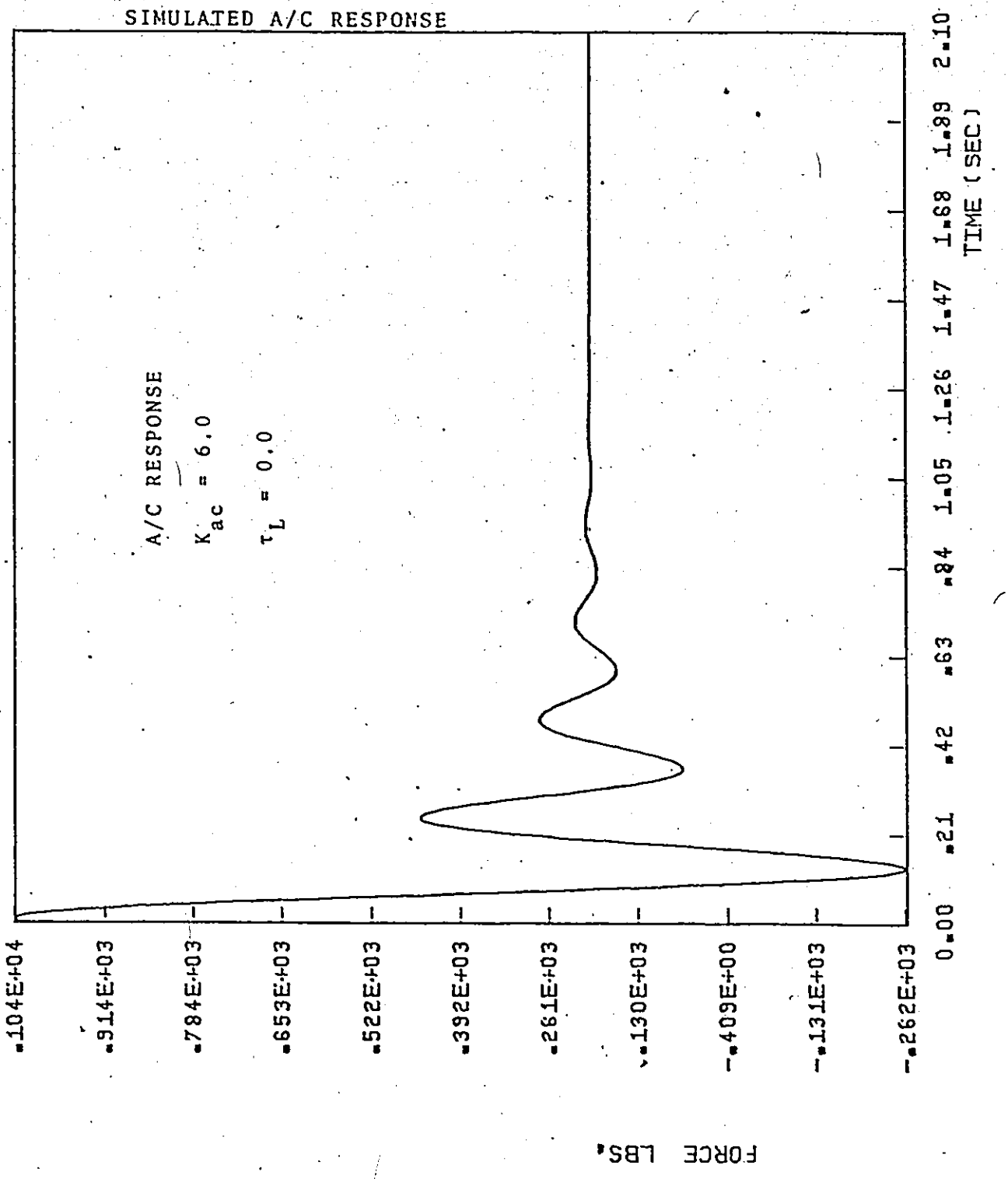
SIMULATED A/C RESPONSE
A/C RESPONSE
K_{ac} = 6.0
τ_L = 0.0
.104E+04
.914E+03
.784E+03
.653E+03
.522E+03
.392E+03
.261E+03
.130E+03
-.409E+00
-.131E+03
-.262E+03
FORCE LBS.
0.00
.21
.42
.63
.84
1.05
1.26
1.47
1.68
1.89
2.10
TIME (SEC)

FIGURE 71

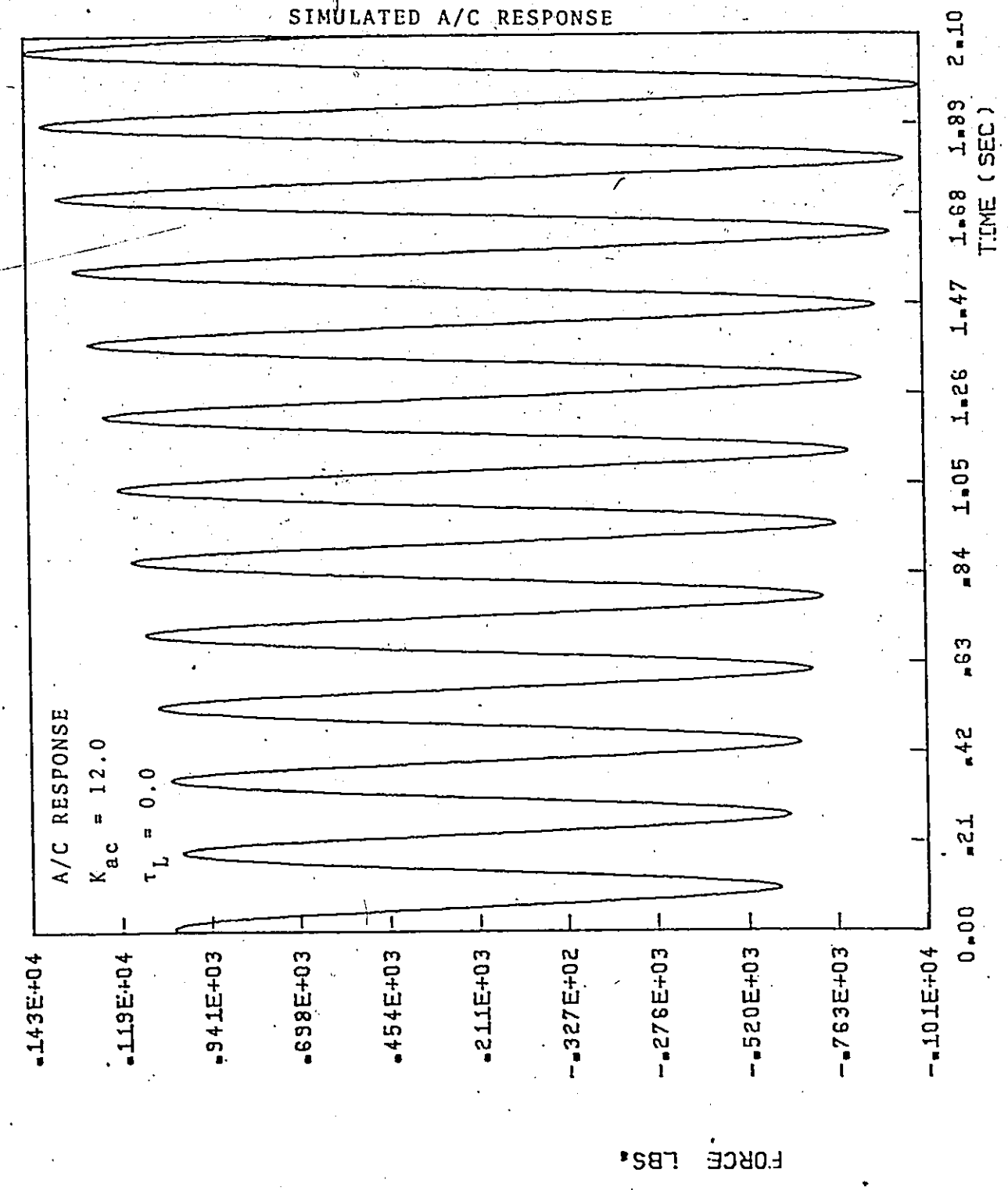
SIMULATED A/C RESPONSE
A/C RESPONSE
K_{ac} = 12.0
τ_L = 0.0
.143E+04
.119E+04
.941E+03
.698E+03
.454E+03
.211E+03
-.327E+02
-.276E+03
-.520E+03
-.763E+03
-.101E+04
FORCE LBS.
0.00
.21
.42
.63
.84
1.05
1.26
1.47
1.68
1.89
2.10
TIME (SEC)

FIGURE 72

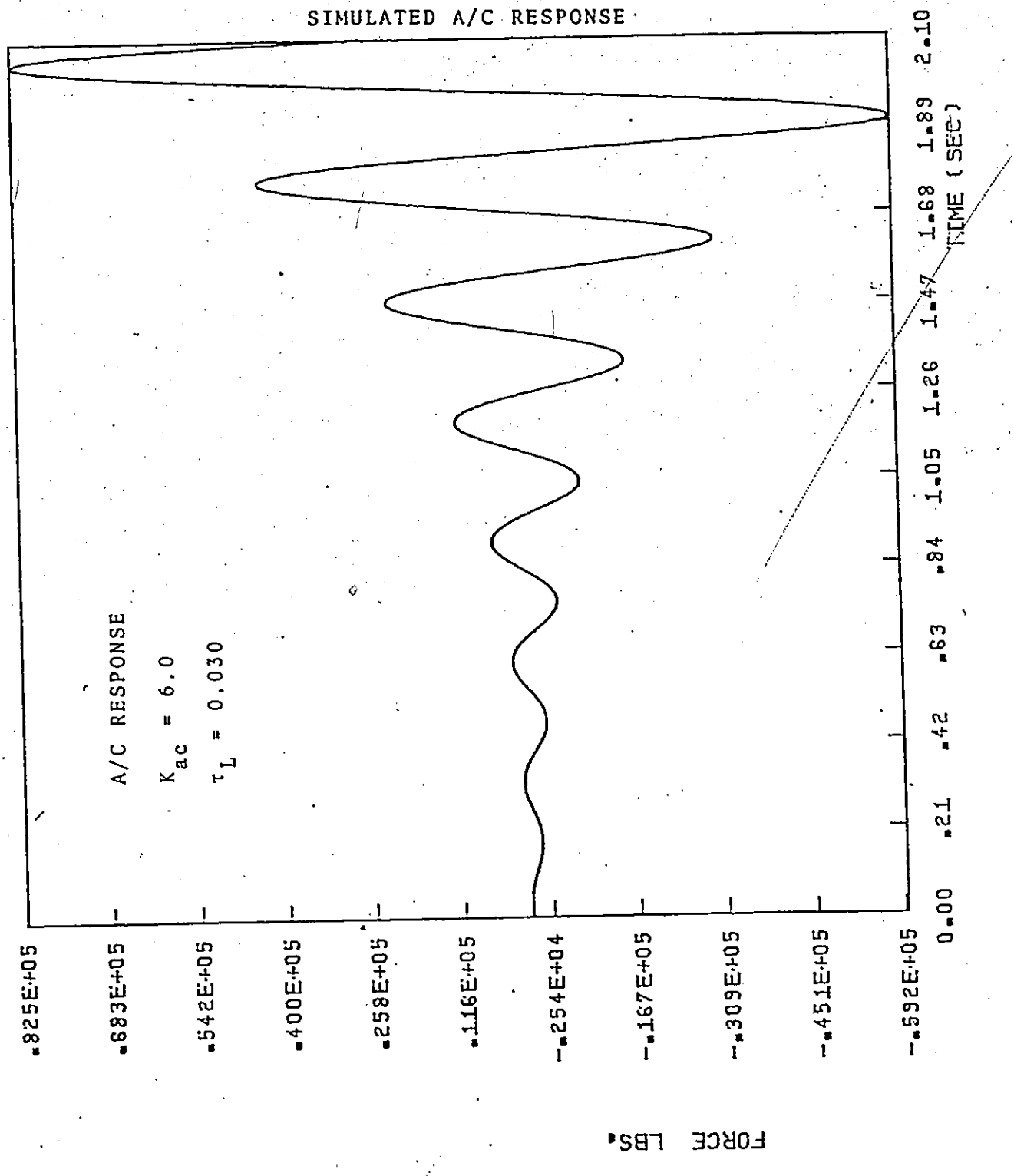
SIMULATED A/C RESPONSE
A/C RESPONSE
K_{ac} = 6.0
τ_L = 0.030
.825E+05
.683E+05
.542E+05
.400E+05
.258E+05
.116E+05
-.254E+04
-.167E+05
-.309E+05
-.451E+05
-.592E+05
FORCE LBS.
0.00
.21
.42
.63
.84
1.05
1.26
1.47
1.68
1.89
2.10
TIME (SEC)

FIGURE 73

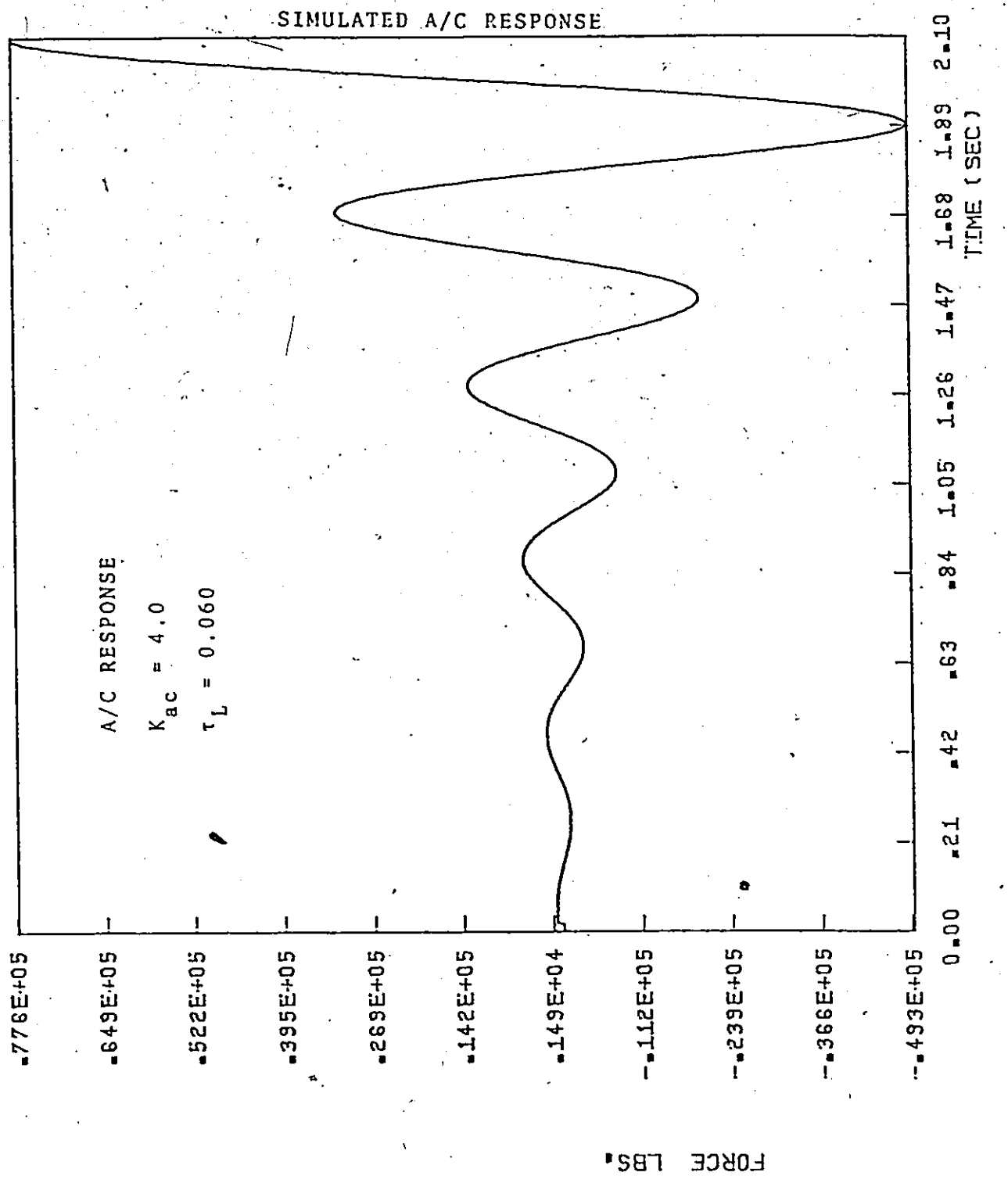
SIMULATED A/C RESPONSE
A/C RESPONSE
K_{ac} = 4.0
τ_L = 0.060
.776E+05
.649E+05
.522E+05
.395E+05
.269E+05
.142E+05
.149E+04
-.112E+05
-.239E+05
-.366E+05
-.493E+05
FORCE LBS.
0.00
.21
.42
.63
.84
1.05
1.26
1.47
1.68
1.89
2.10
TIME (SEC)

FIGURE 74

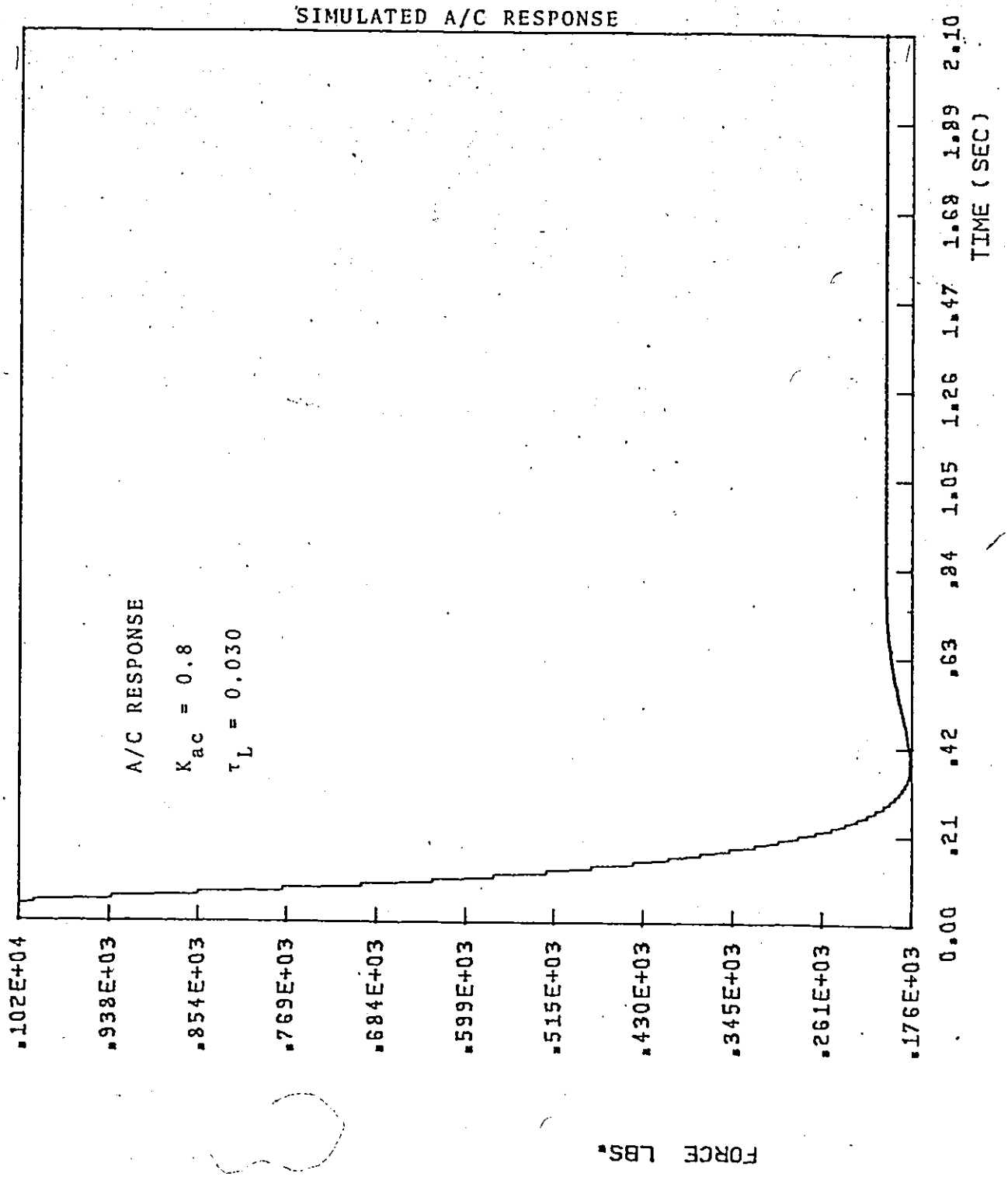
SIMULATED A/C RESPONSE
A/C RESPONSE
K_{ac} = 0.8
τ_L = 0.030
.102E+04
.938E+03
.854E+03
.769E+03
.684E+03
.599E+03
.515E+03
.430E+03
.345E+03
.261E+03
.176E+03
FORCE LBS.
0.00
.21
.42
.63
.84
1.05
1.26
1.47
1.68
1.89
2.10
TIME (SEC)

FIGURE 75.

shows a plot of the resulting cutting force obtained for an A/C gain of 0.8 and a time lag τ_L = 30 milliseconds in the cutting force formula. The system is seen to be quite stable requiring about 300 milliseconds for the cutting force to reach its nominal value. Figure 76 shows the resulting plot obtained when the same A/C gain is used along with a time lag of 60 milliseconds between the cutting force and the table velocity. In the latter case, an undershoot of about 9% of the maximum cutting force is observed. This is obviously the effect of the larger value of time lag introduced in the system. It was arbitrarily decided that oscillations with amplitude of less than 10% of the maximum resulting cutting force are stable.

However, in order to further increase the A/C gain so as to obtain a faster response of the whole system, a second method of stabilization was used, that is the addition of rate feedback. The rate feedback term selected is $\beta\frac{d(error)}{dt}$, where β is considered a damping factor.

Accordingly, the commanded acceleration "ACC" will be:

$$ACC = ERROR \times GAIN + DAMPING$$

And, $$DAMPING = B\frac{d(error)}{dt}$$

The differentiation in the above expression is also evaluated using Euler's method discussed previously. The expression for the new commanded feed rate will then be:

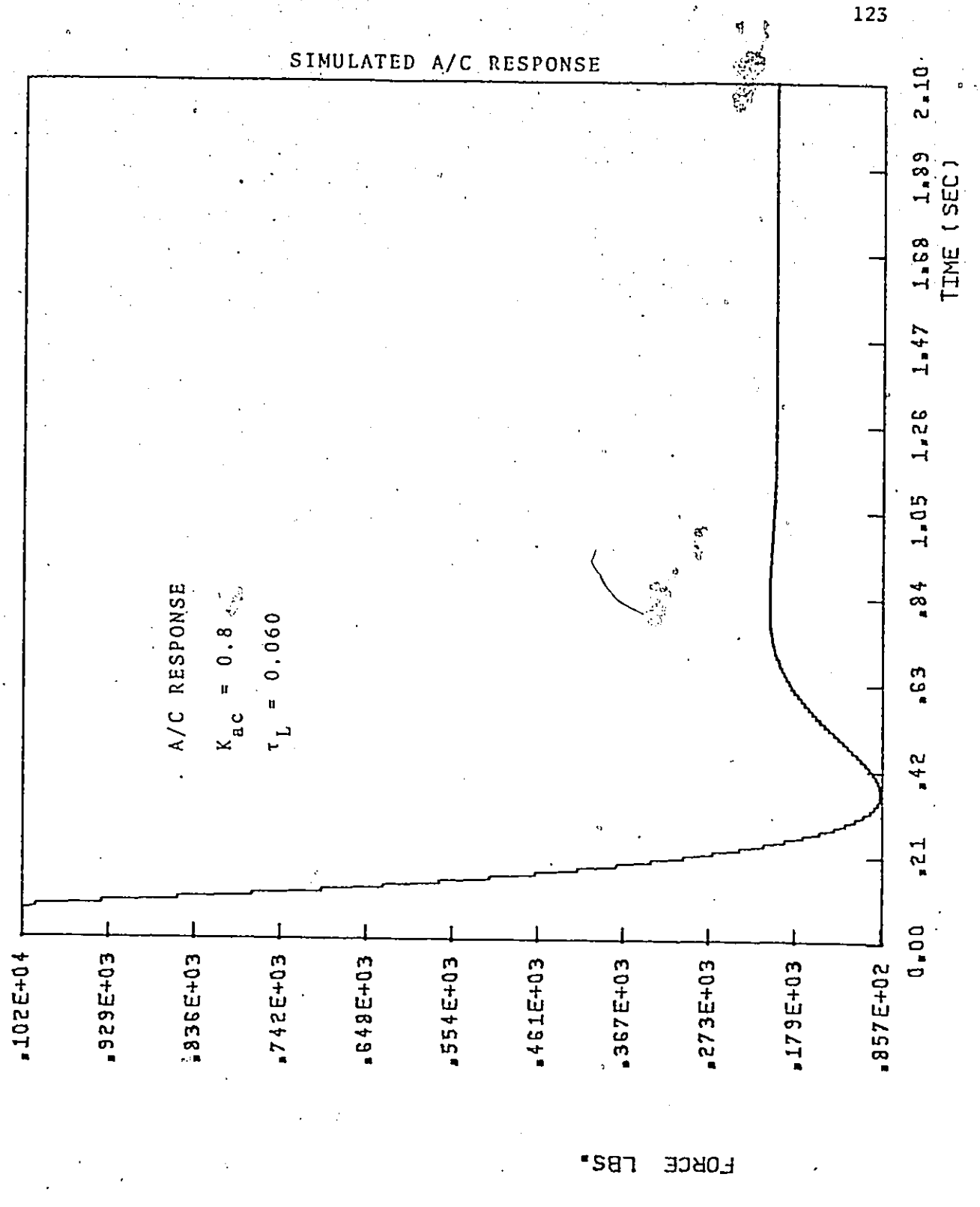
SIMULATED A/C RESPONSE
A/C RESPONSE
K_{ac} = 0.8
τ_L = 0.060
.102E+04
.929E+03
.836E+03
.742E+03
.648E+03
.554E+03
.461E+03
.367E+03
.273E+03
.179E+03
.857E+02
FORCE LBS.
0.00
.21
.42
.63
.84
1.05
1.26
1.47
1.68
1.89
2.10
TIME (SEC)

FIGURE 76

$$x13(t) = x13(t-\tau_d) + ACC \times delay$$

The influence of using this damping term on the overall performance of the system is next discussed. Figure 77 shows the resulting cutting force obtained for the case where an AC gain of unity is used along with 30 milliseconds time lag. When the same case was again considered with the use of a damping term having a damping factor of 0.05, the resulting cutting force is shown in figure 78. Keeping the AC gain equal to unity and introducing 60 milliseconds time lag in the system, the resulting cutting force is again plotted with and without the use of the damping term. The results obtained are shown in figures 79 and 80. A further increase in the A/C gain to 2.0 while introducing a time lag of 30 milliseconds in the cutting force formula yield the response shown in figure 81. The same case was again considered with the use of a damping factor of 0.08. The plot of the resulting cutting force is shown in figure 82. In the latter case the system is seen to be quite stable requiring about 180 milliseconds for the cutting force to drop to its nominal value.

However, it was found that the system became unstable when a relatively larger value of damping factor "β" was used. Figure 83 shows the plot obtained for the resulting cutting force when using a damping factor $\beta = 0.6$ in the previously mentioned case. The system turned to be unstable with a frequency of about 9.6 Hz. It is then fair to comment that

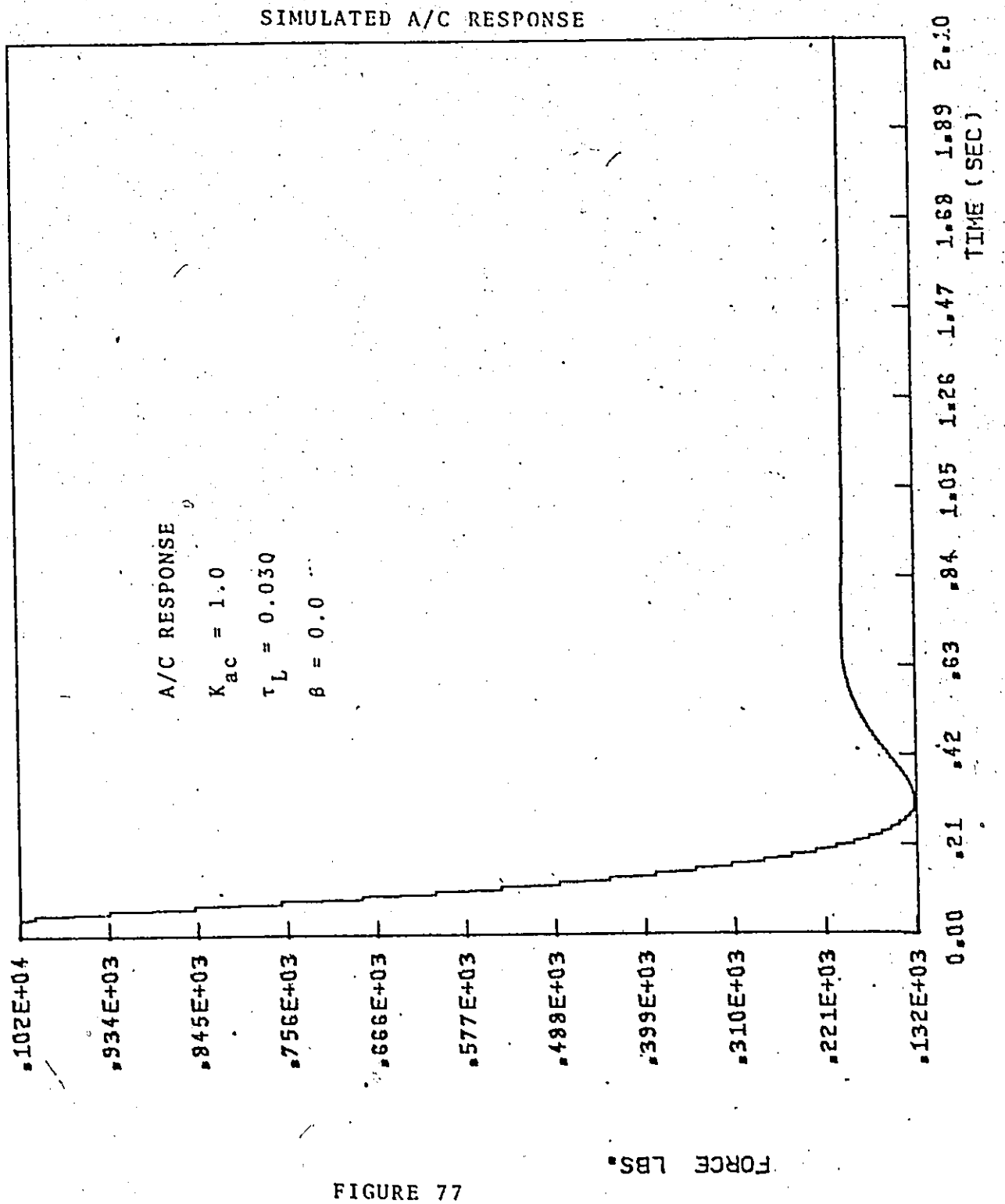
SIMULATED A/C RESPONSE
A/C RESPONSE
K_{ac} = 1.0
τ_L = 0.030
β = 0.0
.102E+04
.934E+03
.845E+03
.756E+03
.666E+03
.577E+03
.488E+03
.399E+03
.310E+03
.221E+03
.132E+03
FORCE LBS.
0.00
.21
.42
.63
.84
1.05
1.26
1.47
1.68
1.89
2.10
TIME (SEC)

FIGURE 77

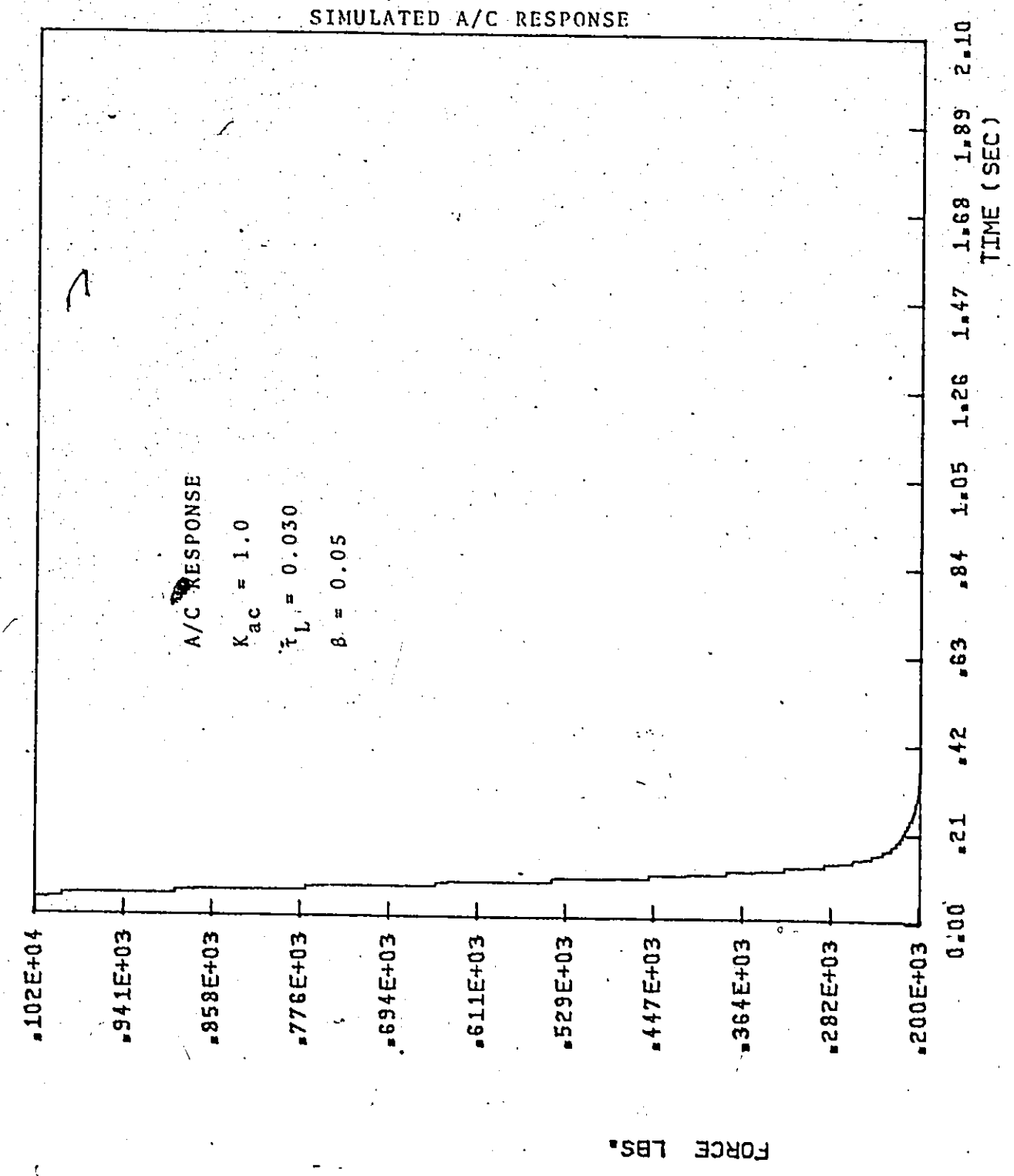
SIMULATED A/C RESPONSE
A/C RESPONSE
K_{ac} = 1.0
τ_L = 0.030
β = 0.05
.102E+04
.941E+03
.858E+03
.776E+03
.694E+03
.611E+03
.529E+03
.447E+03
.364E+03
.282E+03
.200E+03
FORCE LBS.
0.00
.21
.42
.63
.84
1.05
1.26
1.47
1.68
1.89
2.10
TIME (SEC)

FIGURE 78

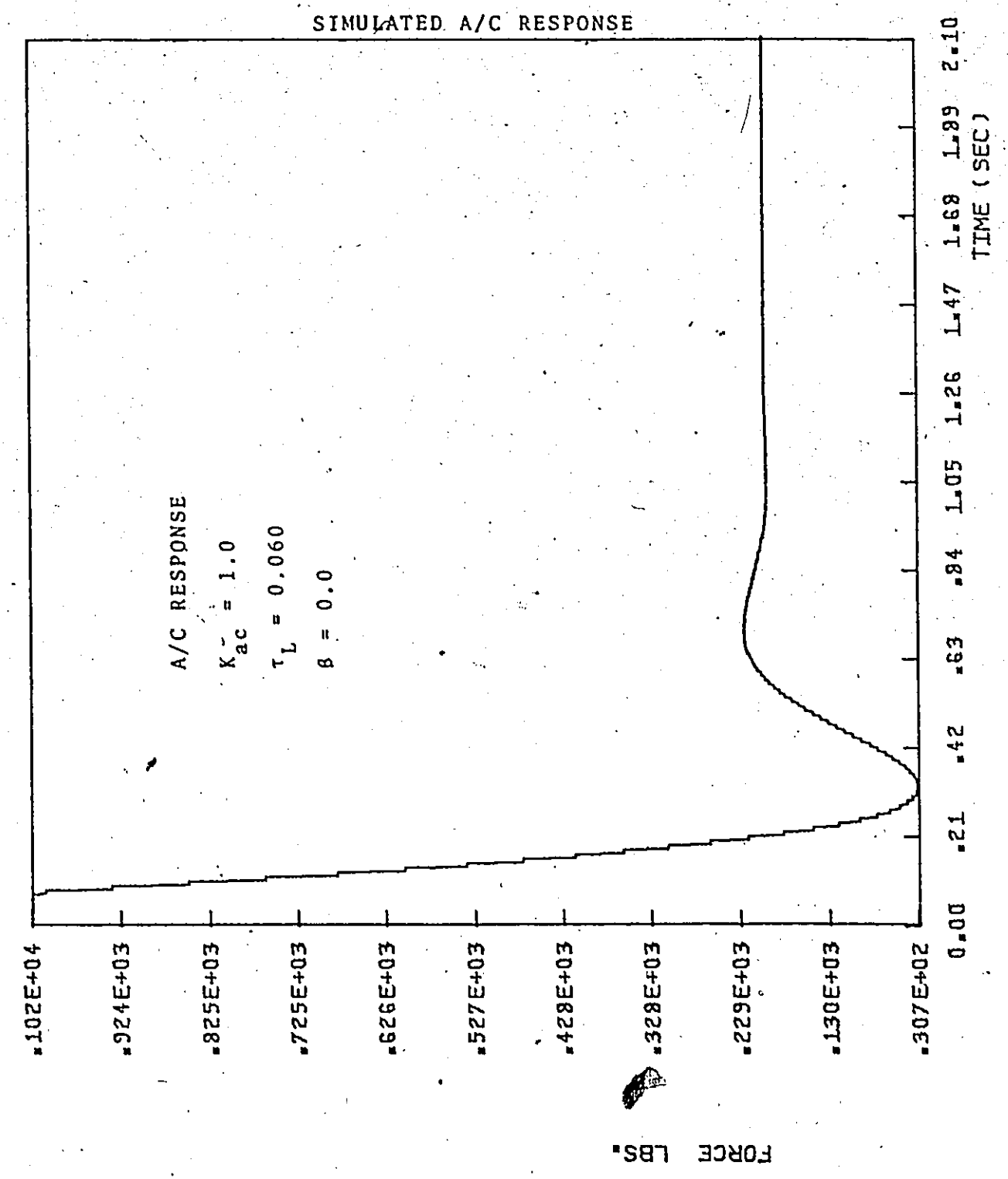
SIMULATED A/C RESPONSE
A/C RESPONSE
K_{ac} = 1.0
τ_L = 0.060
β = 0.0
.102E+04
.924E+03
.825E+03
.725E+03
.626E+03
.527E+03
.428E+03
.328E+03
.229E+03
.130E+03
.307E+02
FORCE LBS.
0.00
.21
.42
.63
.84
1.05
1.26
1.47
1.68
1.89
2.10
TIME (SEC)

FIGURE 79

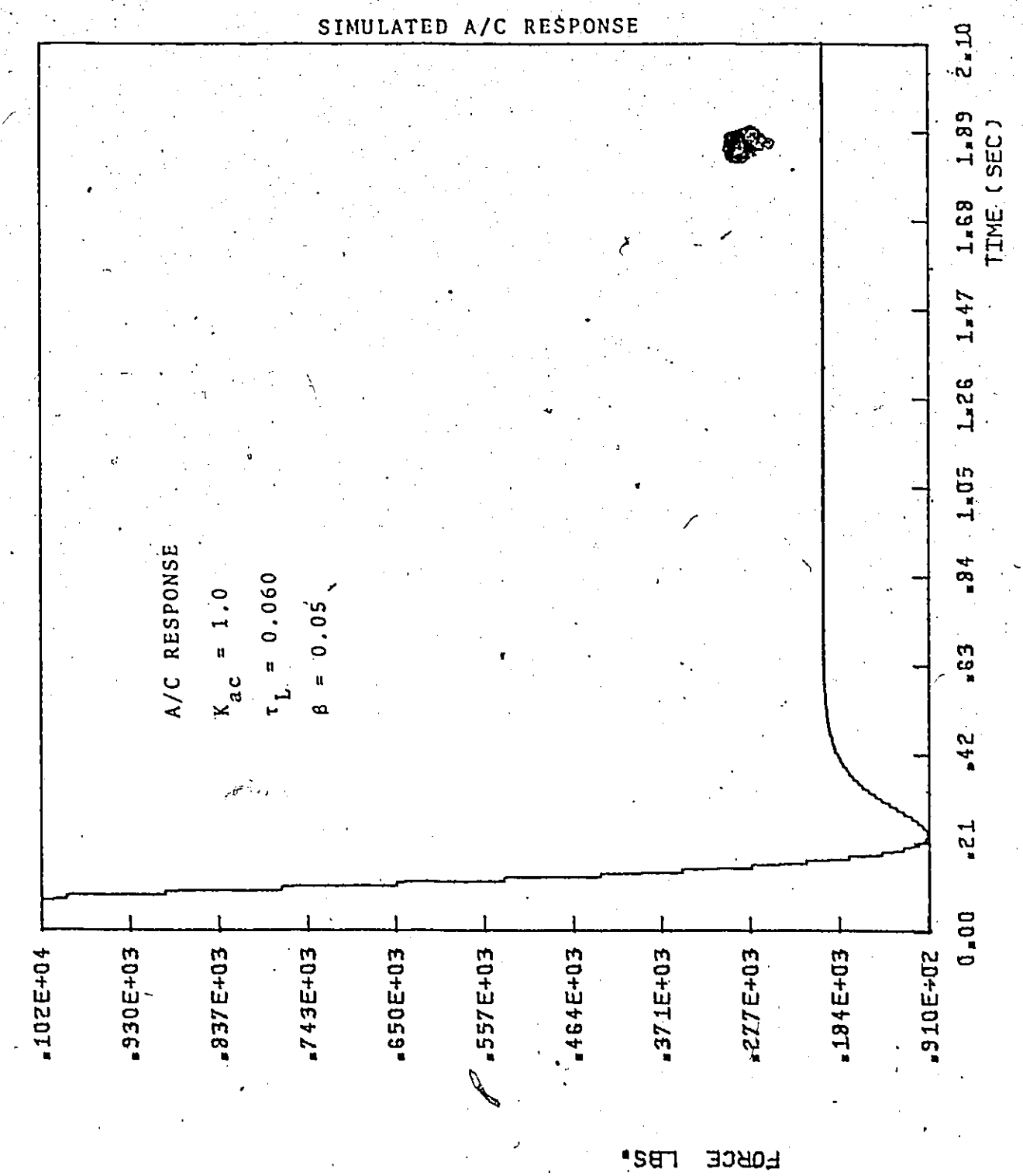
SIMULATED A/C RESPONSE
A/C RESPONSE
K_{ac} = 1.0
τ_L = 0.060
β = 0.05
.102E+04
.930E+03
.837E+03
.743E+03
.650E+03
.557E+03
.464E+03
.371E+03
.277E+03
.184E+03
.910E+02
FORCE LBS.
0.00
.21
.42
.63
.84
1.05
1.26
1.47
1.68
1.89
2.10
TIME (SEC)

FIGURE 80

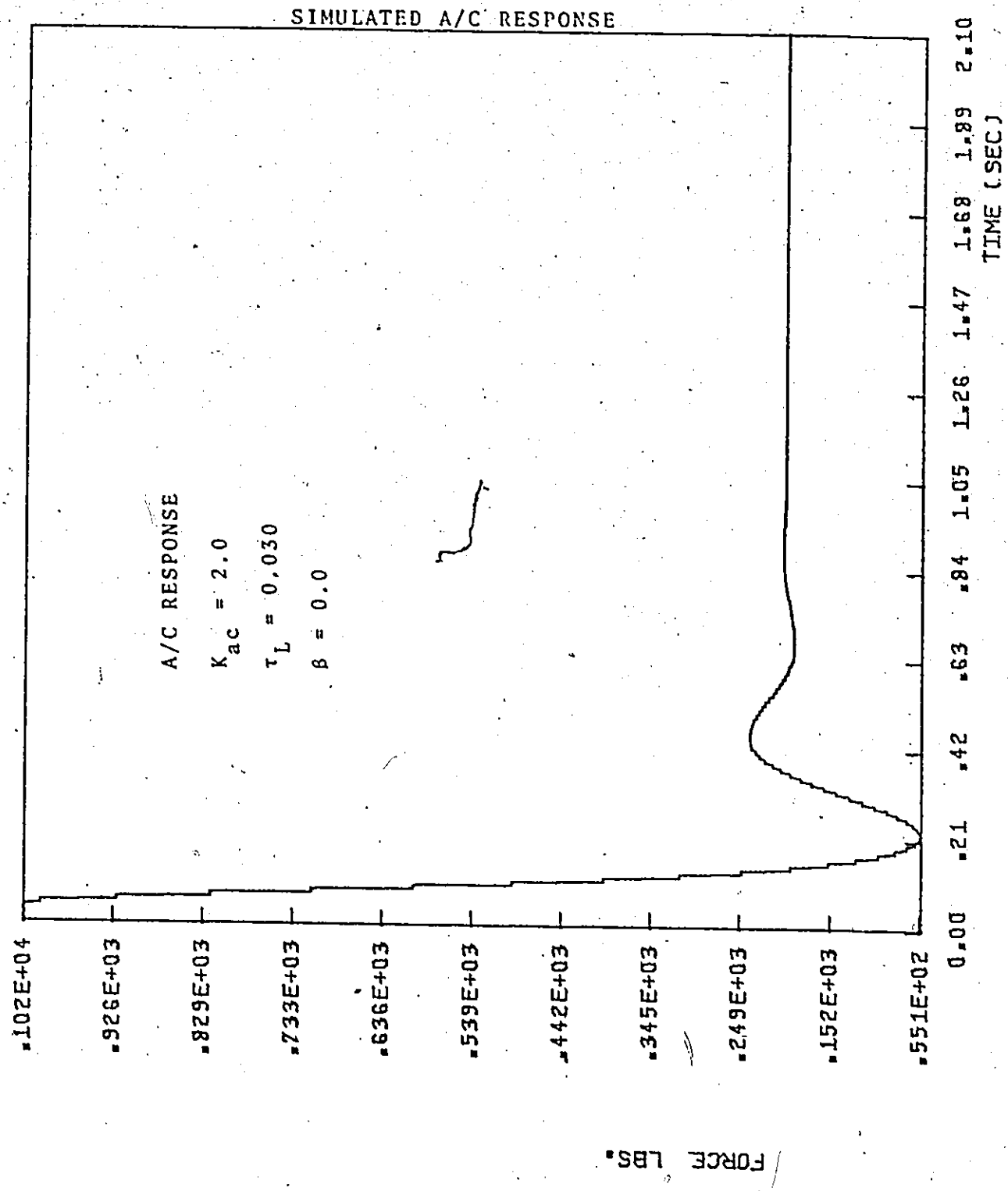
SIMULATED A/C RESPONSE
A/C RESPONSE
K_{ac} = 2.0
τ_L = 0.030
β = 0.0
.102E+04
.926E+03
.829E+03
.733E+03
.636E+03
.539E+03
.442E+03
.345E+03
.249E+03
.152E+03
.551E+02
FORCE LBS.
0.00
.21
.42
.63
.84
1.05
1.26
1.47
1.68
1.89
2.10
TIME (SEC)

FIGURE 81

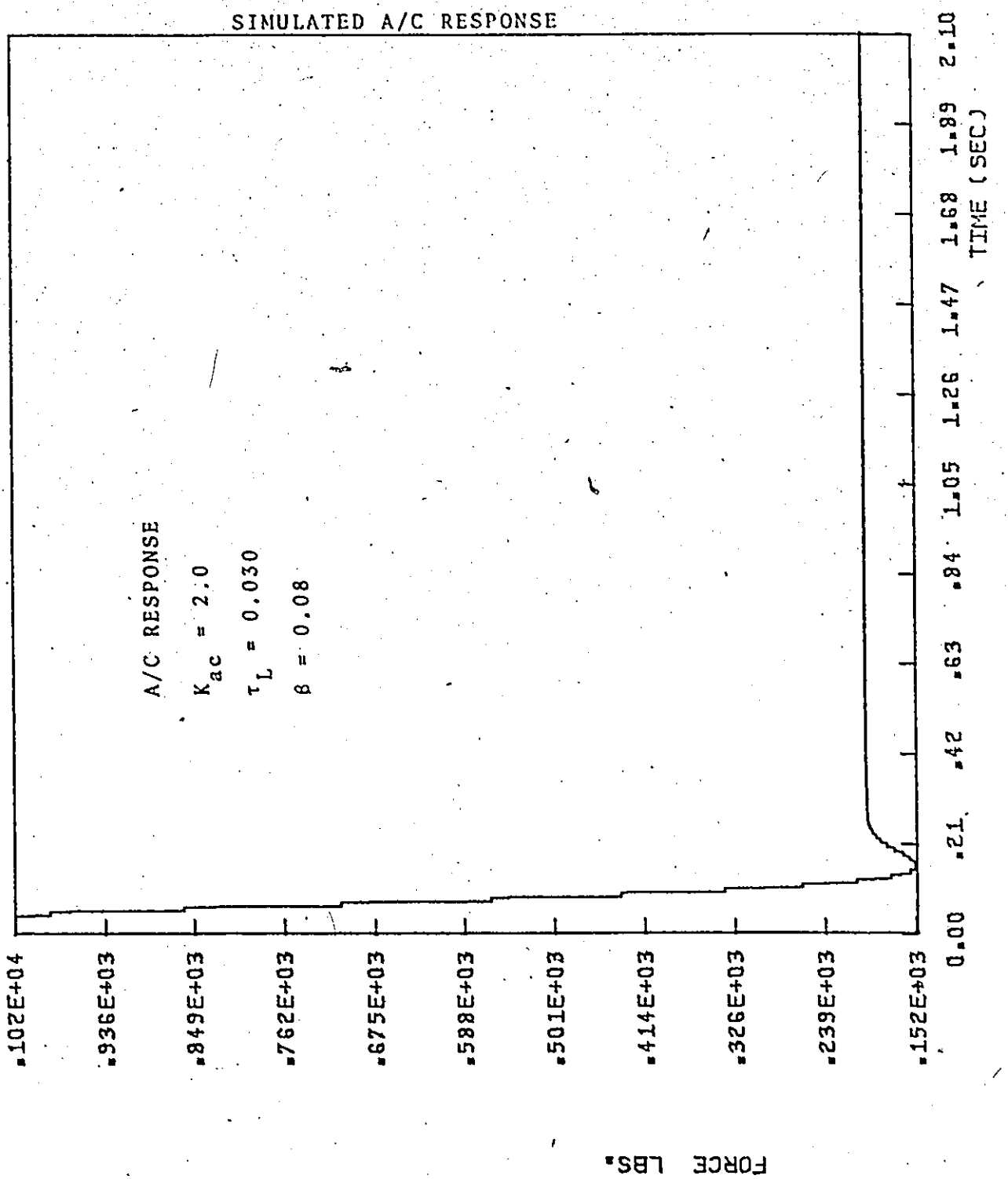
SIMULATED A/C RESPONSE
A/C RESPONSE
K_{ac} = 2.0
τ_L = 0.030
β = 0.08
.102E+04
.936E+03
.849E+03
.762E+03
.675E+03
.588E+03
.501E+03
.414E+03
.326E+03
.239E+03
.152E+03
FORCE LBS.
0.00
.21
.42
.63
.84
1.05
1.26
1.47
1.68
1.89
2.10
TIME (SEC)

FIGURE 82

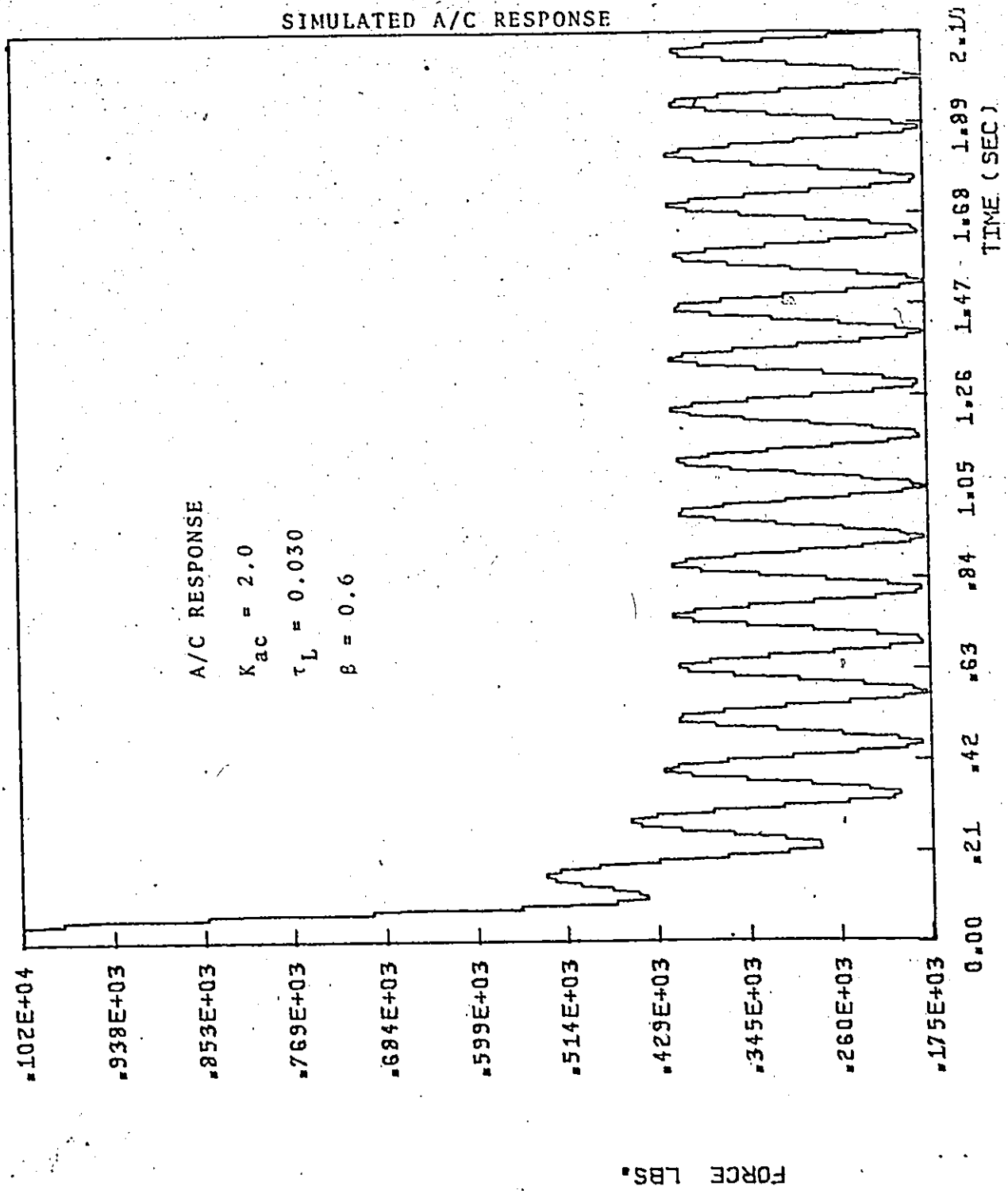
SIMULATED A/C RESPONSE
A/C RESPONSE
K_{ac} = 2.0
τ_L = 0.030
β = 0.6
.102E+04
.938E+03
.853E+03
.769E+03
.684E+03
.599E+03
.514E+03
.429E+03
.345E+03
.260E+03
.175E+03
FORCE LBS.
0.00
.21
.42
.63
.84
1.05
1.26
1.47
1.68
1.89
2.10
TIME (SEC)

FIGURE 83

the term $[\beta \frac{d(error)}{dt}]$ works as a damping term only for a certain range of values used for β.

In all the previous simulated cases a linear cutting force formula was assumed:

i.e. $F = c.v$

where F is the cutting force

c is a constant

and v is the table velocity (feed rate)

Certainly, some of the resulting forces encountered in end milling, as discussed in reference 26 seem to follow this simple relation while other obviously have some superimposed periodic component. Typical plots showing the variation of the cutting force versus the angular position α of the cutting edge are shown in figures 84 and 85. Accordingly, for the case where the cutting force is periodically variable a second formula is assumed:

$$F = (K + c \sin wt)\, v$$

where F is the cutting force K and c are both constants. A reasonable value for both K and c is 1200 lb/inch/sec.

V is the table velocity (feed rate)

w is the frequency of the cutting force in rad/sec, and $w = \frac{2\pi NZ}{60}$, while N is the spindle speed in rev/min, and Z is the number of teeth of the milling cutter. Figures 86 and 87 show the response of the entire system for two different cases when using a periodically variable cutting force formula as explained above. In both cases an AC gain of

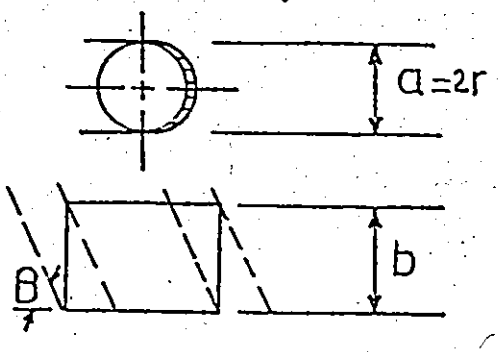

a = depth of cut

b = width of cut

B = 30°

K = specific force = 2150 N/cm^2

S_t = feed per tooth = 0.15 mm

Zr = cutter diameter = 6.35 mm

Z = number of teeth

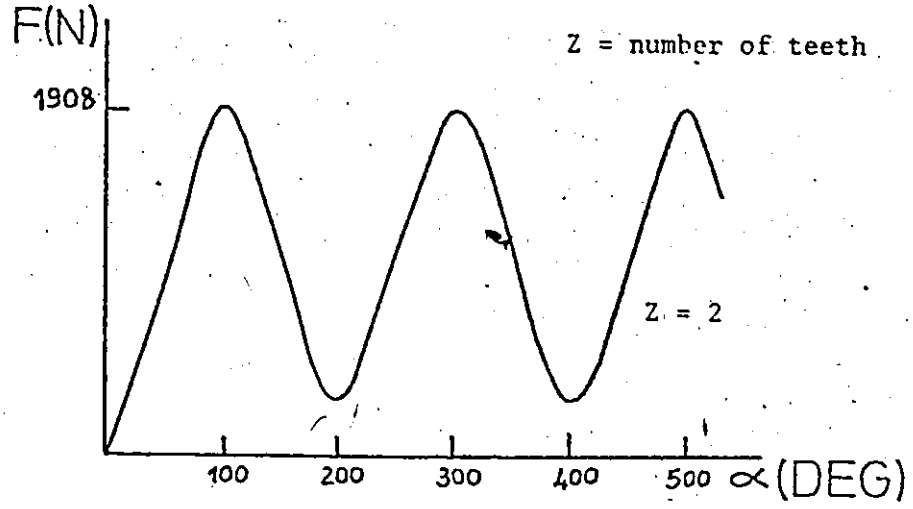

RESULTING CUTTING FORCE IN ENDMILLING

FIGURE 84

[reference 26]

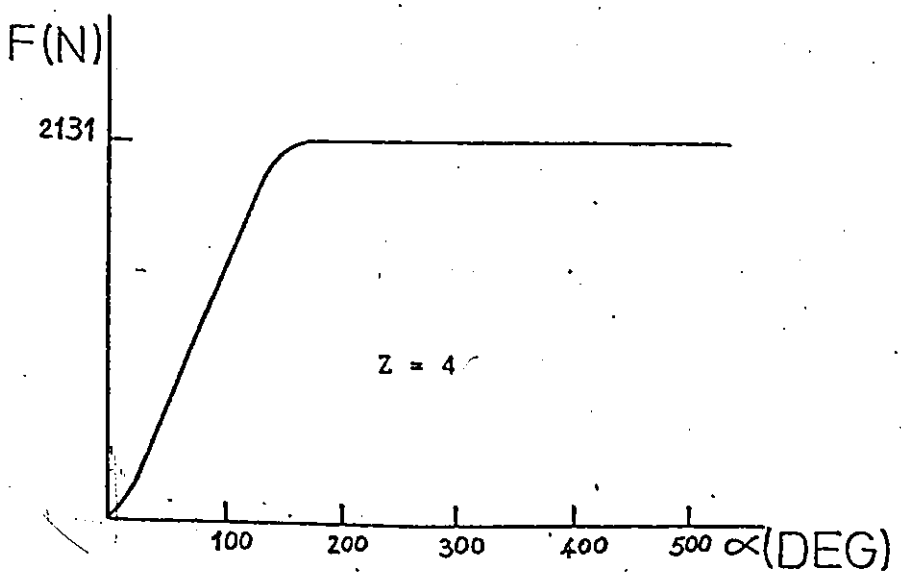

RESULTING CUTTING FORCE IN ENDMILLING

FIGURE 85

[reference 26]

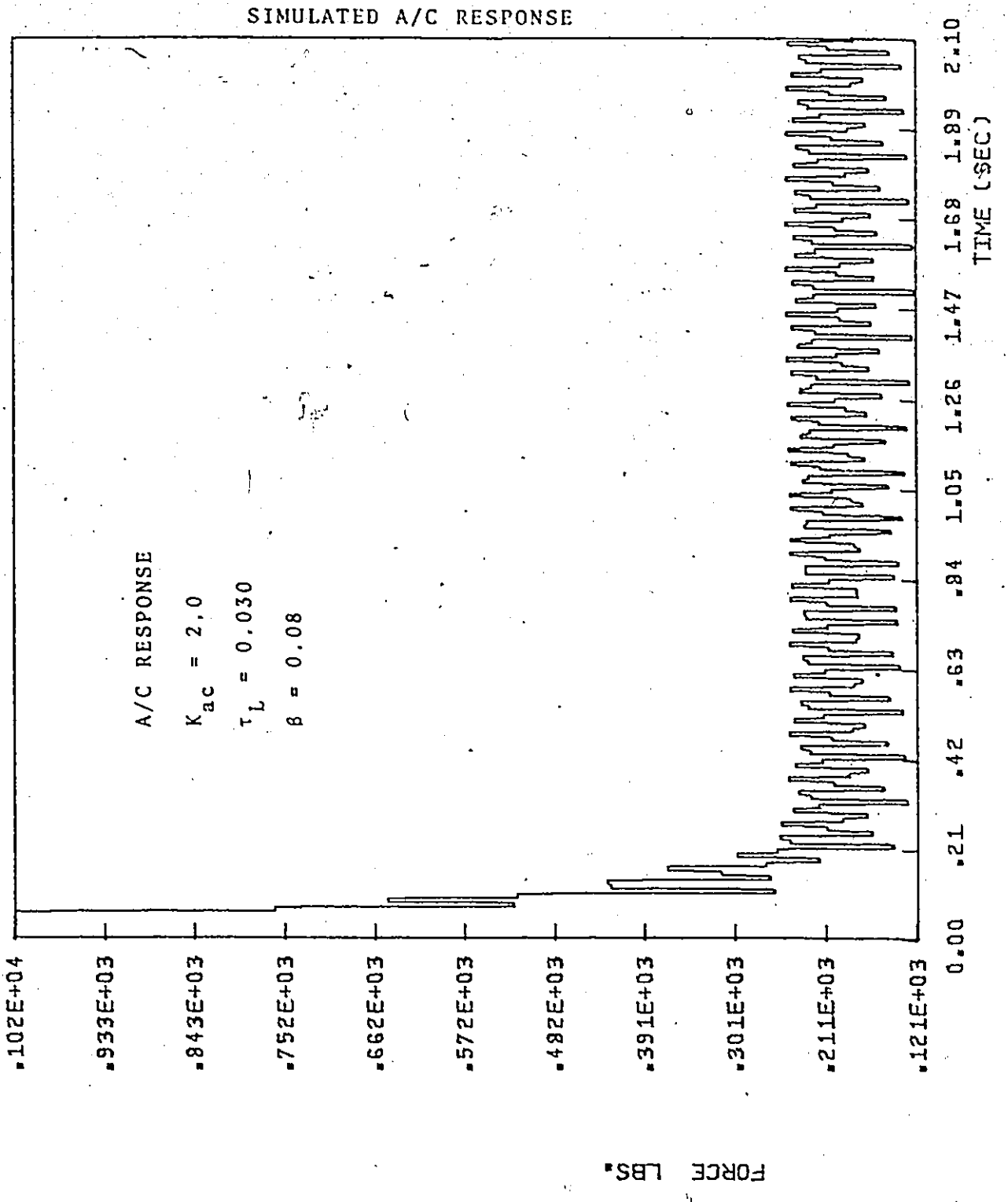
SIMULATED A/C RESPONSE
A/C RESPONSE
K_{ac} = 2.0
τ_L = 0.030
β = 0.08
.102E+04
.933E+03
.843E+03
.752E+03
.662E+03
.572E+03
.482E+03
.391E+03
.301E+03
.211E+03
.121E+03
FORCE LBS.
0.00
.21
.42
.63
.84
1.05
1.26
1.47
1.68
1.89
2.10
TIME (SEC)

FIGURE 86

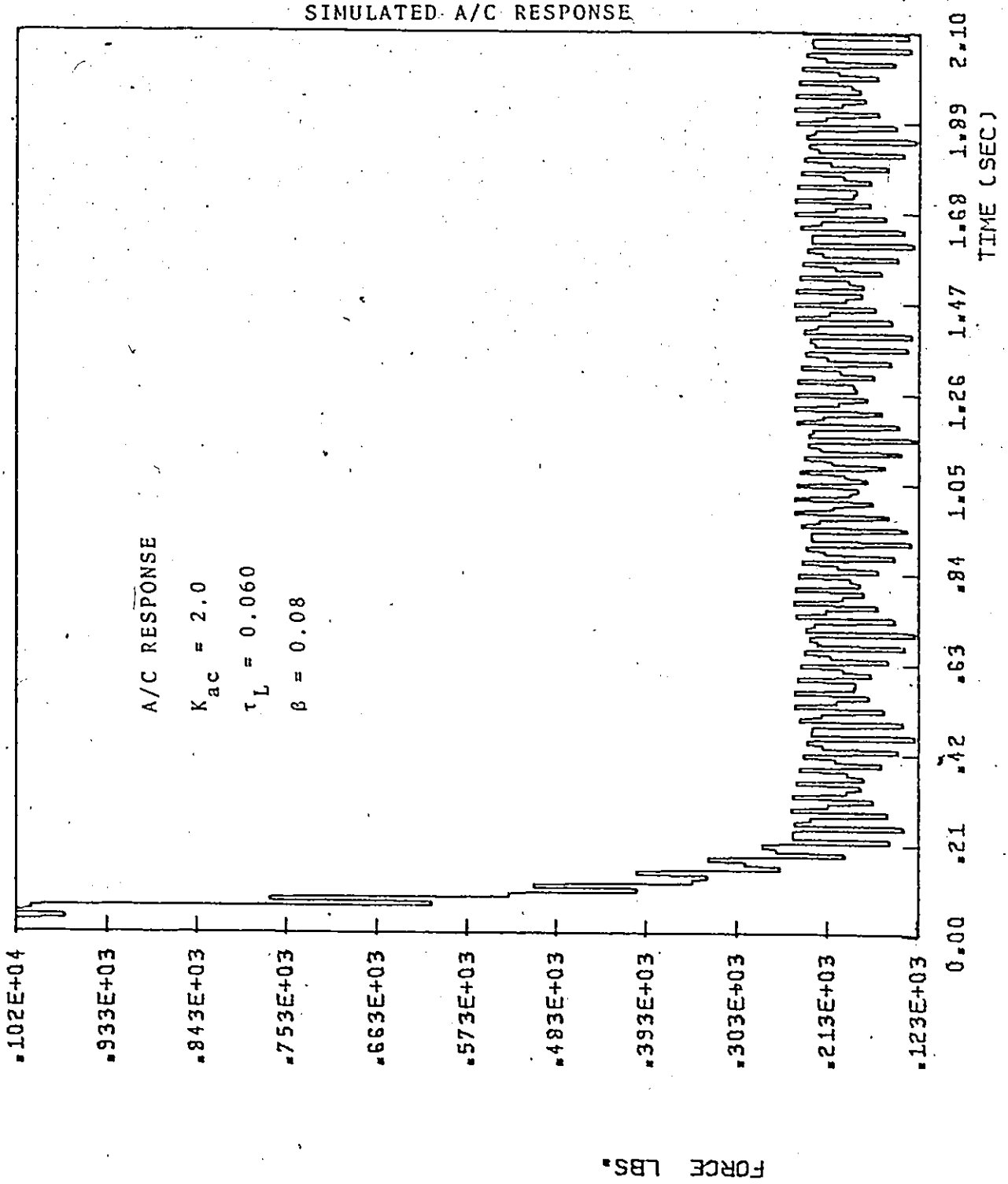
SIMULATED A/C RESPONSE
A/C RESPONSE
K_{ac} = 2.0
τ_L = 0.060
β = 0.08
.102E+04
.933E+03
.843E+03
.753E+03
.663E+03
.573E+03
.483E+03
.393E+03
.303E+03
.213E+03
.123E+03
FORCE LBS.
0.00
.21
.42
.63
.84
1.05
1.26
1.47
1.68
1.89
2.10
TIME (SEC)

FIGURE 87

2.0 along with a damping factor of 0.08 are used. While in the case shown in figure 86 a time lag of 30 milliseconds is introduced in the model and a frequency of 33.3 HZ in the cutting force formula, a time lag of 60 milliseconds is used in the case shown in figure 87 along with a cutting force frequency of 16.6 HZ. It should be noted here that spindle speed is assumed 500 rpm in both cases.

As discussed in detail in chapter 3; increasing the gain of both the position and velocity loops resulted in a faster response of the NC system while still maintaining a reasonable amount of damping in the system. Accordingly, the response of the whole CNC-AC system was next investigated with the suggested increase in both the position and velocity loop gains. Figure 88 shows the resulting cutting force when increasing the positional gain four times, R2 to 47K and decreasing R4 to 10K. An A/C gain of 2.0 was used and a time lag τ_L = 30 milliseconds between the cutting force and the table velocity was introduced in the system. A damping factor β = 0.06 was used. The system is seen to be quite stable and about 120 milliseconds were required before the cutting force dropped to its nominal value.

At this point of the discussion it is worthwhile to comment on the effect of the current limitation discussed in chapter 3 on the system behaviour. All the cases simulated and presented in this chapter were investigated with and without imposing the current limitation in the

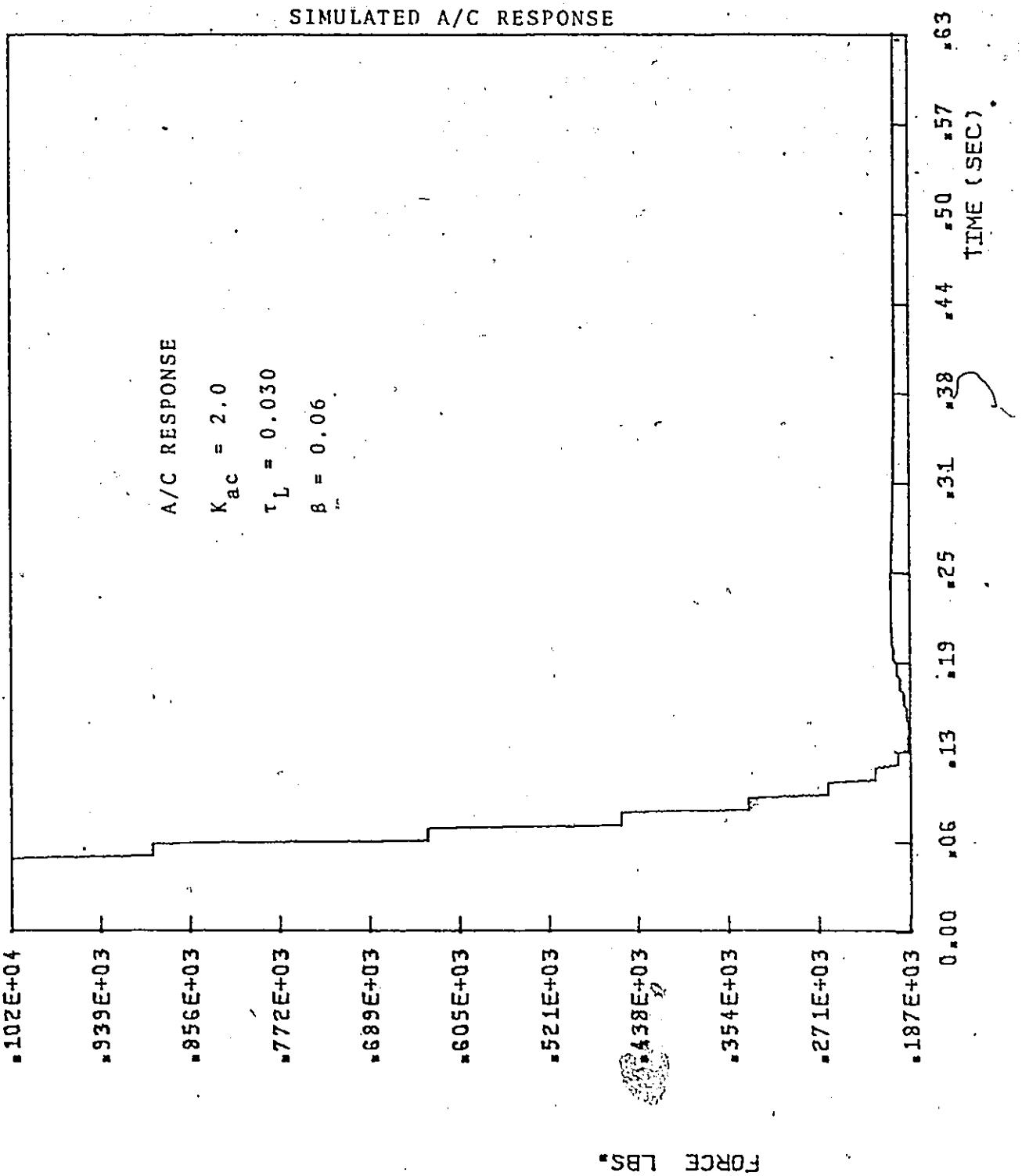
SIMULATED A/C RESPONSE
A/C RESPONSE
K_{ac} = 2.0
τ_L = 0.030
β = 0.06
TIME (SEC)
.00
.06
.13
.19
.25
.31
.38
.44
.50
.57
.63
.102E+04
.939E+03
.856E+03
.772E+03
.689E+03
.605E+03
.521E+03
.438E+03
.354E+03
.271E+03
.187E+03
FORCE LBS.

FIGURE 88

system, and identical results were always obtained in both cases. Accordingly it seemed that the current limitation is active only for very big steps in velocity (e.g. 30 inch/min feed rate) which are very seldom used in mose practical applications of end milling.

A second possible strategy was also investigated using the simulation technique. The suggested algorithm evaluates $\frac{F_{act}}{F_{nom}}$ and immediately starts commanding a new commanded velocity based on the relationship:

$$x13(t) = x13\ (t-\tau_d) \times \frac{F_{nom}}{F_{act}}$$

which still means that in the instant of $F_{act} = F_{nom}$, the commanded velocity is kept constant. Examples of the response obtained from this second algorithm are shown in figures 89 and 90. In the two cases a linear cutting force formula is assumed. In figure 88 a time lag of 30 milliseconds is incorporated in the model. The behaviour of the system is generally acceptable, with the resulting cutting force requiring about 180 milliseconds to drop to its nominal value. When a time lag of 60 milliseconds is introduced in the model, it yields the response shown in figure 89. The effect of the higher value of time lag used is very much pronounced in this case as compared with the previous one. The system sufferrod oscillations of considerable magnitude.

In fact the occurrance of these oscillations in

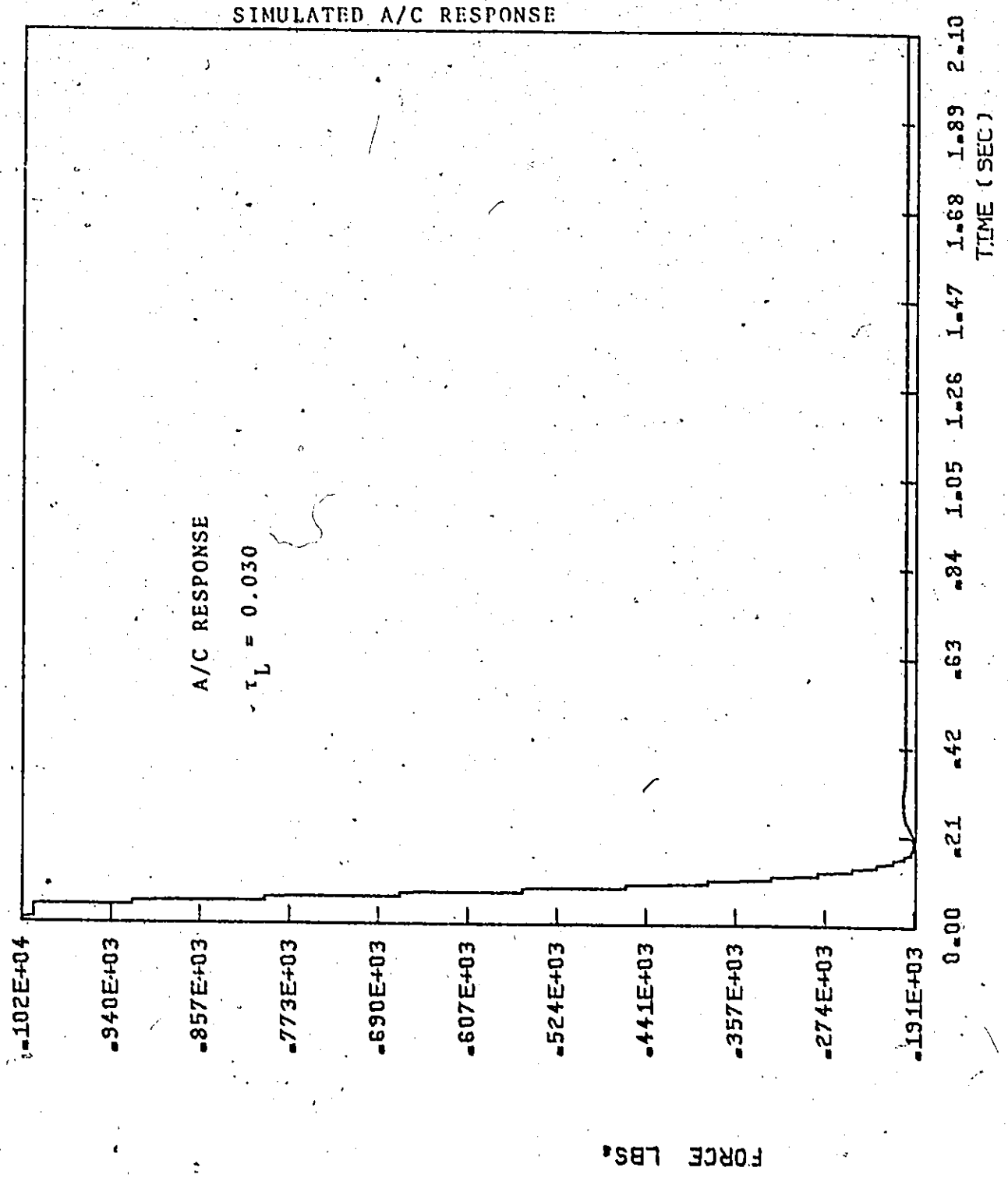
SIMULATED A/C RESPONSE
A/C RESPONSE
τ_L = 0.030
.102E+04
.940E+03
.857E+03
.773E+03
.690E+03
.607E+03
.524E+03
.441E+03
.357E+03
.274E+03
.191E+03
FORCE LBS.
0.00
.21
.42
.63
.84
1.05
1.26
1.47
1.68
1.89
2.10
TIME (SEC)

FIGURE 89

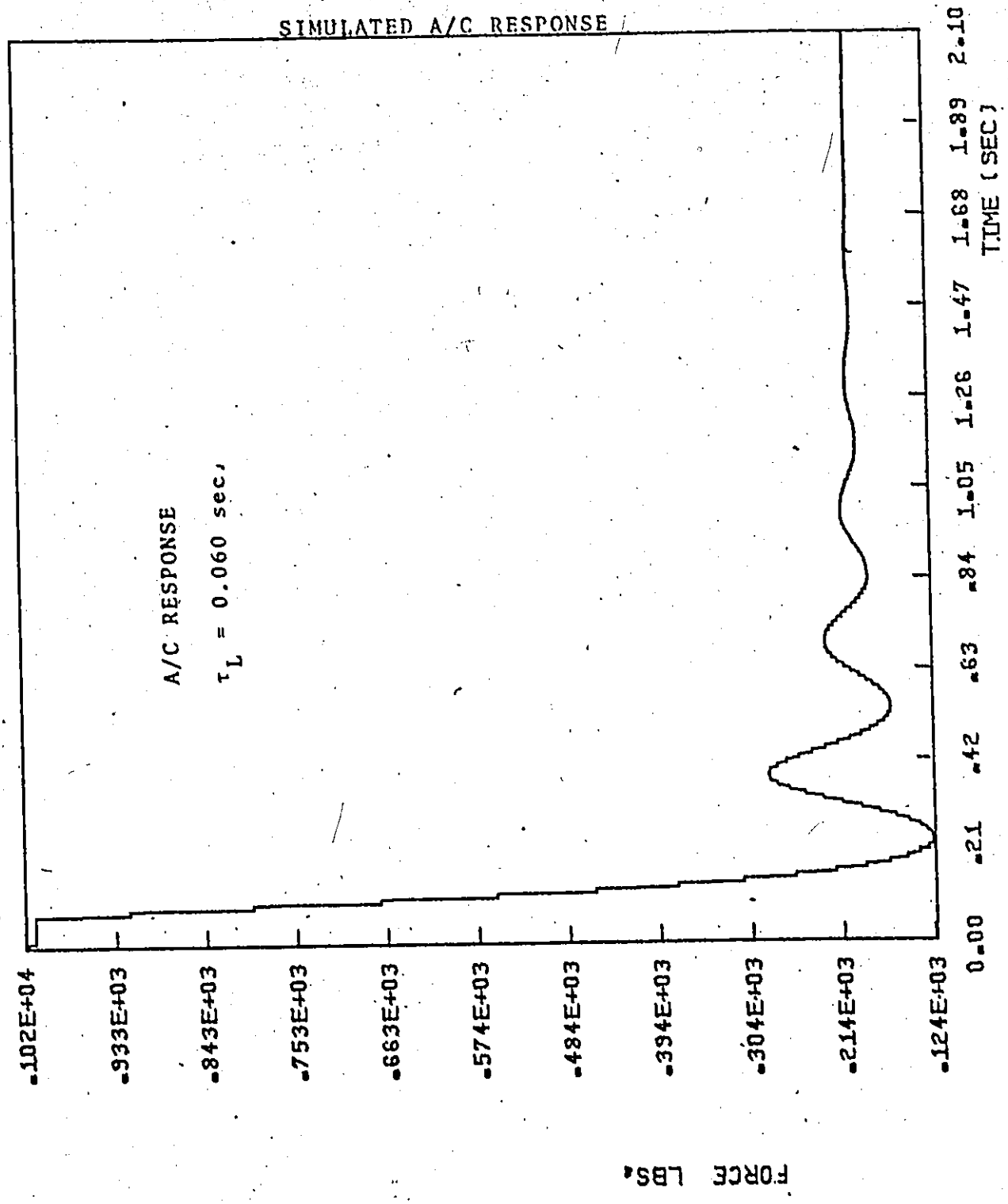
SIMULATED A/C RESPONSE
A/C RESPONSE
τ_L = 0.060 sec.
FORCE LBS.
TIME (SEC)
.102E+04
.933E+03
.843E+03
.753E+03
.663E+03
.574E+03
.484E+03
.394E+03
.304E+03
.214E+03
.124E+03
0.00
.21
.42
.63
.84
1.05
1.26
1.47
1.68
1.89
2.10

FIGURE 90

the system response could be further explained in the following. Referring to figure 91 and at time t_o, a target of v_{nom} is assumed. A deceleration command is initiated, large at the beginning and if the actual velocity would follow immediately, the situation would have been as represented by curves 1 in figure 91. However, due to the delays incorporated in the system, the commanded velocity decreases all the time and drops below v_{nom} (curve 2) when the actual velocity starts to increase but it is still a considerable amount of time below v_{nom} so that actually a deceleration is still commanded. The actual A/C system was not tested. Having stabilized the system, in order to further improve its response time, both the A/C loop gain and the damping term discussed in the A/C simulation require further experimental determination.

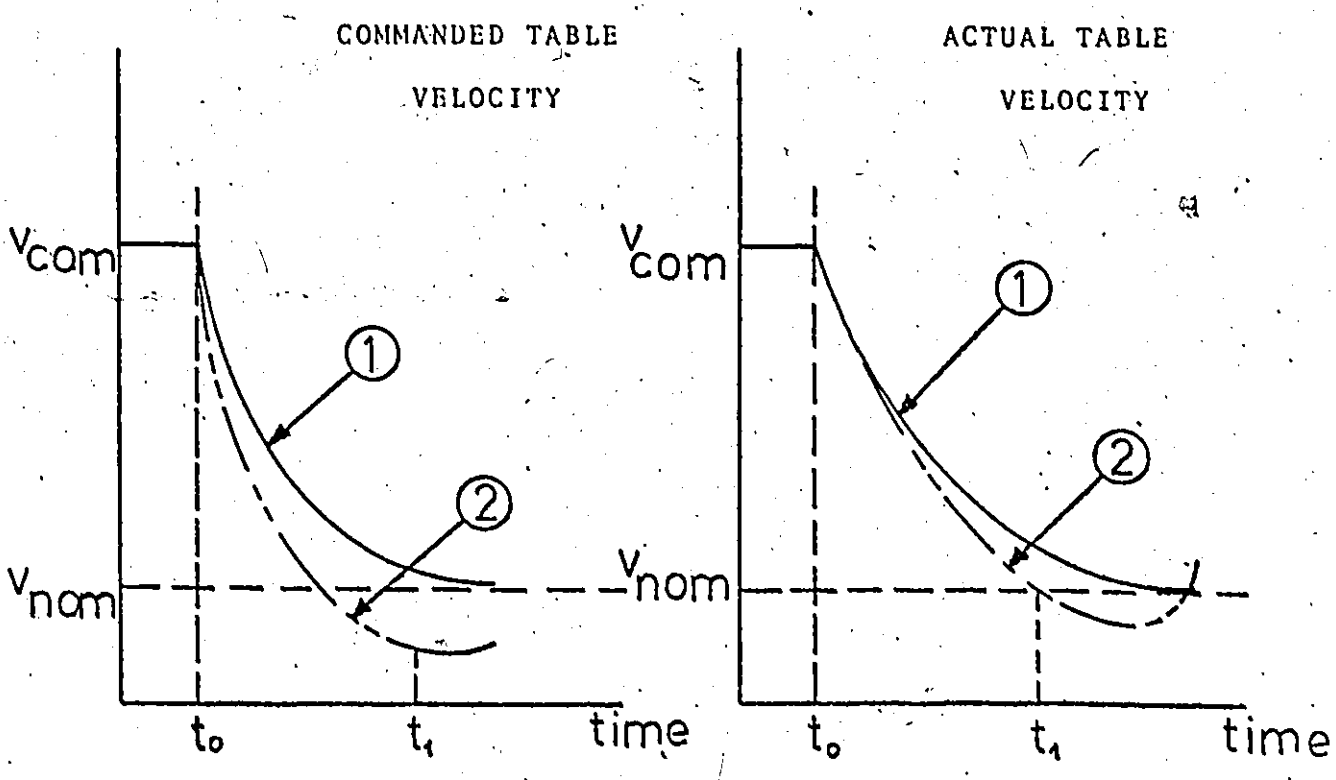

BEHAVIOUR OF COMMANDED AND ACTUAL TABLE VELOCITY

FIGURE 91

CHAPTER 5

CONCLUSIONS

1. In order to improve the response time of the N/C loop, both the gain of the velocity and the position loop has to be increased. While increasing the position loop gain results in a faster response, the velocity loop gain has also to be increased in order to maintain a reasonable amount of damping in the system. This could be achieved by either increasing the value R2 or decreasing R4 in the correcting network.

2. In analyzing the N/C loop, the system is assumed linear and proved to be always stable using various techniques of the classical linear control theory as well as the simulation technique. In reality, the system contains flexibilities and inertias additional to those included in the model and it can become unstable if the gain is too high.

3. The armature current in the servomotor is limited to a value which corresponds to a current analog signal of 3.49 volts. The current limitation results in the limitation of the acceleration of the feed drives. However, this constraint is active only for very large

steps in velocity (e.g. 30 inch/min) which are seldom used in most practical applications of end milling.

4. Analysis of the A/C system by using first various techniques of the linear control theory showed that the system is conditionally stable. A linear A/C algorithm is suggested. Using the simulation technique to test the new strategy, the system behaviour was shown to be quite acceptable when using an A/C gain Kac = 2.0 with a damping factor β = 0.06.

5. The time delay of 10 milliseconds between feed rate corrections which is also the force sampling interval has a small effect on the stability of the system.

6. The time lag between the cutting force and the table velocity is the most important reason for the occurrance of unacceptable oscillations in the system response even when small values of A/C gain are used. In some cases it is responsible for the instability of the whole system.

7. The term $\frac{Bd(error)}{dt}$ works as a damping term only for a certain range of values of B. Using larger values of B, the system turns to be unstable. The effect of this term requires further investigation.

8. The current limitation constraint does not have a great effect on the behaviour of the A/C loop at the currently used values of gains in the velocity,

positional and A/C loops.

9. The analysis described in this work lead to determining the practically optimum values of position gain Kp = 180 volts/inch, R2 = 33K, R4 = 10K, Kac = 2.0 and B = 0.06, which resulted in a response time of the A/C loop to a force step input of 120 milliseconds.

APPENDIX A

Derivation of the Transfer Function of the Closed Velocity Loop and its Response to a Unit Step Input

Appendix "A"

1. Derivation of the Transfer Function of the Closed Velocity Loop:

Referring to figure 92, the transfer function of the individual elements in the loop are:

- Correcting network:

$$T(s) = \frac{R_3}{R_1}\left[\frac{1 + Sc\ R_2}{1 + Sc\ (R_2 + R_3)}\right]$$

Substituting with the corresponding values of R1, R2, R3 and C yields"

$$T(s) = 220\left[\frac{1 + 0.022\ S}{1 + 2.222\ S}\right]$$

- The power amplifier:

$$T(s) = 10.0$$

- The DC motor:

$$T(s) = 0.35\left[\frac{1}{1 + 0.32\ S}\right]$$

- The tacho:

$$T(s) = 1.24$$

- The feedback element $\frac{R1}{R4}$

$$T(s) = 0.217$$

Accordingly, the transfer function of the open velocity loop is:

$$\frac{V_t(s)}{V_c(s)} = 220\left[\frac{1 + 0.022\ S}{1 + 2.222\ S}\right] \times 10 \times 0.35\left[\frac{1}{1 + 0.032\ S}\right] \times 1.24$$

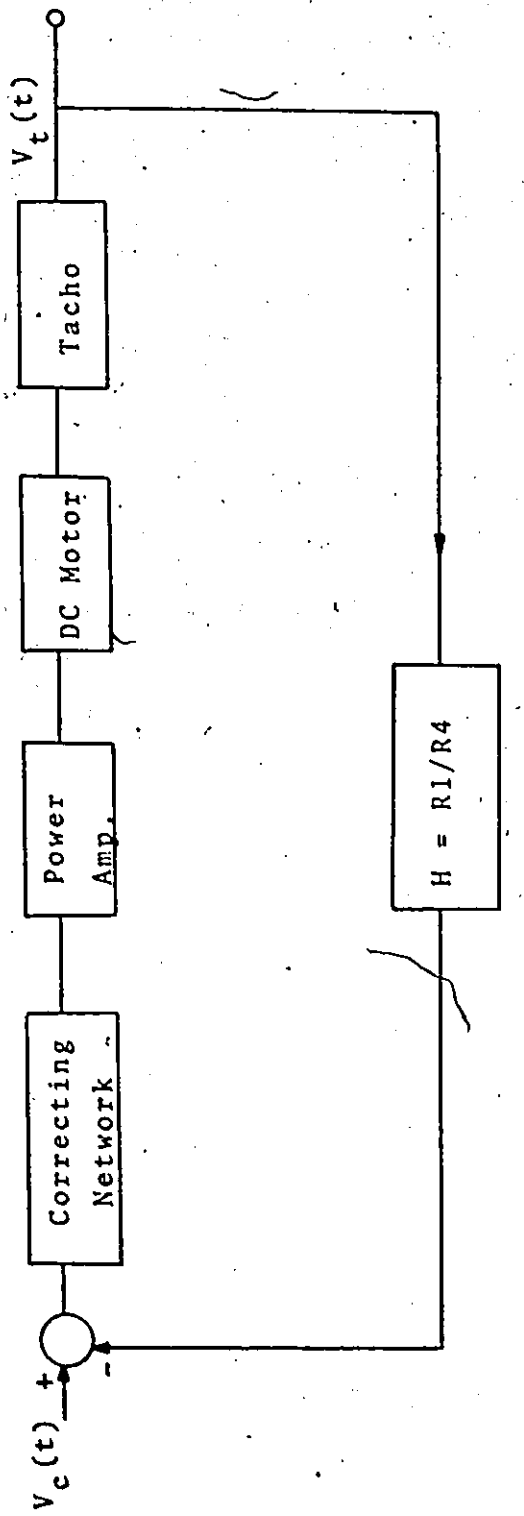

Block Diagram of the Closed Velocity Loop

FIGURE 92

$$\text{i.e. } \frac{V_t(s)}{V_c(s)} = 954.8\left[\frac{1 + 0.022\ S}{(1 + 2.222\ S)(1 + 0.032\ S)}\right]$$

In order to obtain the transfer function of the closed velocity $T_{vc}(s)$, the following relationship is used:

$$T_{vc}(s) = \frac{G(s)}{1 + GH(s)}$$

where $T_{vc}(s)$ is the closed velocity loop transfer function

$G(s)$ is the transfer function of the feed forward elements

$H(S)$ is the transfer function of the feedback elements

Accordingly,

$$T_{vc}(s) = \frac{954.8\left[\frac{(1 + 0.022\ S)}{(1+2.222\ S)(1+0.032\ S)}\right]^6}{1 + 954.8\left[\frac{(1 + 0.022\ S)}{(1+2.222\ S)(1+0.032\ S)}\right].0.217}$$

$$T_{vc}(s) = 295.377\left[\frac{(s + 45.45)}{s^2 + 95.796\ S + 2927.225}\right]$$

2. Response of the Closed Velocity Loop to a Unit Step Response:

The Laplace transform of a unit step input of 1.0 volt is $\frac{1}{s}$, and accordingly:

$$V_t(s) = 295.377\left[\frac{s + 45.45}{s(s^2 + 95.796\ s + 2927.225)}\right] \quad \ldots (1)$$

By arranging the term between brackets [] and using partial fraction expansion:

$$\frac{s + 45.45}{s(s^2+95.796\ s+2927.25)} = \frac{A}{s} + \frac{BS + C}{s^2+95.796\ s+2927.225} \quad \ldots (2)$$

where $A = \lim_{s \to o} \frac{s + 45.45}{s^2 + 95.796\ s + 2927.225}$

$$A = 0.0155$$

From equation (2) it follows that:

$$As^2 + 95.796\ As + 2927.225\ A + Bs^2 + Cs = s + 45.45$$

By equating the coefficients of s^2 in both sides of the above expression:

$$A + B = 0 \quad \text{and} \quad B = -0.0155$$

Again by equating the coefficients of S in both sides:

$$95.796\ A' + C = 1$$

$$C = -0.487$$

Equation (1) can thus be written in the following way:

$$V_t(s) = 295.377\ [\frac{0.0155}{S} - \frac{0.0155\ S + 0.487}{s^2 + 95.796\ S + 2927.225}]$$

Again arranging the term between brackets [] in the above expression:

$$V_t(s) = 4.578\ [\frac{1}{s} - \frac{S + 47.898}{(s+47.898)^2 + (25.159)^2} + 0.6549\ \frac{25.159}{(S + 47.898)^2 + (25.159)^2}]$$

Taking the inverse Laplace transform $L^{-1}[V_t(s)]$ of the above expression to obtain the response in the time domain:

$$V_t(t) = 4.573[1.0 - e^{-t/0.0208}\cos(25.159t) + 0.6549e^{-t/0.0208}\sin(25.159t)]$$

APPENDIX B

Response of the Closed Position Loop to a Unit Step Input in Position as seen from the Resolver and Tacho Outputs

Appendix "B"

1. Response of the Closed Loop to a Unit Step Input in Position as seen from the Resolver Output:

The transfer function of the closed velocity loop is:

$$T_{VC}(s) = 295.377\left[\frac{s + 45.45}{s^2 + 95.796\ s + 2927.225}\right]$$

Referring to figure 93, the transfer function of both the D/A converter and filter is:

$$T(s) = 45.0$$

The synchro is considered as an integrator having a transfer function:

$$T(s) = \frac{1}{10\ S}$$

Accordingly, the open loop transfer function is:

$$\frac{Y(s)}{X(s)} = 1071.932\left[\frac{s + 45.45}{s(s^2 + 95.796\ S + 2927.225)}\right]$$

The loop has a unity feedback element, and accordingly, the closed loop transfer function is:

$$\frac{Y(s)}{X(s)} = 1071.932\ \left(\frac{s + 45.45}{(s + 19.27)(s^2 + 76.67\ s + 2528.23)}\right)$$

Now, considering the resolver response to a unit step input in position:

$$Y(s) = 1071.932\left\{\left[\frac{s + 45.45}{(s+19.27)(s^2+76.67\ s+2528.23)}\right] \times \frac{1}{s}\right\} \quad (3)$$

Using partial fraction expansion technique for the term

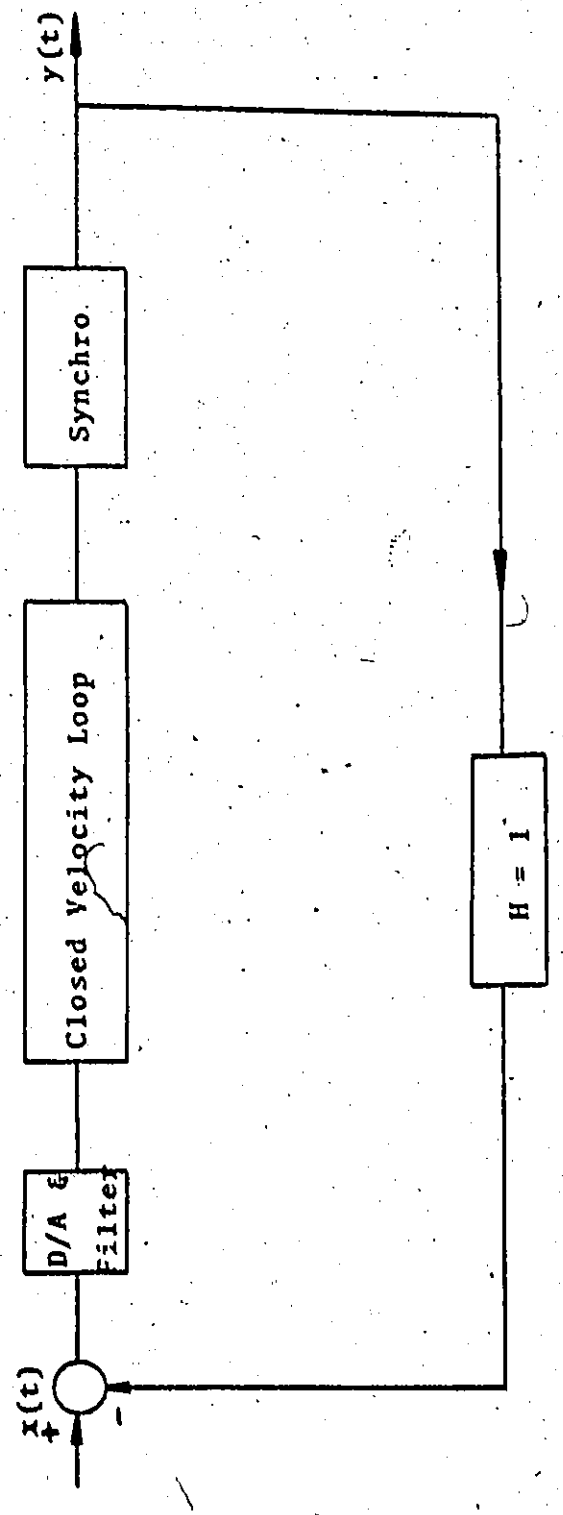

Block Diagram of the Closed Position Loop

FIGURE 93

between brackets {}

$$\frac{s + 45.45}{s(s+19.27)(s^2+76.67s+2528.23)} = \frac{A}{s} + \frac{B}{s+19.27} + \frac{Cs + D}{s^2+76.67s+2528.23} \quad (4)$$

Accordingly,

$$A = \lim_{s\to 0} \frac{(s + 45.45)}{(s + 19.27)(s^2 + 76.67\ S + 2528.23)}$$

Then, A = 0.000932

It follows that

$$B = \lim_{s\to -19.27} \frac{(s + 45.45)}{s(S^2 + 76.67\ S + 2528.23)}$$

B = -0.000955

From equation (4) it follows that:

$$S+45.45 = A(s+19.27)(s^2+76.67s+2528.23) + BS(s^2+76.67s + 2528.23) + (Cs+D)\ S\ (s+19.27)$$

In the above expression, equating the coefficients of S^3 in both sides yields:

A + B + C = 0

Accordingly, C = 0.00023

Again equating the coeffient of s^2 in both sides yields:

$A[76.67s^2+19.27s^2] + B[76.67s^2] + C[19.27s^2] + Ds^2 = 0$

therefore D = -0.0166

Equation (3) could thus, be written in the following manner:

$$Y(s) = 1071.932\left[\frac{0.000932}{s} - \frac{0.000955}{s + 19.27} + \frac{0.00023s-0.0166}{s^2+76.67s+2528.23}\right]$$

Arranging the above expression yields:

$$Y(s) = \frac{0.99904}{S} - \frac{1.02369}{s+19.27} + 0.02465\left[\frac{S + 38.335}{(s+38.335)^2 + (32.537)^2}\right]$$

$$- 0.57592\left[\frac{32.537}{(s+38.335)^2 + (32.537)^2}\right]$$

Now, taking the inverse Laplace transform $L^{-1}[Y(s)]$ of the above expression to obtain the response in the time domain:

$$Y(t) = 0.99404 - 1.02369\ e^{-t/0.0518} + 0.02467\ e^{-t/0.0260} \cos (32.537t) - 0.5764\ e^{-t/0.026} \sin (32.537t)]$$

2. <u>Response of the Closed Position Loop to a Unit Step Input in Position as seen from the Tacho Output:</u>

The transfer function of the closed position loop $T_{PG}(s)$ with output measured at the tacho is:

$$T_{PC}(s) = 1072.1 \times 1.24\left\{\frac{S + 45.45}{(S+19.27)(S^2+76.67S+2528.23)}\right\} \times 10\ S$$

$$T_{PC}(s) = 13294.04\left\{\frac{S + 45.45}{(s+19.27)(s^2+76.67S+2528.23)}\right]$$

Now investigating the unity step input response:

$$V_t(s) = 13294.04\left[\frac{S + 45.45}{(s+19.27)(s^2+76.67S+2528.23)}\right]$$

where the Laplace transform of a unity step input is $\frac{1}{S}$

Accordingly, and using partial fraction expansion one obtains:

$$V_t(s)' = 13294.04\left[\frac{0.01841}{s+1927} - \frac{0.01841\ S'+0.057}{s^2+76.67S + 2528.23}\right]$$

Arranging the term between brackets,

$$V_t(s) = 244.74\left[\frac{1}{s+19.27} - \frac{s+32.537}{(s+38.335)^2 + 2528.23}\right.$$

$$\left. + \frac{32.537}{(s+38.335)^2 + (32.537)^2}\right]$$

Now taking the inverse Laplace transform $L^{-1}[V_t(s)]$ to yield the response in the time domain:

$$V_t(t) = 244.74\left[e^{-t/0.0519} - e^{-t/0.0261}\cos(32.537t) + 1.083\, e^{-t/0.0261}\sin(32.537t)\right]$$

APPENDIX C

Response of the Closed Position Loop to a Ramp Input

Appendix "C"

Response of Closed Position Loop to a Ramp Input

A ramp input was applied to the closed position loop and the tacho output was considered

The ramp is described by:

$f(t) = 0.5t$ inch for $o < t < t_1$

and $f(t) = 0.01$ inch for $t_1 < t < \infty$

where $t_1 = 0.02$ sec.

The transfer function of the closed position loop considering the tacho output is:

$$\frac{V_t(s)}{x(s)} = 13294.04\left[\frac{s(s+45.45)}{(s+19.27)(s^2+76.67S+2528.23)}\right]$$

The Laplace transform of the ramp is:

$$F(s) = \frac{a}{s^2} - \frac{a}{s^2} e^{-t_1 s}$$

where $a = 0.5$ and $t_1 = 0.02$ sec.
The response of the tacho to the above ramp input is thus obtained as follows:

$$V_t(s) = 13294.04\left[\frac{S(s+45.45)\ 0.5\ (1-e^{-0.02s})}{(s+19.27)(s^2+76.67S+2528.23)s^2}\right]$$

$$V_t(s) = 6647.020\left[\frac{(s+45.45)}{s(s+19.27)(s^2+76.67S+2528.23)}\right](1-e^{-0.02s})$$

or

$$V_t(s) = 6647.020(1-e^{-0.02S})\ Q \qquad \ldots (5)$$

where,

$$Q = \left[\frac{(s+45.45)}{s(s+19.27)(s^2+76.67S+2528.23)}\right]$$

Now, factoring only the term Q using partial fraction expansions:

$$\frac{s + 45.45}{S(S+19.27)(S^2+76.67S+2528.23)} = \frac{A}{s} + \frac{B}{s+19.27} + \frac{CS+D}{s^2+76.67S+2528.23}$$

Accordingly

$$A = \lim_{s\to 0} \frac{s + 45.45}{(s+19.27)(s^2+76.67S+258.23)}$$

thus,

$$A = 9.329 \times 10^{-4}$$

and,

$$B = \lim_{s\to -19.27} \frac{S + 45.45}{S(s^2+76.67s+2528.23)}$$

thus,

$$B = -9.553 \times 10^{-4}$$

It follows also that:

$$A(s+19.27)(s^2+67.67s+2528.23) + BS(s^2+76.67S+2528.23) + (CS+D)S(s+19.27) = s + 45.45$$

Equating the coefficients of s^3 in both sides of the above expression yields:

$$A + B + C = 0$$

and

$$C = 2.2 \times 10^{-5}$$

Also,

$$76.67\ B + 19.27\ C + D + 95.94\ A = 0$$

And accordingly,

$$D = -0.01667$$

The term Q thus becomes:

$$Q = \frac{9.329\times10^{-4}}{S} - \frac{9.553\times10^{-4}}{S+19.27} + \frac{2.2\times10^{-5}S-0.01667}{S^2+76.67S+2528.23}$$

The above expression can be further rewritten in the following manner:

$$Q = \frac{9.329\times10^{-4}}{S} - \frac{9.553\times10^{-4}}{s+19.27} + 2.2\times10^{-5}\{\frac{s+38.335}{(s+38.335)^2+(32.537)^2} - 24.07[\frac{32.537}{(s+38.335)^2 + (32.537)^2}]\}$$

The inverse Laplace transform of the term Q is $F_1(t)$ where:

$$F_1(t) = 9.329\times10^{-4} - 9.553\times10^{-4}e^{-t/0.0519} + 2.2\times10^{-5}[e^{-t/0.0261} \cos(32.537t) - 24.07e^{-t/0.0261} \sin(32.537t)]$$

From equation (5) it follows that the inverse Laplace transform of $V_t(s)[L^{-1}V_t(s)]$ is:

$$V_t(t) = 6647.02[F_1(t) - F_1(t-0.02)]$$

Accordingly,

$$V_t(t) = 6.201-6.349e^{-t/0.0519}+0.148e^{-t/0.0261} \cos(32.537t) - 3.58e^{-t/0.0261} \sin(32.537t)-\{6.201-6.349e^{-(t-0.02)/0.0519} +0.148e^{-(t-0.02)/0.0261} \cos[32.537(t-0.02)]-3.58 e^{-(t-0.02)/0.0261} \sin[32.537(t-0.02)]\}$$

For $t < 0.02$ sec., the term between brackets {} is zero.

APPENDIX D

A/C SIMULATION ROUTINE

```
HWTW,HT1,T30.                    A/C SIMULATION                          ELBES
ATTACH,PLOTLIB.
FTN(S=Y,OPT=0)                                                    162
LOSET,LIB=PLOTLIB.
LGO.
*       6400 END OF RECORD
      PROGRAM SIMUL (INPUT,OUTPUT,TAPE5=INPUT,TAPE6=OUTPUT,TAPE10)
C     ****************************************************************
C       PROGRAM SIMUL USES THE STATE SPACE METHOD TO SIMULATE THE
C       RESPONSE OF THE CNC-A/C SYSTEM
C       THE LOOP IS SUBJECTED TO A FORCE STEP INPUT
C     ****************************************************************
C
        DIMENSION X(15),XPREV(15),CASE1(15),CASE2(15)
        DIMENSION V(20),FORCE(1000)
        DIMENSION TIMSTP(1000),TT(101),F1(101)
        INTEGER DELFLG,FORFL
        REAL KAC
        DATA CASE1/0.1,0.07,2.73,0.026,0.078,0.531,0.046,0.2,
       1  2.3,2.37,0.053,1023.,0.8531,0.0,3.0/
        DATA CASE2/0.02,0.0021,0.2833,0.0028,0.0009,0.9786,0.014,
       $ 1.2135,0.2678,0.2659,0.0059,117.434,0.0979,0.0,0.0/
        DATA TIMSTP/0.0021/
C       FMAX AND FMIN ARE TWO CONSTRAINTS IMPOSED ON THE MAXIMUM AND
C       THE MINIMUM ALLOWABLE FEED RATE IN UNITS INCHES/SEC
        DATA FMAX,FMIN/1.5,0.005/
C
C       DEFINE PARAMETERS OF THE CORRECTING NETWORK
C
        DATA R3/2200000.0/
        DATA C/0.000001/
        DATA R1/10000.0/
C       AKV IS THE GAIN OF THE POWER AMPLIFIER
C
        DATA AKV/10.0/
C       DEFINE PARAMETERS OF THE DC MOTORS
C
C       AKM IS THE GAIN OF THE DC MOTOR (REV/SEC/VOLT)
        DATA AKM/0.35/
        DATA B/3.0112/
C       AKE IS THE VOLTAGE CONSTANT OF THE MOTOR (VOLT/REV/SEC)
        DATA AKE/3.96/
C       TM IS THE DC MOTOR TIME CONSTANT IN SECONDS
        DATA TM/0.032/
C
C     THE TIME STEP IS SET AT 0.0021 SECONDS.
C
        NPLOT = 1
C
C     FOR MULTIPLE RUNS, INSERT THE STATEMENT....  DO 804 MNO=1,(NO. RUNS)
        DO 804 MNO=1,6
C
        READ(5,31)ICASE,KDELAY,FORFLG
        READ(5,32) SAMPL,CONST,FREQ,FNOM,B,KAC
        READ (5,666) AKB
        READ (5,777) R2
        READ (5,888) C4
C
```

```
      AVER=CONST
      TIMDEL = SAMPL*FLOAT(KDELAY+1)
      DO 30 II=1,15
      IF(ICASE.EQ.1) XPREV(II) = CASE1(II)
      IF(ICASE.EQ.2) XPREV(II) = CASE2(II)
30    CONTINUE
C
C     ICASE DETERMINES THE INITIAL CONDITIONS. I.E. CASE 1 OR CASE 2
C     FOR A NOMINAL  FORCE OF 200 LBS, CASE 1 REPRESENTS AN EXCESSIVE
C     CUTTING FORCE AND CASE 2 REPRESENTS A SUB-OPTIMAL FORCE.
C
C       CASE1 OR CASE2 REPRESENT THE STEADY STATE OPERATION OF THE M/C
C       LOOP ALONE (I.E BEFORE ATTACHING THE A/C LOOP)
C     KDELAY DETERMINES THE TIME LAG BETWEEN CUTTING FORCE AND FEEDRATE
C     A VALUE OF KDELAY=N MEANS TIME LAG IS N+1 TIMES DELAY IN A/C LOOP
C
C     FORFLG IS A FLAG DENOTING THE DESIRED CUTTING FORCE FUNCTION.
C     I.E.  FORFLG = 0 GIVES A LINEAR FORCE AND FORFLG=1 GIVES A
C     SINUSOIDAL FORCE.
C
C       SAMPL IS THE FORCE SAMPLING INTERVAL (TIME DELAY BETWEEN FEED
C       RATE CORRECTIONS)
C
C     CONST IS THE SCALING FACTOR IN THE FORCE FUNCTION.
C
C     FREQ IS THE FREQUENCY IN HZ OF THE FORCE.IT IS ZERO IF LINEAR.
C
C       FNOM IS THE DESIRED NOMINAL FORCE IN LBS.
C
C     B IS THE DAMPING FACTOR IN THE A/C ALGORITHM
C
C       KAC IS THE A/C GAIN
C
      DELFLG = 1
      IF(SAMPL.EQ.0.0) DELFLG = 0
C
C     DELFLG = 1 INDICATES A DELAY IN THE A/C LOOP.
C
      WRITE(6,20)
      WRITE(6,21)ICASE
      WRITE(6,22) TINCR,FORT
      WRITE (6,23) SAMPL,CONST
      IF(FORFLG.EQ.0)WRITE(6,24)
      IF(FORFLG.EQ.1)WRITE(6,25) FREQ
      WRITE(6,26) KAC
      WRITE(6,27)B,TIMDEL
      OMEGA = 6.2831*FREQ
      IF(DELFLG.EQ.0) SAMPL = TINCR
      T= -TINCR
      X(1) = XPREV(1)
      TIME = 0.0
      IDELAY = 1
      DO 29 IJ=2,15
29    X(IJ) = 0.0
C
C
      DO 100 I=1,1000
      T = T+ TINCR
      IF (T .EQ. 0.0) GO TO 12
```

```
C     X(1) IS THE DISTANCE COMMAND IN INCHES.
      X(1)  = XPREV(1)  + XPREV(13)*TINCR
   12 X(4)=XPREV(2)*TINCR+XPREV(4)*(1.0-(TINCR/((R2+R3)*C)))
C     X(6) IS THE MOTOR SPEED IN REV/SEC
      X(6)=XPREV(6)+((2*TINCR*AKM*XPREV(15))/TM)
     $-((TINCR*XPREV(6)/TM)*(1-AKM*AKE))
C     X(7) IS THE OUTPUT OF THE RESOLVER IN INCHES
      X(7)=XPREV(7)+TINCR*XPREV(6)/10.
C     X(11) IS THE INPUT TO THE D/A CONVERTER AND FILTER
      X(11)=X(1)-X(7)
C     X(10) IS THE OUTPUT FROM THE D/A CONVERTER AND FILTER
      X(10) = AKP*X(11)
C     X(8) IS THE TACHO OUTPUT IN VOLTS
      X(8)=1.24*X(6)
C     X(9) IS THE VELOCITY FEEDBACK IN VOLTS
      X(9)=(R1/R4)*X(8)
C     X(2) IS THE INPUT TO THE CORRECTING NET WORK
      X(2)=X(10)-X(9)
C     X(3) IS THE OUTPUT OF THE CORRECTING NET WORK
      X(3)=((R2*R3)/(R1*(R2+R3)))*X(2)+(R3/((R1*C)*(R2+R3)))*X(4)
C     X(5) IS THE OUTPUT OF THE POWER AMPLIFIER
      X(5)=AKV*X(3)
C     X(15) IS THE ARMATURE CURRENT IA
      X(15)=(X(5)-AKE*X(6))/R
CCCCCC
     NOW TO DETERMINE THE CUTTING FORCE X(12)
CCCCCC
     THIS LOGIC KEEPS THE CUTTING FORCE LAGGING BEHIND THE FEED BY
     THE FACTOR TIMDEL.
CCCCCC
      IF(DELFLG .EQ. 0) GO TO 55
CC    ONLY CALCULATE FORCE AND NEW FEEDRATE AFTER CORRECT
CC    DELAY TIME.
      IF(T.LT.(SAMPL-.0001)) GO TO 10
      IF(KDELAY.EQ.-1) GO TO 59
   55 IF(IDELAY .LE. KDELAY) V(IDELAY)=X(6)/10.0
      IF(FORFLG.EQ.0)X(12)=CONST*V(1)
      IF(FORFLG .EQ. 1) X(12)=(AVER+ABS(CONST*SIN(OMEGA*TIME)))*X(6)
     $/10.0
      IF(IDELAY.LE.KDELAY) GO TO 56
      KKK = KDELAY -1
      DO 57 M=1,KKK
   57 V(M)=V(M+1)
      V(KDELAY)  = X(6)/10.0
   56 IDELAY=IDELAY+1
      GO TO 54
   59 IF(FORFLG .EQ. 0) X(12)=CONST*X(6)/10.0
      IF(FORFLG .EQ. 1) X(12)=(AVER+ABS(CONST*SIN(OMEGA*TIME)))*X(6)
     $/10.0
CCCCCC
     **********    ADAPTIVE CONTROL POLICY    **************
CCCCCC
     COMPUTE EF THE RELATIVE FORCE ERROR.
CCCCCC
   54 EF=(1.0-X(12)/FORT)
      X(14) = EF
C     COMPUTE THE DAMPING TERM B*D(EF)/DT
      DAMP=B*(X(14)-XPREV(14))/DELAY
```

```
C
CC    COMPUTE THE REQUIRED ACCELERATION
C
      ACC=EE*KAC+DAMP
   51 T=0.0
      GO TO 9
   10 ACC=0.0
C
CC    DETERMINE THE NEW COMMANDED FEEDRATE.
C
    9 X(13)=XPREV(13)+ACC*SAMPL
C
      IF(X(13) .GT. FMAX) X(13)=FMAX
      IF (X(13) .LT. FMIN) X(13)=FMIN
C
C
    6 DO 11 J=1,15
   11 XPREV(J)=X(J)
CCCCC
CCCCC
C     NOW DETERMINE THE ACTUAL FORCE RESULTING FROM THE CUTTING PROCESS
  102 FORCE(I)=X(12)
      TIMSTP(I) = TIME
  103 TIME=TIME+TINCR
  100 CONTINUE
CC    PRINT THE RESULTING CUTTING FORCE ONLY EVERY 10 STEPS
      TT(1)=0.0
      F1(1)=FORCE(1)
      DO 305 I=10,1000,10
      II=(I/10)+1
      F1(II)=FORCE(I)
      TT(II)=TIMSTP(I)
  305 CONTINUE
      WRITE (6,61)
      WRITE (6,67) ((TT(II),F1(II)),II=1,101)
C
      JJ=1
      CALL RESPONS (TIMSTP,FORCE,1000,JJ)
  804 CONTINUE
      CALL PLOT (X,Y,999)
      STOP
31    FORMAT(I2)
32    FORMAT(F7.1)
   20 FORMAT(1H1,10H**********,*LINEAR A/C ALGORITHM *,
     $ 10H********** //)
21    FORMAT(1H ,5X,* INITIAL CONDITIONS USED ARE CASE *,I1/)
22    FORMAT(1H ,5X,* TIME INCREMENT = *,F6.4,* SEC*//6X,
     $ * NOMINAL FORCE  = *,F6.1,* LB */)
   23 FORMAT(1H ,5X,*FORCE SAMPLING INTERVAL=*,F6.4,*SEC*//6X,
     $ * FORCE CONSTANT = *,F9.1/  )
24    FORMAT(1H ,5X,* LINEAR CUTTING FORCE */)
25    FORMAT(1H ,5X,* SINUSOIDAL CUTTING FORCE WITH FREQ = *,
     $ F8.3,* H7 */)
   26 FORMAT(1H ,5X,*A/C GAIN=*,F5.1/)
27    FORMAT(1H ,5X,* DAMPING FACTOR =  *,F4.2//6X,
     $ * TIME LAG IN ACHIEVING NEW FORCE = *,F5.3,* SEC *//)
   61 FORMAT(1H ,5X,*TIME*,5X,*ACTUAL FORCE*,//)
```

```
 67   FORMAT(F9.4,F14.6)
 666  FORMAT(F20.6)
 777  FORMAT(F20.6)
 888  FORMAT(F20.6)
      END
      SUBROUTINE RESPONS (X,Y,M,JJ)
C     SUBROUTINE RESPONS PLOTS THE RESULTING CUTTING FORCE VS TIME
      DIMENSION X(M),Y(M)
      SI=0.1
C
      CALL PLOT (0.0,0.0,-3)
      CALL DATE(D1)
      CALL LETTER (0.0,7.270.0,1.0,10.0,9HELDESTAHI)
      CALL LETTER (10,0.1,270.0,2.0,10.0,01)
C
      IF (JJ .EQ. 1) GO TO 32
   32 CALL LETTER (11,0.1,90.0,17.0,5.0,11HFORCE  LBS,)
   9A CALL LETTER (10,0.1,0.0,11.0,7.50,1CHTIME (SEC))
C
      XL=12.5
      YL=10.0
      XMARG=6.5
      YMARG=4.0
C
      CALL FACTOR (M,X,Y,XL,YL,XMARG,YMARG )
      CALL PLOT (XMARG,YMARG,3)
      CALL PLOT (XL,YMARG,2)
      CALL PLOT (XMARG,YMARG,3)
      CALL PLOT (XMARG,YL,2)
      CALL PLOT (XL,YL,2)
      CALL PLOT (XL,YMARG,2 )
C
      CALL PLOT (XL,YMARG,2 )
C
      YSTEP= (YL-YMARG)/10.0
      XOR=XMARG
      YOR=XMARG
C
   2  CALL PLOT (XOR,YOR,3)
      CALL PLOT (XOR-0.1,YOR,2)
      CALL INCHTO (XMARG,YOR,XO,YP)
C
      ENCODE (10,5,YO) YP
C
C
      CALL LETTER (10,0.1,0.0,5.4,YOR-0.05,YO)
C
      IF (YOR .LE. YL) YOR=YOR+YSTEP
      IF (YOR .LE. YL) GO TO 2
      XSTEP=(XL-XMARG)/10.0
      YYM=YMARG
      NN=1
C
   4  CALL PLOT(XOR,YYM,3)
      CALL PLOT (XOR-0.1,YYM,2)
      CALL INCHTO (XOR,YYM,XH,YH)
      ENCODE (4,6,XO ) XH
C
      CALL LETTER (4,0.1,0.0,XOR-0.23,YYM-0.3,XO)
```

```
C
      NNN1=NNN+1
   10 XOR=XOR+XSTEP
      IF (XOR .LE. XL) GO TO 7
C
      CALL UNITTO (X(1),Y(1),X1,Y1)
C
      NM=N-1
      DO 4 I=1,NM
C
      CALL UNITTO (X(I+1),Y(I+1),XN,YN)
C
    4 CONTINUE
C
      CALL PLTHPL (X,Y,N)
      CALL PLOT (12.0,0.0,-3)
C
      RETURN
C
    5 FORMAT (F10.3)
    6 FORMAT(F4.2)
      END
      6400 END OF RECORD
END LISTING
      6400 END OF RECORD
      6400 END OF RECORD
      6400 END OF RECORD
```

COTOT %2T

REFERENCES

1. Wilson, Frank W., "Numerical Control in Manufacturing", McGraw-Hill book company 1963.
2. Childs, James J., "Principles of Numerical Control", 2nd ed., Industrial Press 1969.
3. Raven, Francis H., "Automatic Control Engineering", McGraw-Hill book company 1968.
4. Distefano, Stubberud and Williams, "Feedback and Control Systems", Schaum's outline series, McGraw-Hill book company 1967.
5. Shinners, Stanley M., "Modern Control System Theory and Application", Addison Wesley 1972.
6. Davies, W.D.T., "System Identification for Self Adaptive Control", Wiley-Interscience 1970.
7. Macneil, Peter R., "Computer Adaptive Control in Milling", M.Eng. thesis, McMaster University, Hamilton, Canada, April 1975.
8. Mail Vaganam, "An Adaptive Control Algorithm for a CNC Milling Machine", M.Eng. thesis, McMaster University, Hamilton, Canada, April 1974.
9. Koren, Y. and J. Tlusty, "CNC/AC System for a Milling Machine - Part I", Metal Working Research Group Report No. 43, Hamilton: Mechanical Engineering Department, McMaster University, March 1974.

10. Koren, Y. and J. Tlusty, "CNC/AC System for a Milling Machine - Part III", Metal Working Research Group Report No. 46, Hamilton: Mechanical Engineering Department, McMaster University, June 1974.

11. Tlusty, J., Y. Koren and P. Macneil, "Numerical and Adaptive Control for Die Sinking", Proceedings of the International Conference on Production Engineering, Tokyo, Japan Society of Precision Engineering, 1974.

12. Koeniaberger, F. and J. Tlusty, "Structures of Machine Tools", Vol. 1, 1st ed., Oxford: Pergamon Press, 1970.

13. Bendix Corporation, Michigan, U.S.A., "Adaptive Control of Milling Machines", Tool and Manufacturing Engineer, Vol. 62, No. 5 (May 1969), pp. 50-54, Adapted from ASTME paper MS68-638.

14. Hartley, D., "Adaptive Control of Cutting Force and Power", N.T.I.R.A. research report No. 46, May 1972.

15. Shillam, N.P., "The On-line Control of Cutting Conditions Using Direct Feedback", paper presented at the 12th International M.T.D.R. Conference, Manchester, U.K., September 1971.

16. Weck, M., E. Verhaag and M. Gather, "Adaptive Control for Face-Milling Operations with Strategies for Avoiding Chatter Vibrations and for Automatic Cut Distribution", Annals of the C.I.R.P., Vol. 24/2, 1975.

17. Koji Nakasawa, "Improvement of Adaptive Control of Milling Machine by Non-Contact Cutting Force Detector",

Annals of the C.I.R.P., Vol. 24/2, 1975.

18. Stute, G. and F.R. Goetz, "Adaptive Control for Variable Gain in ACC Systems", Annals of the C.I.R.P., Vol. 24/2, 1975.

19. Valek, Robert J., "How to go Adaptive Control", Tool and Manufacturing Engineer, Vol. 59, No. 1, pp. 18-21, July 1967.

20. Mesniaeff, P.G. "The Technical ins and outs of Computerized Numerical Control", Control Engineering, March 1971.

21. Evans, L., "Computerized Numerical Control Revised", Control Engineering, August 1972.

22. Kenneth L. Slawson, "Computer Control Adds Flexibility to N/C", Tool and Manufacturing Engineer, Vol. 60, No. 3, (March 1968), pp. 48-50.

23. Taft, C.K., F.N. Lutz and M. Mazok, "Dynamic Accuracy in Numerical Control Systems - Part I", Tool and Manufacturing Engineer, Vol. 58, No. 5 (May 1967), pp. 18-20.

24. Taft, C.K., F.N. Lutz and M. Mazok, "Dynamic Accuracy in Numerical Control Systems - Part II", Took and Manufacturing Engineer, Vol. 58, No. 6 (June 1967), pp. 80-83.

25. Bedini, R. and P.C. Pinotti, "On-line Measurement of Bending and Torque in Milling", Annals of the C.I.R.P., Vol. 2, No. 3, 1974.

26. Tlusty, J. and P. MacNeil, "Dynamics of Cutting Forces in End Milling", Annals of the C.I.R.P., Vol. 24/1/1975.